



UNIVERSITÀ POLITECNICA DELLE MARCHE
SCUOLA DI DOTTORATO DI RICERCA IN SCIENZE DELL'INGEGNERIA
CURRICULUM IN INGEGNERIA INFORMATICA, GESTIONALE E DELL'AUTOMAZIONE

An infrastructure for decision-making to support neonatal clinical care and research

Ph.D. Dissertation of:
Annalisa Cenci

Advisor:
Prof. Primo Zingaretti

Curriculum Supervisor:
Prof. Francesco Piazza

XVI edition - new series



UNIVERSITÀ POLITECNICA DELLE MARCHE
SCUOLA DI DOTTORATO DI RICERCA IN SCIENZE DELL'INGEGNERIA
CURRICULUM IN INGEGNERIA INFORMATICA, GESTIONALE E DELL'AUTOMAZIONE

An infrastructure for decision-making to support neonatal clinical care and research

Ph.D. Dissertation of:
Annalisa Cenci

Advisor:
Prof. Primo Zingaretti

Curriculum Supervisor:
Prof. Francesco Piazza

XVI edition - new series

UNIVERSITÀ POLITECNICA DELLE MARCHE
SCUOLA DI DOTTORATO DI RICERCA IN SCIENZE DELL'INGEGNERIA
FACOLTÀ DI INGEGNERIA
Via Brezze Bianche – 60131 Ancona (AN), Italy

To my family

Ringraziamenti

Il primo ringraziamento va, senza dubbio, ai miei genitori, i due punti di riferimento della mia vita, senza i quali non sarei arrivata dove sono ora. Grazie perché posso sempre contare su di voi, perché sapete essermi vicini nei momenti difficili e gioire per i miei traguardi.

Un grazie enorme anche a mia sorella e a mio fratello, su cui posso sempre contare, e alla famiglia che si allarga..

Un grazie speciale anche a te Italo, perché con te posso essere sempre me stessa, perché mi capisci e mi sei vicino più di chiunque altro, anche nei momenti più stressanti, che tanto spesso sono capitati in questi anni di dottorato. Grazie per tutto!

Altro tipo di ringraziamento, ma non meno importante e sincero, va ai professori Primo Zingaretti ed Emanuele Frontoni, che mi hanno dato la possibilità di intraprendere questo stimolante percorso di ricerca. Grazie a Primo per i suoi preziosi consigli che mi hanno spronato a fare sempre meglio e ad Emanuele per la passione che mette nel suo lavoro e che cerca di trasmetterci quotidianamente.

Ringrazio tutti i membri del VRAI, del DII e dell'Università che ho avuto il piacere di conoscere in questi anni, Rama, Michele, Rocco, Chiara, Mirco, Roberto e Roberto, Gloria. Grazie per avermi dato una mano quando potevate o anche solo per avermi allietato la giornata con una battuta.

Un grazie particolarmente sentito va ai miei due compagni di lavori, viaggi, avventure, chiacchiere e risate, che in questi tre anni da colleghi si sono trasformati in amici fidati su cui so che potrò contare anche in futuro.

Un grazie anche al Prof. Virgilio Paolo Carnielli, al personale del reparto della UTIN dell'ospedale pediatrico "G. Salesi" di Ancona e alla JEF srl senza la cui collaborazione questo lavoro di dottorato non sarebbe stato possibile.

A tal proposito mi sento di ringraziare tutte le persone della JEF con cui mi trovo molto bene e da cui sto imparando molto. Grazie a Moira, Bianca, Luca, Andrea, Marco, Salvatore e a tutto il team di sviluppo.

Anche qui un grazie particolare, che viene dal cuore, va a te Ilaria. 7 anni fa ti ho conosciuta come mia correlatrice. Da correlatrice sei passata a collega e, poi, a molto più che collega. Ormai se per me un'amica vera e leale. Posso dire, mai stata più sincera, che se non fosse stato per te non sarei arrivata fin qui. Mi hai sempre spronato a continuare e ad andare avanti, credendo in me

più di quanto facessi io, sopportando le mie ansie e sollevandomi il morale con il tuo perenne buonumore. Grazie!

Ultimo, ma non per importanza, un grazie alle mie amiche di sempre, Mari, Vale, Anna e Marti; grazie perché, nonostante lo studio, il lavoro e i mille impegni che ci tengono lontane, siete sempre lì pronte ad accogliermi a braccia aperte, a farmi divertire e a farmi sentire a casa come se ci vedessimo ancora tutti i giorni!

E per finire un grazie davvero sentito a tutti coloro, amici e parenti, che, anche se non ho citato, mi hanno aiutato ad arrivare a questo importante traguardo.

Ancona, October 2017

Annalisa Cenci

Sommario

I dispositivi medici, in genere, sono unità individuali, per cui una tipica sala ospedaliera in un reparto di terapia intensiva ospita un gran numero di dispositivi stand-alone, ognuno con una propria interfaccia utente.

Le culle dei neonati pretermine presso l'Unità di Terapia Intensiva Neonatale (UTIN) dell'Ospedale Pediatrico "G. Salesi" di Ancona sono circondati da numerosi dispositivi per il monitoraggio, la diagnosi e il trattamento di diverse malattie e tutti questi dispositivi forniscono un'enorme quantità di dati che, fino ad ora, venivano visualizzati solo su monitor e periodicamente trascritti in una cartella clinica cartacea. Le note manuali, quindi, venivano regolarmente, ma non immediatamente, trascritte in un foglio elettronico sul PC dell'unità neonatale con il rischio di errori e dimenticanze.

In questo contesto, i medici hanno espresso la necessità di raccogliere automaticamente i dati da tutti questi dispositivi per garantire che non venissero trascurati dettagli importanti per la cura del paziente, essendo consapevoli che l'automazione di questo processo può facilitare e migliorare l'implementazione delle procedure della loro pratica clinica quotidiana.

Alla luce di quanto espresso, l'obiettivo di questa tesi è quello di permettere l'interfacciamento e l'integrazione delle strumentazioni biomediche della UTIN in un'unica infrastruttura cloud, che consenta la comunicazione tra diversi dispositivi medici e un unico database. L'architettura proposta consente l'automatizzazione del processo di raccolta, trasmissione, memorizzazione, elaborazione e disponibilità dei dati dei dispositivi per il personale medico. Questa è garantita dalla realizzazione di un'interfaccia web che supera le funzionalità di una semplice Cartella Clinica Elettronica (CCE), grazie allo sviluppo di moduli clinici innovativi. Essi contengono applicazioni, funzionalità, tecniche di estrazione e analisi dei dati e algoritmi decisionali, che forniscono in output consigli, reminder, allarmi, e importanti indicatori, in grado di supportare i medici nella previsione e nella diagnosi di malattie come l'ittero neonatale o le disabilità motorie, nel monitoraggio dei parametri fisiologici e di sviluppo, come la frequenza respiratoria e i parametri di crescita, e nelle decisioni da prendere riguardo problemi clinici, come gli apporti nutrizionali giornalieri e i follow-up.

Tutte le soluzioni sopra descritte sono state validate attraverso una serie di esperimenti condotti nella UTIN sotto l'attenta supervisione del primario del

reparto, il Prof. V. P. Carnielli.

Abstract

Medical devices, generally, have been unique units, so that a typical hospital room in an intensive care ward hosts a big number of stand-alone devices, each one with its own user interface.

Preterm infants' cribs in Neonatal Intensive Care Unit (NICU) of "Women's and Children's Hospital G. Salesi" of Ancona are surrounded by many devices for the monitoring, diagnosis and treatment of several diseases and all these devices provide a huge amount of data that, until now, was only displayed on monitors and periodically transcribed in a paper medical record. Then manual notes were regularly, but not immediately, transcribed in an electronic sheet on the PC of the neonatal unit with the risk of errors and forgetfulnesses. In this context, physicians have expressed the need to automatically gather data from all these devices to ensure that no important details for patient care were overlooked, as they are aware that the automation of this process could facilitate and improve the implementation of the procedures of their daily clinical practice.

In the light of the above, the objective of this thesis is to allow the interfacing and integration of biomedical instrumentations of the NICU into a single cloud-based infrastructure that enables the communication between different medical devices and a unique database. The proposed architecture permits the automation of the process of device data collection, transmission, storage, processing and availability for medical staff, that is guaranteed through the implementation of a web interface that exceeds the functionalities of a simple Electronic Medical Record (EMR), thanks to the development of innovative clinical tools. They contain applications, functionalities, data extraction and analysis techniques and decision making algorithms, which provide in output advices, reminders, alarms, and important indicators that can support physicians in predicting and diagnosing diseases, such as neonatal jaundice or motor disabilities, in monitoring physiological and developmental parameters, such as respiratory rate and growth parameters, and in making decisions about clinical problems, such as daily nutritional intakes and follow-ups.

All the solutions described above have been validated through a series of experiments conducted in the NICU under the careful supervision of the Head Physician, Prof. V. P. Carnielli.

Contents

1	Introduction	1
1.1	Context	1
1.2	Objectives and main contributions	4
1.3	Structure of the thesis	6
2	State of the art	9
2.1	Health Information System Infrastructures	10
2.2	Electronic Medical Records and Electronic Health Records	12
2.3	Evidence-Based Medicine and Decision Support	16
3	A new infrastructure for neonatal care	19
3.1	SINC cloud-based healthcare architecture	20
3.1.1	Data Platform	22
3.1.2	Cyber Security	23
3.2	Medical Device Network	24
3.2.1	Patient Monitor	24
3.2.1.1	Communication Protocol	25
3.2.1.2	Patient Monitor Data	27
3.2.2	Bilirubinometer	28
3.2.2.1	Communication Protocol	29
3.2.3	Transcutaneous Bilirubinometer	31
3.2.3.1	Communication Protocol	32
3.3	The end-user web interface	34
3.3.1	Authentications, Authorizations and Privacy Policy	35
3.3.2	Applications, Tools and Services	36
3.3.2.1	Clinical Tools	37
3.3.2.1.1	Anagraphic Tool	37
3.3.2.1.2	Growth Tool	38
3.3.2.1.3	Nutrition Tool	40
3.3.2.1.4	Bayley Tool	43
4	Decision-Making Tools	47
4.1	Bilirubin Tool	47
4.1.1	Related Works	49
4.1.2	SIN Guidelines	51

4.1.3	Scenario	55
4.1.4	Data Analysis: Bilirubin Decision-Making Algorithm . .	57
4.2	Activities Monitoring Tools	61
4.2.1	The physical architecture	61
4.2.2	Respiration Tool	62
4.2.2.1	Related Works	63
4.2.2.2	Data Analysis: Respiratory Rate Algorithm . .	64
4.2.3	Movement Tool	65
4.2.3.1	Related Works	68
4.2.3.2	Data Analysis	69
4.2.3.2.1	Acquisition and Movements Detection Algorithm	70
4.2.3.2.2	Data processing	71
KPIs Extraction	73	
Markov Chain Model	74	
4.2.3.2.3	Extremities Tracking Algorithm . . .	75
4.2.4	Infant Semantic Segmentation	77
4.2.4.1	Related Works	78
4.2.4.2	Convolutional Neural Networks	78
4.2.4.2.1	U-Nets	78
4.2.4.2.2	SegNet	80
4.2.4.2.3	ResNet	81
4.2.4.2.4	FractalNet	81
4.2.4.3	Adopted Metrics	82
5	Results and discussion	85
5.1	SINC cloud-based healthcare architecture evaluation	85
5.1.1	The web interface usability test	86
5.2	Bilirubin Tool	87
5.2.1	Data Analysis Results	89
5.2.2	Discussion	91
5.3	Respiration Tool	93
5.3.1	Data Analysis Results	94
5.3.2	Discussion	96
5.4	Movement Tool	96
5.4.1	Data Analysis Results	100
5.4.1.1	MIA (Motion Infant Analysis) dataset	100
5.4.1.2	KPIs and MC Transition Matrix	101
5.4.2	Discussion	107
5.5	Semantic Segmentation	108
5.5.1	PIDS (Preterm Infants' Depth Silhouette) Dataset . . .	108

5.5.2	Data Analysis Results	112
5.5.2.1	Quantitative Evaluation	112
5.5.2.2	Qualitative Evaluation	115
5.5.3	Discussion	115
6	Conclusions and Future Works	119
6.1	Discussion	119
6.2	Thesis contributions	121
6.3	Future Works	123
	Appendices	125
	Appendix A	127

List of Figures

- 3.1 The current scenario. 19
- 3.2 The cloud-based healthcare infrastructure. 20
- 3.3 The patient monitor: Datascope Passport 2. 24
- 3.4 Time trend of the parameters extracted from the patient monitor. 27
- 3.5 The bilirubinometer: Ginevri One Beam. 28
- 3.6 The bilirubinometer driver interface developed in Python for
Ginevri One Beam input. 31
- 3.7 The transcutaneous bilirubinometer: Dräger JM-105. 31
- 3.8 SINC authentication. 35
- 3.9 SINC home. 36
- 3.10 SINC “Anagraphic Tool” - Patient’s registry. 39
- 3.11 SINC “Growth Tool” interface - Patient’s growth data. 39
- 3.12 SINC “Growth Tool” interface - Patient’s growth parameters. . 40
- 3.13 SINC “Growth Tool” interface - Patient’s growth graphs. . . . 41
- 3.14 SINC “Nutrition Tool” interface - Patient’s nutrition adminis-
tration. 43
- 3.15 SINC “Bayley Tool” - Automated Bayley test interface. 44

- 4.1 TcB hour-specific percentile nomogram. 53
- 4.2 TSB hour-specific percentile nomogram. 53
- 4.3 Nomogram for PT. Total bilirubin is plotted against PA in hours.
The groups of GA are represented with lines of different colours. 54
- 4.4 Nomogram for BET. Total bilirubin is plotted against PA in
hours. The groups of GA are represented with lines of different
colours. 55
- 4.5 Nomogram for BET in case of haemolytic disease. Total biliru-
bin is plotted against PA in hours. 55
- 4.6 Bilirubin Decision-Making workflow diagram. 60
- 4.7 Representation of the configuration scheme of the system. . . . 61
- 4.8 Followed pattern for preterm infants’ movements analysis. . . . 70
- 4.9 In figure 4.9a a depth frame from RGB-D sensor is shown. Fig-
ure 4.9b is the result of clustering process; it highlights 4 clusters
that correspond to the 4 infant’s limbs. 72

List of Figures

4.10	Different movements states in which infant can be in. Red rounds indicate the “in movement” limbs.	75
4.11	Longest path approach steps.	76
4.12	Illustration of the U-Net architecture. Image taken from [1]. . .	79
4.13	Illustration of the cascade of vanilla U-Net and shape regularization networks. Image taken from [2].	79
4.14	Illustration of implemented modified U-Net architecture.	80
4.15	Illustration of the SegNet architecture. Image taken from [3]. . .	80
4.16	Residual Unit. Image taken from [4].	81
4.17	Illustration of the FractalNet architecture. Image taken from [5].	82
5.1	SINC “Bilirubin Tool” interface.	88
5.2	SINC “Bilirubin Tool” interface - Risk Factors.	89
5.3	Screenshot of interface developed with the Qt Framework while it is running on Cubieboard2.	94
5.4	Example of respiration signal measured from RGB-D camera (blu line) and of the filtered signal (red line) on a time window of 10s.	95
5.5	Scatter plot and regression line of RR mean values.	95
5.6	“Movement Tool” graphic interface.	97
5.7	“Colour-map” of the movements extracted from the software. . .	97
5.8	“Movement Tool” graphic interface with velocity information. . .	98
5.9	“Movement Tool” interface screenshots that represent a sequence of fast movement 5.9a, slow movement 5.9b and the absence of movement 5.9c during a real-time acquisition.	99
5.10	“Movement Tool” graphic interface with extremities tracking. . .	100
5.11	States activation sequence during time.	101
5.12	Transition matrix \mathbf{P} of infant’s movements.	104
5.13	Temporal evolution of $\mathbf{P}(i i)$ probabilities related to each state.	104
5.14	Transition matrix \mathbf{P} of infant’s movements during different periods of the day.	106
5.15	Example of a PIDS Dataset positive instance. It consists of 16 bit original depth image (5.15a), 8 bit scaled depth image (5.15b) and the corresponding ground truth (5.15c).	110
5.16	Example of a PIDS Dataset negative instance. It consists of 3 images where the infant is not present in the frame: a 16 bit original depth image (5.16a), a 8 bit scaled depth image (5.16b) and the corresponding ground truth (5.16c), a completely black mask.	110

5.17	Example of a PIDS Dataset partial instance. It consists of 3 images where the infant is partially visible in the frame: a 16 bit original depth image (5.17a), a 8 bit scaled depth image (5.17b) and the corresponding ground truth (5.17c). Figure 5.17d is the corresponding RGB image used to facilitate ground truth annotation.	110
5.18	Example of a PIDS Dataset decentralised infant’s instance. . .	111
5.19	Example of a PIDS Dataset vertically positioned infant’s instance.	111
5.20	Example of a PIDS Dataset instance acquired when lights are very low.	112
5.21	Jaccard index trends over the 200 epochs for each CNN architecture.	113

List of Tables

3.1	Bedside-to-VISA protocol technical specifications.	26
3.2	Bedside-to-VISA protocol string.	26
3.3	Communication protocol of Ginevri One Beam.	30
3.4	Communication string of Ginevri One Beam.	30
3.5	HL7 Protocol	34
4.1	Evidence hierarchy from the centre for evidence-based-medicine.	52
4.2	Infants' characteristics (Gestational Age and Weight).	64
5.1	Database Traffic.	85
5.2	Database Connections.	85
5.3	Query Statistics.	85
5.4	Mean RR values measured by RGB-D camera and patient monitor.	95
5.5	Data results and KPIs.	103
5.6	PIDS Dataset infants characteristics (Gestational Age and Weight).	109
5.7	PIDS Dataset acquisition sessions and relative instances.	112
5.8	Jaccard and Dice indices of different CNN architectures.	113
5.9	Semantic segmentation results of different ConvNet architectures.	114
5.10	Jaccard Index results.	117
5.11	Qualitative result of prediction.	118
1	U-Net Indexes results.	128
2	U-Net2 Indexes results.	129
3	U-Net3 Indexes results.	130
4	ResNet Indexes results.	131
5	SegNet Indexes results.	132
6	FractalNet Indexes results.	133

Chapter 1

Introduction

1.1 Context

Technologic advances in neonatal intensive care and their impact on short term and long-term outcomes have been the major focus of neonatal clinical research. Neonatal mortality reached an unsurpassable minimum by the late 1990s. However, this has been associated with high rates of neonatal morbidity and neurodevelopmental impairment.

Preterm birth is defined as all births before 37 completed weeks of gestation or fewer than 259 days since the first day of a woman's last menstrual period [6]. Preterm births can be further sub-divided based on gestational age (GA): extremely preterm (<28 weeks), very preterm (28 - <32 weeks) and moderate preterm (32 - <37 completed weeks of gestation). Moderate preterm births may be further split to focus on late preterm birth (34 - <37 completed weeks).

Every year there are more than 15 million worldwide preterm births, that is more than 1 in 10 babies, and the number of cases continues to rise.

Prematurity is the leading cause of newborn deaths (babies in the first 4 weeks of life) and now the second leading cause of death after pneumonia in children under five years of age. It was responsible for nearly 1 million deaths in 2015. Three-quarters of them could be saved with current, cost-effective interventions. Many of the surviving infants face a lifetime of significant disability, including learning and motor disabilities.

Preterm birth affects the anatomical and functional development of all organs, inversely with GA, as well as the acquisition of skills for survival in an extra-uterine environment.

In the case of preterm infants and low weight infants, the risk of mortality and morbidity increases; typical complications linked to prematurity occur in infants of very low GA (between 23 and 28 weeks) and weighing less than 1 *kg*.

Across 184 countries, the rate of preterm birth ranges from 5% to 18% of babies born; 7-9% of pregnancies do not reach the normal 40-week gestation period; 1% of newborn babies come to light before the 32nd week of gestation

and 0.5% even before the 28th week.

In Italy, preterm births represent the 6.9% of the total birth rate; among the 40000 premature births born every year, 5600 have a body weight less than 1500 g. The care of these young patients, who would not be able to survive independently, require highly specialized staff and cutting-edge technologies. In the last five years, the development of biomedical technologies for intensive neonatal care has allowed the survival of patients born before the 23rd week of gestation and of a weight at birth less than 400 g. To date, the survival of preterm infants has even reached more than 90%.

The sooner babies are born, the less prepared their bodies are for the outside world. They need special care to overcome the following challenges:

- breathing: many preterm babies start breathing on their own when they are born, but others need to be resuscitated. If the lungs are not fully developed and lack surfactant (a substance that helps keep the lungs expanded), preterm babies may have difficulty breathing. Sometimes, premature babies that start off breathing are not strong enough to continue on their own. They exhaust themselves and may stop breathing (apnoea).
- brain: Preterm babies are at risk of bleeding in the brain, during birth and in the first few days after birth; about 1 in 5 babies weighting less than 2kg have this problem. Preterm babies can also have brain injuries from a lack of oxygen. Bleeding or lack of oxygen to the brain can result in cerebral palsy, developmental delays, motor impairments and learning difficulties.
- neonatal jaundice: it is caused by an accumulation of bilirubin (redish-yellow pigment present in the bile and produced by haemoglobin catabolism) in the subcutaneous tissue and in the sclere; when bilirubin exceeds the limit values, the newborn is placed under a UV light lamp that promotes the elimination of bilirubin from the blood to the intestine.
- cardiovascular difficulty: there is often a delayed adaptation of the circulatory system to post-natal life.
- feeding: Preterm babies can have trouble feeding because the coordinated suck and swallow reflex is not yet fully developed. They may need additional support for feeding. They often experience gastrointestinal difficulties and reduced food tolerances, so that additional support for feeding is needed: total parenteral nutrition (i.e., venous feeding) or gavage feeding (milk administration by means of an orogastric tube, which goes directly from the mouth to the stomach) is often used.
- infections: Severe infections are more common among preterm babies. Their immune systems are not yet fully developed, and they have a higher risk of dying if they get an infection.

- staying warm: Preterm babies lose body heat more easily, putting them at risk of life-threatening hypothermia. They need extra energy and care to stay warm and grow.
- eyes: Preterm babies' eyes are not ready for the outside world. They can be damaged by abnormal growth of blood vessels in the retina. The condition is usually more severe in very premature babies and if they are given a too-high level of oxygen. This can result in visual impairment or blindness.

As said, preterm babies are at risk of developing disabilities that will affect them for their entire lives, strongly depending on how early they were born, the quality of care they received during and around birth and the days and weeks that follow.

Hospitals with neonatal intensive care units can provide specialized care for preterm infants with serious health problems. They have special equipment and specially trained doctors and nurses who provide around-the-clock care for preterm babies who need extra support to keep warm, to breathe and to be fed, or who are very sick.

Preterm infants are housed in incubators or heated cribs, which provide temperature control and recreate the maternal uterine environment. Sometimes a "nest" with sheets is made inside the incubator to increase the sense of containment enjoyed by the baby in his mother's womb.

Continuous monitoring of the vital functions of the small patient is required, which will then be connected to multiple probes and devices that generate alarms whenever the limit levels set by the staff of the neonatal intensive care ward are exceeded.

The hospital ward taken into consideration in this thesis is the Neonatal Intensive Care Unit (NICU) of the Women's and Children's Hospital "G.Salesi" in Ancona.

Here, infants' cribs are surrounded by many devices for the monitoring, diagnosis and treatment of the above described diseases and all these devices provide a huge amount of data that was only displayed on monitors. A member of the medical staff, usually the nurse on duty, periodically transcribed these data in a paper medical record. Then the manual notes were regularly, but not immediately, transcribed by nurses in an electronic sheet on the PC of the neonatal unit with the risk of errors and forgetfulnesses.

In this context, physicians have expressed the need to automatically gather data from all these devices in order to ensure that no important details for patient care were overlooked, as they are aware that the automation of this process can facilitate and improve the implementation of the procedures of their daily clinical practice. In this sense they have also contributed to the development of innovative systems, methods and algorithms for the study of

some important healthcare problems related to preterm infants.

1.2 Objectives and main contributions

In the light of the above, the first objective of this thesis was to allow the interfacing and integration of biomedical instrumentation in the neonatal intensive care ward into a single cloud infrastructure that allowed the digital storage of all data from the various instruments.

In order to carry out optimal care processes, in fact, a maximum correlation and integration between all the physiological data collected by the instrumentation connected to the infant was required. Often the critical clinical situation is caused by a combination of pathologies, therefore the interactions between several physiological parameters must be studied.

In particular, the developed architecture was tested with the integration of three different type of instruments located in the NICU of the “Women’s and Children’s Hospital G.Salesi”:

- Patient monitor;
- Bilirubinometer;
- Transcutaneous bilirubinometer.

Medical communication protocols are used to enable the communication and data transfer between the above mentioned infant’s monitoring devices and the unique database of the platform. For this purpose, Python drivers for input devices are being developed in order to communicate with the devices and acquire data.

Then, a process of data collection from different instrumentation was carried out by standardising the data and by forwarding them to the cloud, through import Web Services. A system built with these characteristics guarantees the interoperability property of the collected data allowing on-line sharing of the data.

At this point, another objective achieved by this thesis was to provide the medical staff with a valid tool to visualize this enormous amount of data. Data visualization plays a fundamental role in the interpretation of data. The visualization does not simply have an aesthetic purpose of presenting the results, but gives access to information and interpretations that otherwise would remain latent. For this reason, a web interface has been designed and developed based on specifications given by healthcare personnel and medical guidelines. It acts like a web-portal and works as an application on Mobile Devices and Desktop Workstations, where medical staff members can access all available information.

Moreover, it is equipped with the main characteristics of the patient clinical record, but it exceeds the functionalities of a simple Electronic Medical Record

(EMR), thanks to the development of innovative clinical tools, which contain functionalities, data analysis techniques and decision-making algorithms, useful to speed up and facilitate the work of doctors. These tools allow them to follow guidelines of daily clinical practice more closely, by automating steps and medical procedures, with the aim of improving patient care.

The processing of the data displayed on these clinical tools is, in fact, the result of decision-making systems, whose development and implementation is a further objective of this thesis in order to support the early diagnosis of diseases.

In particular, an algorithm has been developed to support the diagnosis of neonatal jaundice and the management of therapies to treat the disease. It consists in an evidence-based automated decision support system (DSS) for guideline based care to facilitate the implementation of clinical practice guidelines for neonatal jaundice.

Another proposed algorithm supports the physician in fluid administration within nutrition task, another allows the automation of a clinical test used in follow-ups to assess the development of preterm infants.

Worthy of note is the implementation of an algorithm deployed to analyse preterm infants' respiratory rate, which is able to activate an alarm signal when respiratory rate values go out of the physiological range, and of a method that, through computer vision techniques and machine learning algorithms, is able to detect infant's movements in real-time from depth stream and to extract from the sequence of depth images, collected by an RGB-D sensor, some important features and indicators that can be used by clinicians to objectively study infants' movements during their development.

The validation of these algorithms was made possible only thanks to the creation of a new device, another objective achieved in this work. It is a novel non-contact and non-invasive RGB-D system that consists in an RGB-D camera and in an embedded board, where the algorithms used to extract and analyse data from the depth images acquired by the camera are run in real-time.

All the above described solutions and algorithms have been validated through a series of experiments, conducted in the NICU of "G.Salesi" Hospital under the careful supervision of the Head Physician, Prof. V. P. Carnielli, which have also led to the creation of two datasets.

The work of this thesis is culminated in the funding of a regional project, named SINC, made in collaboration with the "Women's and Children's Hospital G. Salesi" of Ancona, as the coordinator of all the regional Neonatal Intensive Care Units, and where the Head Physician, Prof. V. P. Carnielli, a neonatologist of international fame, is the scientific director and validator of technological solutions, the Departments of Information Engineering and of Industrial Engineering and Mathematical Sciences of the Polytechnic University

of Marche and four local companies. SINC “System Improvement for Neonatal Care” project started in January 2017 and will last three years.

The objective of the SINC project is to develop an innovative integrated system that allows an enrichment of the instrumentation available for neonatology and that will be able to automatically communicate the data to a cloud in order to guarantee the distribution of information and protocols of care on the territory, creating a new regional organizational model, on the basis of that developed in this thesis for the NICU of “G. Salesi” Hospital.

One of the project’s objectives is to manage a cloud infrastructure that makes services and utilities available throughout the region and that is able to integrate monitoring data collected by medical devices to facilitate patient diagnosis and treatment. The aim is to create and experiment a new hospital and territorial model for the integrated management of neonatal care and therapies between the various levels of hospital specialization in the Marche Region, which will be supported by distributed data management systems.

1.3 Structure of the thesis

The thesis is organized in six Chapters, which describe the design and development of a healthcare infrastructure that has allowed the interconnection of several biomedical devices in a NICU and the communication of data coming from these instruments to a single DB, which is exploited in order to permit the automatization of the process of device data collection, transmission, storage, processing and availability for medical staff.

Chapter 2 reviews the state-of-the-art about the main topics addressed. It discusses the results achieved in the creation of distributed healthcare infrastructures for the integration of medical devices in hospital wards and the problems still outstanding in this regard, and then goes into more detail on the current situation regarding the development and use of Electronic Medical and Health Records, Evidence-Based Medicine and Decision Support Systems in general and particularly in Italy and in the Marche region.

Chapter 3 describes the proposed cloud-based infrastructure, that allows the communication between the three different type of medical devices of the NICU of the “Women’s and Children’s Hospital G.Salesi” through communication protocols that are thoroughly described, and the developed web-based platform, where data coming from these instruments can be displayed and analysed.

The functionalities of the implemented tools of the platform are briefly described in this Chapter, while in Chapter 4 the attention is focused on three of these tools, which have seen the application of decision-making algorithms and computer vision techniques applied with the aim of support physicians in everyday clinical practice.

Chapter 5, then, discusses the results related to the analysis of the data collected by the various instruments and stored in the various platform tools, which are processed using the algorithms described in the previous chapter through a series of experiments conducted within the NICU.

Finally, conclusions are reported in Chapter 6, as well as some future research directions.

Chapter 2

State of the art

Medical devices generally are monolithic units so that a typical hospital room in an intensive care ward hosts a number of stand-alone devices, each one with its own user interface, its own proprietary software, its own display and often its own built-in computer. Graphical user interfaces are all different and non-uniform and this can create confusion and misunderstandings among the healthcare personnel who has to use all the devices simultaneously.

Moreover, the devices are physically separated blocks and they can also be located on different bed sides so that the medical staff has to go from one device to another to use it, e.g., to see data on device display, to change device settings and to set up new vital parameters or new alarm values. In this way, the staff has to deal with different interfaces implemented on devices located in different places, which contributes to create mental confusion and poor organization and makes it more difficult for the physicians to rapidly take stock of the situation on the patient's state of health. Furthermore, in a hospital ward there are many figures with different roles, e.g., the head physician, specialists in various fields and nurses, and each of them needs a tailored user interface suited to his own expertise and that shows him device data and information in the most suitable way to make him perform his job well and quickly.

Finally, around patient's bed there are devices for the monitoring, the diagnosis and the treatment of different diseases and it would be appropriate to bring together data coming from all these devices to ensure that the physician could have a general idea about the patient's health conditions in order to not neglect any important detail for the patient's care. On the contrary, data are usually saved separately for each device and they are not always sent to the patient Electronic Medical Record (EMR), if it exists, so that it becomes difficult to search and find them, to create correlations between them and to make them available in real time to the clinician when he is visiting the patient, whereas this would bring great benefits to medical research [7].

Nowadays many devices already have some connection mechanisms that use serial ports, Ethernet, IEEE 802.11 or Bluetooth wireless, but they are typically used to unidirectionally log data and events from these devices towards

the computer, permitting the reading of the measured value on a PC display. However, this is no longer sufficient: as demand increases for better health-care paradigms, it is evident that there is the need of having integrated and cooperating (interoperable) medical devices. Thus, the goal is to go beyond the simple connectivity to move towards a more complex device integration that offers the possibility to stream device data directly into electronic medical records (EMRs), to create a database for further statistic investigations of data so collected and to integrate the information derived from multiple medical devices into a single customised display.

In this thesis, a cloud computing solution is proposed for the creation of a cloud infrastructure that exceeds the simple EMR. A cloud-based DBaaS (Database-as-a-Service) is created with the abilities of storing and cooperatively sharing medical data based on the HL7 message required for interoperability of medical information of different types. A database is created serving as a data consumer which allows the integration between device data, EMR data, personal patient's data, patient's medical history and so on. This permits to aggregate device data in one place, making easier the recorded data maintaining. This facilitates data searching in order to allow the doctor to make faster diagnosis, by having all relevant information available. Moreover, the identification of statistical trends and patterns is simplified by using data mining and machine learning techniques that can lead to the discovery of correlations between collected data and illnesses, which otherwise would not have been possible to observe by clinicians [8] and that could be an useful tool to support a long-period management of a university hospital [9].

2.1 Health Information System Infrastructures

Health Information Systems (HISs) can be described as the interaction between individuals, processes and technologies used to support fundamental information operations, management and availability, with the aim to improve healthcare services [10].

They provide information and enhance the knowledge creation in health care environments through data processing [11]. In particular, they are considered mechanisms for storing, processing, analysing and transmitting information required for planning, organization, execution and evaluation of health services.

The above depicted scenario presents the opportunity to create an integrated cloud-based network that automates the process that begins with data collection from multiple devices and ends with information accessibility from medical staff. To achieve this goal diverse cut-edge technologies were studied.

In the past, the healthcare information systems have been extensively implemented with traditional Management Information System (MIS) mode, but

this does not comply with the current requirements of healthcare system. Lee et al. in [12] propose a service-oriented architecture (SOA)-based system that permits the integration of data from personal health devices and the creation of tailored users interfaces, but this work does not provide concurrency or constant and reliable service capabilities. Kulkarni and Ozturk in [13] implement a system called mPHASiS that leads to an end-to-end solution. Nonetheless, it is based on the Java programming language that makes the system less efficient for reasons of performance of Java Virtual Machine (JVM).

The proposed solution is based on the idea of cloud computing with which it is possible to provide customers with pervasive, affordable and on-demand services. Cloud computing owns the characteristics of parallel computing, distributed computing, and grid computing, but it improves the user experiences over the Internet compared to these. Lots of applications are moved towards a cloud platform because it is able to supply services for diverse application scenarios [14, 15]. Nowadays, also lots of works on medical information systems are based on cloud services [16, 17]. Cloud infrastructure can provide the flexibility and scalability of service-oriented systems unlike the transaction-oriented MIS mode.

The proposed model provides support to ad hoc integration of diverse medical devices, distributed processing, and open accessibility. A cloud-based infrastructure is presented where medical devices are plugged in and begin to cooperate, i.e. to collect and transmit data. The computer resources achievable with this environment are set up to receive, store, process, and distribute the information. The method described in this thesis permits the creation of an ad hoc integration network of different medical devices and of a distributed data processing.

The main requirement of the optimal solution is that it has to quickly implement the methods to collect process and distribute infant's vital data, from the crib to remote accessibility, by integrating all different medical devices [18, 19].

Moreover, it has to be flexible and extensible, i.e., it has to hold up diverse medical devices in different numbers that can be added to the system in different times [20]. Then, the proposed system has to guarantee the security and the safety of shared data, by ensuring strong access control and data encryption [21, 22].

To ensure data interoperability [23] it is necessary to realise data extraction process from various instruments, normalising the database according to a record format defined in the XML language and specifically to the logic related to language HL7 [24]. A database made with these characteristics enables online sharing of encrypted healthcare data, reported in a standard language, allowing a complete interoperability of shared data.

The architecture has to guarantee also the system availability in any possible

operational conditions, by ensuring its reliability [25] and it has to be scalable and compatible with the use in large healthcare environments and with the aggregation of different institutions [26].

In King et al. [27] they discuss about all these main problems and about their possible solutions with respect to the creation of a distributed architecture for the integration of medical devices in a hospital ward. They discuss about interoperability of data collected from devices, displays and databases of different vendors and about standardisation of device data streams and their reliability, security and safety, also in terms of privacy. However, the work is not concentrated on concrete solutions, leaving room to other works for putting into practise the proposed ideas.

2.2 Electronic Medical Records and Electronic Health Records

All health information systems, as well as many other technologies, can be interfaced with a systematic collection of information: the electronic medical record (EMR).

The medical record is the tool used to manage patient's clinical data, which are collected during meetings with healthcare professionals for prevention purposes, or when episodes of disease occur.

EMR is therefore the electronic evolution of the classic paper-based medical record, which has lost its effectiveness because the continuous improvement of the treatment process has led the paper version to become increasingly voluminous and easily damageable, with a wide variety of sources from which to obtain documents and information, and has made it more difficult to consult and find the necessary information for healthcare professionals in a timely manner [28].

Moreover, handwritten medical records may be lowly legible, and this can contribute to medical errors. Some pre-printed forms and the standardization of abbreviations were stimulated to improve reliability of paper-based medical records, but without remarkable results.

Thus, EMR may help with the standardization of digitized forms, terminology and data input in order to facilitate the collection of data for epidemiology and clinical studies [29].

The EMR can enable information to be used and shared over secure networks through digital formatting; track care (e.g. prescriptions) and outcomes (e.g. blood pressure); trigger warnings and reminders, send and receive orders, reports, and results; decrease billing processing time and create more accurate billing system; enable information to move electronically between organizations [30].

As regards interoperability, EMRs would facilitate the coordination of health-care transfer in non-affiliated healthcare structures [31]. A lot of information is conveyed in the EMR which can include laboratory results, radiology results, pharmacy orders, medical prescription, discharge/transfer orders and any other data from auxiliary services. In this way, some EMR-based systems are capable of automatically monitoring clinical events, by analysing patient data to predict, detect and potentially prevent adverse events. Furthermore, data from an EMR can be used for statistics on issues such as quality improvement, physicians' self-audit and resource management.

The EMR, actually, is the patient record created by providers for specific encounters in hospitals and ambulatory environments and it is limited to a single healthcare structure. It can serve as a data source for the electronic health record (EHR). The terms EHR and EMR, in fact, have often been used interchangeably, although differences between the models are now being defined [32, 33].

The EHR is a more comprehensive collection of the electronic health information of individual patients or populations. It is a more comprehensive form involving integration and network access of data from different clinical applications and heterogeneous systems.

According to the definition of the International Organization for Standardization (ISO) the EHR is a repository of patient data in digital form, stored and exchanged securely, and accessible by multiple authorized users [34]. It contains retrospective, concurrent, and prospective information and its primary purpose is to support continuing, efficient and quality integrated health care.

EHR should contain, for each patient, all information resulting from their interaction with different healthcare professionals, hospital wards and structures in order to facilitate an integrated vision of patient data [35]. It grows over time: it self-feeds, preserves and organises the complete collection of personal health history.

Main requirements of an EHR include the definition of a flexible data structure to allocate information in each patient's profile, of a clinical information registry concerning subsequent consultations and prescriptions, and of a repository of all medical and clinical history individualized and complete [36].

A system that manages the EHR must be able to meet three main demands:

- the integration of data from different sources (e.g. hospitals, private clinics, health care professionals);
- the correct acquisition of data;
- support for clinical decisions.

These interlinked characteristics within the EHR permit to achieve the goal pursued by the system: patient care. In order to achieve this goal, however, the EHR must also have interoperability characteristics, since processed data come

from different sources and are produced autonomously [37]. It must ensure the integration between different types of information (e.g. clinical, financial, administrative data) and not be limited in geographical terms, because it must link the various access points of users (general practitioner, physicians, healthcare professionals, and patients) and the different healthcare structures [38]. It should also ensure the integration of data provided by the various EMRs to obtain what IHE (Integrating the Healthcare Enterprise) calls a “longitudinal” view of the health status of individual patients.

In Italy, EMRs are quite widespread, but only within individual hospital wards and they are used more administratively than clinically.

According to a survey [39, 40] conducted in 2016 by the Healthcare Information and Management Systems Society (HIMSS), that has created the EMR Adoption Model (EMRAM), an eight-stage model that permits to assess the quality of the adopted EMRs on a scale from 0 to 7, in Italy the 6th level EMR covers only the 2,2% out of a total of 135 EMRs evaluated by HIMSS, while there are not 7th level EMR, compared to the 8,6% and 2,9%, respectively, in the Netherlands (total = 35) and the 32,7% and 6,1% in the USA (total = 5478). The majority of the Italian healthcare structures are placed on stage 5 (34,8%) and 2 (34,1%) and the 6,7% still occupy stage 0 compared to 0% in the Netherlands and to 1,6% in USA.

There are many reasons for this situation. In fact, even if the EMR spread requires infrastructure investments, which are still lacking, the painful point is the lack of confidence, if not resistance, that healthcare workers show towards the EMR. On the one hand, a cultural and “self-protection” resistance to the transparency of the data that the EMR sets in motion, and on the other hand - even more significant - a technological approach that does not make the EMR confident with the doctor, especially if it is in situations of urgency and speed. Doctors often denounce the adoption of complicated and redundant technological procedures, heterogeneous levels of integration, overlapping programs, excessive access and safety filters, which make “complex” the use of the EMRs [41, 42, 43, 44].

In any case, even Italy is increasingly moving towards the digitalization of the medical record, especially after the enactment of the Article 12 of Act 221/2012 that officially introduced the EHR, called “*Fascicolo Sanitario Elettronico*”, defined as “*the set of data and digital documents relating to health and socio-medical information produced by current and past clinical events concerning the patient*” [45]. Under Article 12.2, the EHR can be used for a triple purpose:

- a prevention, diagnosis, treatment and rehabilitation;
- b study and scientific research in the medical context;
- c health planning, verification of the quality of care and evaluation of healthcare.

Moreover, the n. 237 of October 2017 of the Official Gazette contains the publication of Circular n. 4, “*Documento di progetto dell’Infrastruttura Nazionale per l’Interoperabilità dei Fascicoli Sanitari Elettronici (art.12 - comma 15-ter – D.L. 179/2012)*”, available in the transparency section of the website of the Italian Agency for the Digital Agenda (AgID) [46], where EHR characteristics, its objectives and structure are illustrated in the light of the latest legislative changes affecting it.

The results of Government and regions efforts to promote the EHR can be seen in the following percentages: in 2015, the 40% of reports and the 9% of medical records were dematerialised; according to Federfarma, the 72% of medical prescriptions were dematerialized, up sharply from 26% in December 2014; the 16% of the reports were delivered online to the citizen, while bookings and payments made via the web were 12% and 8% respectively. The share of those who have heard about EHR (32%) doubled compared with the previous year, even if only 5% have actually used it, considering that at the moment, according to AgID data of April 2016, only six Italian regions have an EHR already active and operational (Emilia-Romagna, Lombardy, Tuscany, Sardinia, and Valle d’Aosta), while in 11 others, including Marche Region, regional EHRs are being implemented.

As mentioned above, the Marche Region is also making progress in disseminating the guidelines concerning the regional EHR infrastructure, with the aim of illustrating all the integration services envisaged in this area, in order to facilitate future suppliers of systems that will interact with the regional EHR in the implementation of integration interfaces [47].

On the basis of this document and those mentioned above, a web-based solution was therefore designed and developed, which allows the integration of data from different devices with those from the medical record. This solution was achieved by considering and preparing the communication with the regional EHR.

The final and future objective is, in fact, to go towards the creation of a network that includes all neonatologies of the Marche region, favouring the sharing of health data and the coordination of their flows, in order to facilitate transfers between the different hospital structures, which may take place after a first analysis of the patient’s vital signals has already been made by the reception centre, and, vice versa, to allow the continuity of monitoring of the newborn once from the central hospital (“G. Salesi”) is transferred to a neonatology that is closer to his parents’ residence to end there the last days of hospitalization.

The database created is also available for a “transversal” interoperability with all the colleagues who have need of continuity of care with respect to the same patient, and “vertical” interoperability with other databases and Na-

tional Health Service (NHS) operators. All services are backed by a guarantee for the highest security of data, encrypted both during transfer and storage, and access, in compliance with current legislations in terms of security and privacy, is strictly permitted only to those who have the appropriate permissions. Users can remotely access patient data, using both the PC and mobile devices (smartphones and tablets).

2.3 Evidence-Based Medicine and Decision Support

Evidence-based medicine (EBM) aims to improve quality of care reducing the wide healthcare practice variations, and the inefficiencies, dangers, and inequalities that have resulted from nonoptimal patient care as pointed out in “Crossing the quality chasm” by the Institute of Medicine [48].

EBM originated in 1992, from a series of studies started more than 10 years earlier at the Department of Clinical Epidemiology and Biostatistics of the Canadian McMaster University for the best use of scientific literature for medical updating.

From these roots, the EBM has developed the concept that “evidence” must play a leading role in therapeutic decisions, meaning with the term “evidence” up-to-date and methodologically valid information from medical literature. Originally defined as “*a new emerging paradigm for medical practice*”, the EBM received, four years later, a more cautious definition: EBM is “*the conscientious, judicious and explicit use of current best evidence in making decisions about the care of individual patients*”, then recognizing the need to integrate “evidence” with individual clinical skills of the healthcare professional (“expertise”) [49].

EBM has developed in two areas of application: public health macro-decisions or related to homogeneous population groups and individual patient medical practice.

EBM use has been approved by international healthcare organizations such as the WHO and the Institute of Medicine. but it has resulted to be far from easy to implement. About thirty years after its birth, it has so far found little application, especially in Italian clinical information systems. While there are several free or pay websites where clinical evidence and guidelines can be found and used, there has been no software integration between these sources and patient clinical data.

One of the tools used for the practice of EBM is Clinical Decision Support defined as “*providing clinicians or patients with computer-generated clinical knowledge and patient-related information, intelligently filtered or presented at appropriate times, to enhance patient care*” [50], where clinical knowledge means, for example, the evidence contained in up-to-date guideline recommen-

datations.

Clinical Decision Support Systems (CDSSs) are interactive software, very important within the medical industry, designed to assist doctors and other healthcare professionals (e.g. nurses) in the formulation of diagnosis, treatment decisions and management of therapies, through the collection and the elaboration of information coming from several sources.

In fact, knowledge-based CDSSs apply rules to data to be analysed by models or other methods via an inferential motor and provide results to the end user.

There are many different clinical applications in which CDSSs are used.

They can be used to warn changes in patients' condition from patient monitor data analysis [51], to help the evaluation of the clinical guidelines used to assist physicians in finding alternative treatment and diagnosis [52], or to identify similar factors between different cases that lead to complications [53].

A CDSS is used in a diabetic clinic to determine if a diabetics treatment would be safe given patient history, laboratory test results and known allergies and pathologies of a diabetic patient [54].

Generally, when a patient's case is complex or the healthcare professional who has to make the diagnosis is inexperienced, a CDSS can support to decide which is the therapeutic treatment to be suggested based on up-to-date treatment guidelines.

CDSSs are also used extensively in Neonatal Intensive Care Units (NICUs), given the very critical conditions in which small patients live and the many ethical problems associated with them.

In [55] a prototype of integrated eXtended Markup Language (XML)-based CDSS is implemented in a NICU, with the aim to evaluate the effectiveness of real-time decision support and of the longterm impacts on physician decision-making. In [56] it is used to define, detect and generate clinical alerts from collected medical device data.

In [57] a decision-making support system based on specific outcome information for individual NICU patients is used to provide support for parents and healthcare professionals in ethically determining and deciding which treatments to perform.

In [58] a web services-based infrastructure to support CDSSs for processing multi-domain medical data from obstetrics, perinatal and neonatal hospital wards is proposed. It is used to reduce medical errors, to assist physicians in decision-making process, to improve patient care also by the optimization of alert detection systems.

In Italy, CDSSs are still not very widespread, while in the rest of Europe and North America they represent a growing phenomenon.

The report "Clinical Decision Support Systems Market by Component (Services, Software), Delivery Mode, Product Type (Integrated, Standalone), Model

(Knowledge-Based), Type (Therapeutic, Diagnostic), User Interactivity (Active, Passive), Application - Forecasts to 2021”, made by MarketsandMarkets [59], studies the global clinical decision support systems market over the forecast period of 2016 to 2021. This global market is expected to reach USD 1.519,2 Million by 2021 from USD 856,3 Million in 2016, at a CAGR of 12.2%.

The cause of this lack of diffusion in italian healthcare system is due to physicians’ aversion and to a great distrust of technology and CDSSs use as underlined in [60], but also to the lack of a passage in the current legislation (which is instead foreseen in many European and extra-European health systems, starting from Belgium, the Netherlands and the United Kingdom) or which “the practice of the health professional” is explicitly encouraged to use a scientifically based CDSS (guidelines and good practices).

Despite this, having ascertained the excellent results deriving from the use of CDSSs in clinical practice, they are beginning to spread also in Italy in various fields of clinical application [61, 62, 63].

In fact, the results of the study conducted in [60] suggest that the CDSSs adoption path is marked by a progressive evolution of clinicians’ perceptions towards the system. A trend is emerged which moves from positions that are adverse to the adoption of CDSSs - characterized by strong resistances and a very little “perceived mastery” - to an hoped optimal situation, in which CDSSs are seen as a working tool at the service of clinicians, integrable (and not interchangeable) with their skills, adaptable to their needs and to the local organizational specificities.

In this thesis, decision-making models and algorithms are applied in the NICU environment to preterm infants’ data in order to generate alarms from the analysis of medical devices data, to help physicians in the administration of nutrients and in the diagnosis and treatment of neonatal jaundice, and to support the prediction of neuromotor disabilities from depth images as shown in next chapters.

Chapter 3

A new infrastructure for neonatal care

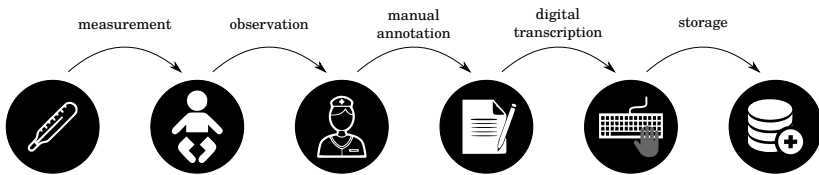


Figure 3.1: *The current scenario.*

The hospital ward that is taken into consideration for testing the new infrastructure is the Neonatal Intensive Care Unit (NICU) of the “Women’s and Children’s Hospital G.Salesi” in Ancona, where preterm infants are taken into care [64]. As said, preterm birth affects the anatomical and functional development of all organs, inversely with GA. The degree of organs immaturity is a critical aspect for these babies, which leads them to have many health problems. For this reason, the primary physiological functions of these babies have to be continuously monitored and often infants have to undergo major treatments and therapies. Hence, infants’ cribs are surrounded by lots of devices for the monitoring, the diagnosis and the treatment of different diseases. It is desirable that all these devices communicate between each other and with a unique database in order to create an integrated device network.

Nowadays, on the contrary, the majority of these devices only provide the ability to read data on their digital displays. Consequently, a member of the medical staff, generally the nurse in charge, has to collect infant’s data at bedside by writing them down to a paper medical chart on a regular basis. Then manual notes are regularly, but not immediately, transcribed by nurses in a PC of the Neonatal Unit. After that, data are transmitted to a local server that stores and organizes them together with the patient data collected in the EMR. Only at this moment, the medical staff can access data through an interface application. Focusing on the problem of infants’ vital data collection,

distribution and processing, it is clear that current solution based on manual note writing is a slow and laborious process, susceptible to errors in the two phases of manual taking notes and of digital transcription on EHR. Moreover, there is an important delay between data generation and their availability and accessibility to medical staff. Fig. 3.1 shows this process based on manual taking notes.

In this thesis, a method to make automated and faster this process that starts from crib data gathering and ends with the remote access to data by clinicians is proposed. Medical communication protocols or proprietary software are used to automatically enable the communication and the data transfer between the devices and the unique database, which collects data from all medical devices.

3.1 SINC cloud-based healthcare architecture

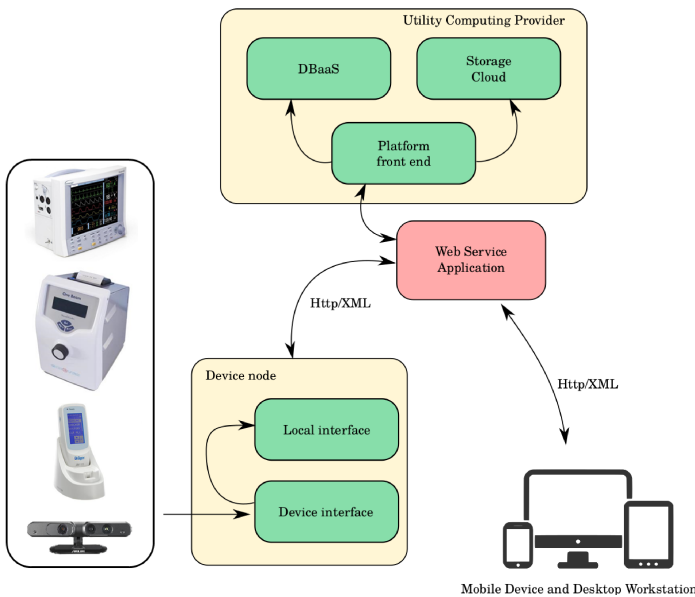


Figure 3.2: *The cloud-based healthcare infrastructure.*

Fig. 3.2 shows the implemented system architecture that allows the developing and the deploying of the process automation of data collection, storage, processing and distribution through a medical device network that uses cloud computing.

At the preterm infant's crib there are device nodes that are provided with hardware components such as serial port or USB port, forming the device inter-

face, and with software to collect, encode, encrypt and transmit data through configurable communication channels to be stored, forming the local interface. Data are picked up through applications of extraction, specifically concerted for every different type of devices, which use medical communication protocols or proprietary software to enable the direct data communication and transfer.

After extracting and standardising into XML, through Web Service of importation, data are carried to the cloud database, where they are aggregated.

For security reasons, both during the import process and the storage phase in the aggregate DB, data are encrypted and accessed, using “strong” credentials as well as other medical authorities (or other health professions, as far as relevant information about an individual is concerned) authorized by the physician.

The intrinsic interoperability, obtained by using different device types and vendors and language independent XML technologies and the widespread HTTP as a transport, implies that devices can communicate each other and with the EHR by using Web Services [65].

Web Services, in fact, are web application components that permit the interoperability between different technologies that work in a same network. These services hide their internal complexities such as data types and business logic from their users, but expose their programming interfaces and their locations using UDDI (Universal Description, Discovery, and Integration) protocols. They make available a software interface, described in a format which can be automatically processed, which permits the interaction between other systems and the Web Service itself by activating the functions available on the interface (services or requests of remote procedures) through special “messages” of request. Such request messages are included in an “envelope” that is formatted according to the standard XML, encapsulated and transported via Web protocol. In our case, the XML-based language for describing Web services application software interface is Web Services Description Language (WSDL), which is recommended by the World Wide Web Consortium (W3C). These interfaces, publicly exposed, guarantee the procedures of import data and access to the database by different authorized medical staff members for respective allowed functions. The XML-based protocol for accessing Web Services is Simple Object Access Protocol (SOAP), which is always recommended by W3C and the Web protocol on which SOAP operates is HTTP, the most commonly used and the only one that was standardised by the W3C.

Web services act like a broker between local medical devices and remote services. They are able to capture collected data from devices and to send them to suitable storage service hosted on cloud. They also allow the local storage for pre-processing, e.g., they allow data to be aggregated or simply analysed before the transfer to the main system.

On the other hand, Web Services work as an access point. Users through a web interface that acts like an application that works on Mobile Devices and Desktop Workstations, with which the hospital ward is equipped, can interact with data on the cloud database. Web Services receive requests from that interface to recover data from the cloud database.

The function of the Utility Computing Provider is to provide logical and physical infrastructure for data storage, processing and delivery services.

Its main components are the Platform front end interface, the Cloud Storage and the DBaaS (Database-as-a-Service). The platform front end interface is able to allow the management of the storage contents and to directly communicate with users. The interface can be a web client or a standalone application. The cloud storage is the model of data storage in which the digital data is stored in logical pools and it is based on highly virtualized infrastructure. Database-as-a-service [66] is one of cloud computing secondary service models and a key component of XaaS. This may be considered a subspecialty of the bigger Software-as-a-service model. In essence, DBaaS is a cloud database, which is a database that typically runs on a cloud computing platform. It is a cloud computing service model with which there is no need to physically launch a virtual machine instance for the database so that in such a configuration, application users do not have to install and maintain the database themselves. All of the administrative tasks, installation and maintenance are taken care of by the database service provider and application owners pay according to their usage.

3.1.1 Data Platform

The relational database for the storage and management of data is configured according to a structure optimized in terms of performance and zero data redundancy.

As DBaaS the Amazon Relational Database (Amazon RDS) for MySQL is used, since it makes it easy to set up, operate, and scale MySQL deployments in the cloud. The use of this DBaaS provides to the system all the features that we have discussed in section 2.1, which are the main requirements to obtain an efficient cloud-based healthcare infrastructure for medical device integration. It makes it easy to go from project conception to deployment. It is possible to access the capabilities of a production-ready relational database in minutes and without the need for infrastructure provisioning, and for installing and maintaining database software. It is possible to scale database compute and storage resources often with no downtime: the engine will automatically grow the size of database volume as database storage needs grow. It enhances reliability for critical production databases, including automated backups, database snapshots and automatic host replacement.

For security reasons, it allows data encryption both during the transit, with the use of SSL, and during the cloud storage phase. Also backups, read replicas and snapshots are encrypted. Moreover, data are accessible only by authorized medical staff members by using strong authorization. There is also the possibility to run database instances in a virtual private network.

3.1.2 Cyber Security

The legislation about the protection of personal data (Legislative Decree no. 30 June 2003 n. 196) provides (art. 31) a general safety requirement under which the personal data object of treatment should be kept and controlled, also in relation to acquired knowledge with the technical progress, the nature of the data and the specific characteristics of the treatment, so as to minimize, through the adoption of suitable and preventive security measures, the risk of destruction or loss, even accidental, of the data, unauthorized access or treatment not allowed or inconsistent with the purposes for collection.

The obligation to adopt the “minimum security measures” (arts. 33 et seq.) is also provided. In particular, (pursuant to art. 34) the treatment of personal data carried out with electronics instruments is allowed only if the following measures are adopted:

- computer authentication;
- adoption of procedures for the management of authentication credentials;
- use of a system of authorization;
- periodic update of the identification of treatment allowed to individual officers and employees for management or maintenance of electronic instruments;
- protection of electronic tools and data against illegal treatment of data, unauthorized access and certain computer programs;
- adoption of procedures for storing backups, restoring access data and systems;
- adoption of encryption techniques or identification codes for certain treatments of data disclosing health status or sexual life performed by health organizations.

Under these conditions, in Nu.Sa. data are subjected to protection with a “strong” encryption system that guarantees high degree of security; the assumption is that only the rightful owner - the licensed doctor - has access to the data of his competence through an authentication system (SSO Single Sign On) described below. The cryptography algorithm is held by a third party, the Polytechnic University of Marche.

3.2 Medical Device Network

In order to have continuous and multi-parametric monitoring of premature patients, a system has been developed based on the connection of several biomedical devices to the platform described above. Thus, the architecture was tested with the integration of three different type of instruments located in the NICU of the “Women’s and Children’s Hospital G.Salesi”:

- Patient monitor;
- Bilirubinometer;
- Transcutaneous bilirubinometer.

In the following paragraphs there will be a brief description of each biomedical apparatus listed above.

Furthermore, Python drivers for input devices are developed in order to communicate with the devices and acquire data. They work in a Linux environment, but were tested also on Windows OS.

Communication protocols, that allow the correct flow of data between the above mentioned infant’s monitoring devices and the platform, will be displayed.

3.2.1 Patient Monitor



Figure 3.3: *The patient monitor: Datascope Passport 2.*

Nowadays, patient monitors, commonly called cardiac monitors, are not limited to heart rate monitoring, but also control other important vital functions such as breathing rate, partial oxygen and carbon dioxide pressures in the bloodstream, temperature, pressure.

For this reason, it is preferable to call this instrument “monitor for the control of physiological activities”, as they provide signals useful for monitoring, but

not sufficient for diagnostics. Each parameter is detected by the relative sensor and processed through a set of special amplifiers and circuits; on the screen the trends of the parameters of interest are shown, a widespread application in intensive care units, including neonatal ones.

Associated with the derivation of the ECG (usually I or II) there is often an acoustic signal, activated by a certain threshold for the QRS complex: every time it is surpassed by this complex, there is a standardized beep, usually a pure 800 Hz tone, which indicates the beat.

In addition, patient monitors are equipped with an alarm system, whose thresholds for the various parameters monitored are set by medical personnel.

The patient monitor used in the NICU of “G.Salesi” hospital is the Datascope Passport 2 [67] represented in figure 3.3.

It detects the following parameters:

- Oxygen saturation, SaO₂ [%];
- Heart rate detected by the saturimeter [*bpm*];
- Heart rate detected by the ECG [*bpm*];
- Respiratory rate [*apm*];
- Systolic, diastolic and average pressures [*mmHg*];
- Esophageal temperature [*°C*].

3.2.1.1 Communication Protocol

To communicate with the patient monitor Datascope Passport 2 the Datascope Bedside-to-VISA for serial communication protocol is used.

The patient monitor transmits parameter data and waveform data in a packet format with a synchronization word at the beginning of each packet. The waveform data is in a binary format, the parameter data is in *ASCII* format. The parameter data is interspersed in the waveform data.

The patient monitor continuously transmits data in the following sequence:

- Instrument Identification
- Patient Data
- Alarm Limits
- Patient Data

This protocol specifies communication in one direction only, transmit. No data is received by the patient monitor.

Details of the RS232C interface are summarised in table 3.1.

The Bedside-to-VISA communication protocol consists of a 74 *byte* packet transmitted every 80 *milliseconds* (table 3.2). Each packet consists of two

Table 3.1: *Bedside-to-VISA protocol technical specifications.*

Item	Value
Baud Rate	9600
Parity	none
Stop <i>Bits</i>	1
<i>Bits</i> per character	8

Table 3.2: *Bedside-to-VISA protocol string.*

<i>byte</i> 1	<i>byte</i> 2	<i>bytes</i> 3 - 20	<i>bytes</i> 21 - 38	<i>bytes</i> 39 - 56	<i>bytes</i> 57 - 74
AA Hex	55 Hex	Data + CRC	Data + CRC	Data + CRC	Data + CRC

synchronization *bytes*, followed by four 18 *byte* packets. Each 18 *byte* packet is 17 *bytes* of data followed by 1 *byte* Cyclical Redundancy Check (CRC).

Each 74 *byte* packet contains the following information: 16 ECG samples (200 *Hz* sample rate), 8 samples of each of the three other waveforms (100 *Hz* sample rate), and sixteen characters from the parameter information described later in this document (200 characters per second transfer rate). Each waveform sample consists of 10 bits of data, each ECG sample also includes a pacemaker detect flag. The 74 *byte* packet is split into four 18 *byte* packets. The four 18 *byte* packets split the data up to provide 4 ECG samples, 2 samples of each of the other three waveforms and four characters from the parameter information.

The contents of each *byte* are defined in the Service Manual Supplement.

To check the correct transmission of data, the Bedside-to-VISA communication protocol provides at the end of the sent data string the insertion of 4 redundant control characters, called Cyclic Redundancy Check (CRC).

It consists in adding to the end of the transmitted data sequence redundant bits, so that the entire sequence constitutes a binary number that can be exactly divided by another fixed binary number, which must be the same for sender and receiver, in order to be able to check the integrity of the data by comparing the calculated CRC with the received one.

The CRC code, expressed in hexadecimal, is obtained by cyclically scrolling the input data in a logical network, taking into account not only the value of the bits, but also their position.

An algorithm for calculating the CRC on the received data was then implemented, so that it can be compared with the one sent by the patient monitor and thus verify the correctness of the received string.

This algorithm has been written by adapting the one reported in the Bedside-to-VISA communication protocol, i.e. the algorithm used by the monitor itself to calculate the CRC transmitted at the end of each sent string.

3.2.1.2 Patient Monitor Data

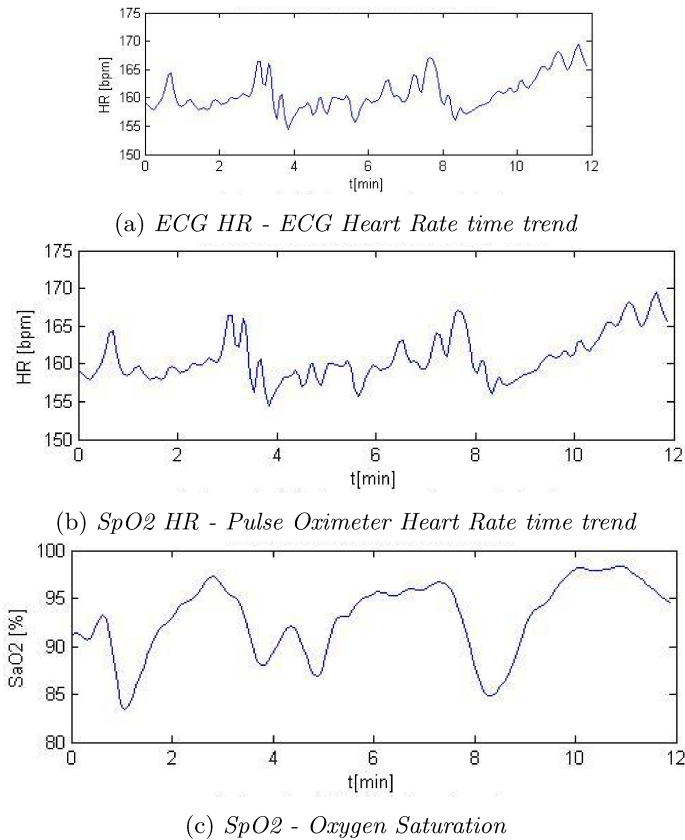


Figure 3.4: Time trend of the parameters extracted from the patient monitor.

By establishing the communication as described above, the following parameters are acquired from the patient monitor:

- SpO2, oxygen saturation;
- HR, the heart rate detected by ECG;
- SpO2 HR, the heart rate measured by the pulse oximeter;
- RR, Respiratory Rate.

Each response string received is used essentially for two purposes:

- Extract the parameters of interest in a log file;
- Extract the CRC (calculated from the patient monitor) to be compared with the CRC calculated using the algorithm implemented.

Figure 3.4 shows the time trend of some of the above listed parameters extracted from the patient monitor.

3.2.2 Bilirubinometer



Figure 3.5: *The bilirubinometer: Ginevri One Beam.*

The bilirubinometer is a biomedical instrument designed to achieve accurate total serum bilirubin concentration (TSB) measurements in newborns through the analysis of micro-blood samples with a heel puncture. Knowledge of accurate bilirubin levels is essential helping in the successful treatment of neonatal jaundice caused by bilirubin aggregation in various body tissues, skin in particular (classic yellow skin colour observed in jaundice patients). Bilirubin aggregation could involve brain tissues causing irreversible patient damage (kernicterus). Thus, newborns require constant monitoring of bilirubin levels.

Bilirubin concentrations are determined either by whole blood or serum analysis using spectrophotometric methods or by skin-reflectance measurements (section 3.2.3).

The three methods of spectrophotometric analysis are the direct spectrophotometric method, the Malloy-Evelyn method, and the Jendrassik-Grof method. Blood samples are required for spectrophotometric analysis. The analysis technique depends on both the type or types of bilirubin being measured and the age of the patient (neonate versus child or adult). The reflected light is generally split into two beams by a dichroic mirror, and wavelengths of $455nm$ and $575nm$ are measured by optical detectors.

Transcutaneous bilirubinometers do not require a blood sample. A light-emitting sensor is placed on the infant's skin (optimally on the forehead or

sternum).

The bilirubinometer used in the NICU of “G.Salesi” hospital is the Ginevri One Beam [68] represented in figure 3.5.

It allows for a prompt photometric analysis of bilirubin in the serum (conjugated and non-conjugated total) using a capillary tube as an optical cell. Bilirubin concentration is determined through a photometric measurement at $455nm$ and $575nm$ wavelengths: the first wave length indicates bilirubin levels while the second informs on any interfering agent presence, essentially haemoglobin. A mathematical model accounts for haemoglobin interference resulting in an accurate bilirubin result.

The HD OLED display indicates both bilirubin (mg/dl and $\mu mol/l$) and interfering agent (g/dl) values. One Beam uses a single optical beam projected onto a fixed point of the sample due to a particular automatic filtering system. The system achieves a “clean” light beam free of any disturbing frequencies reducing negative bilirubin photo-isomerization effects thus ensuring a stable signal. An accurate signal is also achieved as an only one point on the capillary tube is measured eliminating any errors observed in past generation devices with two measure points. Lastly a stronger signal results due to the use of a single rather than a split beam. A particular collimation and beam concentration system allows for reading results even with limited serum sample quantities obtained after centrifugation, as in polycythemia cases (up to 80% haematocritic levels) or partial capillary tube filling. Advanced microprocessor controlled electronic technology enables better signal processing transformed into the corresponding bilirubin level promptly indicated on the display. The printer enables quick printing of any test results.

3.2.2.1 Communication Protocol

In this case, the communication protocol is much simpler than in the previous case, since the bilirubinometer transmits only a parameter data in *ASCII* format and not a waveform data.

An example of *ASCII* output is: “GINEVRI ONE BEAM 09/11/16 11:19 BILIRUB. 06.7mg/dl EMO. 0.28g/dl” and in *HEX* is: “47 49 4E 45 56 52 49 20 4F 4E 45 20 42 45 41 4D 20 30 39 2F 31 31 2F 31 36 20 31 31 3A 31 39 20 42 49 4C 49 52 55 42 2E 20 30 36 2E 37 6D 67 2F 64 6C 20 45 4D 4F 2E 20 30 2E 32 38 67 2F 64 6C 0D 0A”.

The contents of each character are defined in table 3.3.

For the bilirubinometer to verify data integrity, the transmission of the same data unit is repeated 10 times.

In addition, the string is associated with the patient’s ID written on a barcode held in the infant’s crib. In particular, an algorithm has been developed that waits for the code to be read by a wireless barcode scanner and then for the

Table 3.3: *Communication protocol of Ginevri One Beam.*

#Byte	ASCII	HEX	#Byte	ASCII	HEX	#Byte	ASCII	HEX
1	G	47	23	/	2F	45	7	37
2	I	49	24	1	31	46	m	6D
3	N	4E	25	6	36	47	g	67
4	E	45	26		20	48	/	2F
5	V	56	27	1	31	49	d	64
6	R	52	28	1	31	50	l	6C
7	I	49	29	:	3A	51		20
8		20	30	1	31	52	E	45
9	O	4F	31	9	39	53	M	4D
10	N	4E	32		20	54	O	4F
11	E	45	33	B	42	55	.	2E
12		20	34	I	49	56		20
13	B	42	35	L	4C	57	0	30
14	E	45	36	I	49	58	.	2E
15	A	41	37	R	52	59	2	32
16	M	4D	38	U	55	60	8	38
17		20	39	B	42	61	g	67
18	0	30	40	.	2E	62	/	2F
19	9	39	41		20	63	d	64
20	/	2F	42	0	30	64	l	6C
21	1	31	43	6	36	65		0D
22	1	31	44	.	2E	66		0A

string from the bilirubinometer. At the end, the string that arrives at DB through REST API is visible in table 3.4.

Table 3.4: *Communication string of Ginevri One Beam.*

```

s : 4 : "data"; s : 230 :
{"
  "infantID" : 01315052601,
  "vendor" : "GINEVRI",
  "instrument" : "ONEBEAM",
  "datetime" : "6/06/1717 : 35",
  "timestamp" : "2017 - 06 - 1615 : 39 : 01.745882",
  "bilirubin" : 4.2,
  "bilirubinUnit" : "mg/dl",
  "hemoglobin" : 0.24,
  "hemoglobinUnit" : "g/dl"
}";

```

The interface of Python driver is visible in figure 3.6.

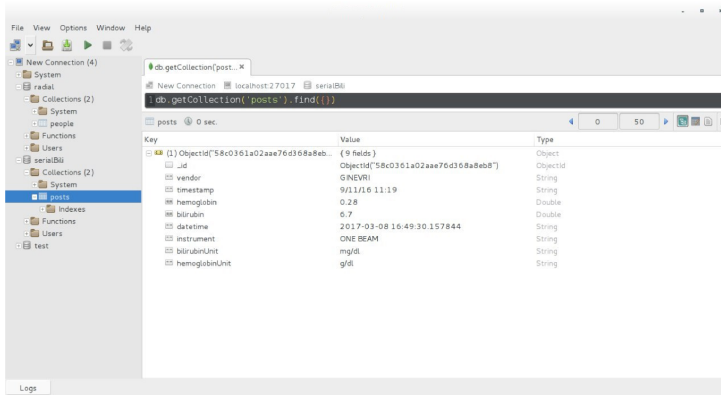


Figure 3.6: *The bilirubinometer driver interface developed in Python for Ginevri One Beam input.*

3.2.3 Transcutaneous Bilirubinometer



Figure 3.7: *The transcutaneous bilirubinometer: Dräger JM-105.*

The current gold standard to measure bilirubin levels is TSB concentration determination from a blood sample obtained by the use of bilirubinometers described above. Although over the years this method has been proven to be successful in preventing kernicterus [69], it has its drawbacks. Invasive blood sampling is painful and stressful for the neonate, resulting in blood loss and an increased risk for osteomyelitis and infections at the site of sampling [70, 71].

A possible alternative for invasive blood sampling is transcutaneous bilirubinometry, a noninvasive and painless method that provides an instantaneous read-out of the cutaneous bilirubin concentration (TcB).

Transcutaneous bilirubinometry is based on optical spectroscopy, which relates the amount of light absorption by bilirubin (i.e., the yellow color of the skin) to the concentration of bilirubin in the skin. The first transcutaneous bilirubinometer was introduced in 1980 [72]. Since then, several more devices have been developed, and important adjustments, such as the correction for the presence of other skin chromophores (i.e., melanin and hemoglobin), were made to improve their accuracy [73, 74, 75, 76, 77]. These “second generation” bilirubinometers are suitable for screening of hyperbilirubinemia, leading to a considerable decrease of the number of hospital readmissions [78] and a decrease of the amount of required blood samples from patients [79]. Hence, the use of transcutaneous bilirubinometers is recommended in clinical practice guidelines on the management of hyperbilirubinemia [80], but only as a first control measure for what concerns NICUs, as will be explained later in section 4.1.3.

The transcutaneous bilirubinometer used in the NICU of “G.Salesi” hospital is the Dräger JM-105 [81] represented in figure 3.7.

Dräger JM-105 has to be placed on the infant’s forehead or sternum, it directs white light into the skin and measures the intensity of the returning wavelengths. It analyses the spectrum of optical signal reflected from the neonate’s subcutaneous tissues: it measures hemoglobin, dermal maturity, melanin, and bilirubin, and then, by using known spectral characteristics of each of these components, subtracts all but the bilirubin to arrive at a measurement.

It has an integrated barcode scanner that can automate data entry, storing patient and nurse ID, medical record number, patient name, and date of birth. Automated data entry permits to save time and reduces the likelihood of manual input errors. In the NICU of “G.Salesi” hospital the infant’s barcode is read with the device incorporated scanner, while the rest of the data is entered with the keypad.

3.2.3.1 Communication Protocol

The communication protocol used by the Dräger JM-105 transcutaneous bilirubinometer is HL7 Standard Protocol.

The HL7 Standard was created and is maintained by Health Level Seven, an American National Standards Institute (ANSI) accredited Standards Developing Organization (SDO) that operates in the healthcare arena [82], consisting of hospital, vendor and consultant volunteers.

Initial efforts began in March of 1987 and continue to date. Now, the HL7 Standard is broadly divided into two categories – Version 2 (V2) and Version 3 (V3). The majority of HL7 messaging employs messages that use the 2.3 or 2.3.1 versions of the standard. Newer versions of the standard, including V3, represent only a small portion of real-world usage in interfacing.

HL7 design is based on a set of general goals. The first goal is to be supportive rather than prescriptive. This is an important philosophy and is absolutely necessary in the very heterogeneous health care computing environment. The second goal is that it be practical, which to the developers of HL7 means that it should function in a wide range of environments, from complex networks (e.g. a full seven level ISO type network) to simple terminal/host environments (e.g. *RS232* connection). The third goal is that the standard should accommodate site specific variations. This has been accomplished by allowing sites to create their own message types and record definitions. The fourth and final goal is to support evolutionary growth. This capability has been built in by requiring that changes to the record definitions be made only by adding fields and never by deleting.

The central paradigm of the protocol is the exchange of messages between applications that want to communicate. HL7 messages transmit data between disparate systems. An HL7 message consists of a group of segments in a defined sequence, with these segments or groups of segments being optional, required, and/or repeatable (referred to as HL7 cardinality). A segment is a logical grouping of fields containing data. The HL7 message type defines the purpose for the message being sent and is present in every HL7 message. Message types are identified by a three-character code, and are used in conjunction with a trigger event. An HL7 trigger event is a real-world event that initiates communication and the sending of a message, and is shown as part of the message type. Both the message type and trigger event are found in the MSH-9 field of the message. MSH segment is the first mandatory segment that gives information about the calling, receiving, triggering event, version of protocol used and so on. Each segment starts with three characters that uniquely identify the segment within the message.

Table 3.5 shows the message exchanged between the Dräger JM-105 transcutaneous bilirubinometer and SINC infrastructure.

It is an *OUL^R22* message type, that is an “Unsolicited Specimen Oriented Observation Message”, of 2.5.1 HL7 version, as it is possible to see from the MSH (Message Header segment).

The Patient Identification segment (PID) is used by all applications as the primary means of communicating patient identification information. In bilirubinometer message this segment contains the *id.code* (01315052601), described above, that is read by the barcode scanner incorporated in the device before the measurement.

The Observation/Results segment (OBX) is used to transmit a single observation. Here, there are 3 OBX segments: the first is used to transmit the value of the transcutaneous bilirubin measurement (5.5), the unit of measurement (*mg/dl*), the measurement date and time (20160309132951), the nurse

As already said, it is connected to the cloud database through WS-SOAP. It consists of a cross-platform solution that can be used with Windows, Linux and Mac, tablet Apple iOS, Android and Windows RT, while maintaining the same user interface. It is a simple and user-friendly interface that does not require special training. It is based on the paradigms of tablet and touch screen in order to minimize necessary interactions to access information and functions. Anyway, it is equipped with a user manual accessible through a click on the portal.

In addition, unlike the traditional medical records, mostly based on “pull” logic where the user needs to know what to look for, it adopts “push” logic where the system suggests to the user what to see and what actions to carry out on the basis of rules and clinical protocols.

3.3.1 Authentications, Authorizations and Privacy Policy

In the SINC architecture, authentication (user and password) is ensured by a system of Single Sign On (SSO). In the system, an algorithm is defined to establish the authorization in relation to the management for access to data clusters. The generation of credentials can be activated from SINC website, where one can also access the procedures for password renewal 3.8.

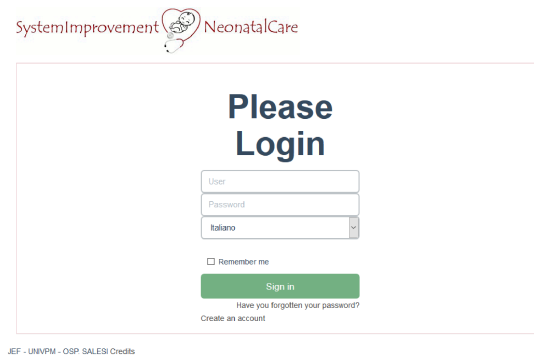


Figure 3.8: *SINC authentication.*

Data are encrypted using an encryption algorithm, both during the flow and storage phase in the cloud. The cloud system of SINC records the accesses to assisted records of the cloud; then each consultation-modification of the database in cloud is tracked completely, allowing one to go back to the information entry source and the time when the logging took place. The database in the cloud is available to physicians that, before being allowed access to the cloud data import service of SINC, must be registered at the portal, so that the proper credentials may be released.

Such credentials are provided during registration and are activated after the physician has agreed to a procedure sent via email. The credentials allow access to the database in cloud and its interoperability using tools made available by SINC.

SINC also provides a system that allows the authentication of infants' parents, permitting direct involvement of the user, aimed to encourage co-responsibility and empowerment policies. The patients parents will be provided with authentication credentials to access an area of the database in the cloud, functionally correlated with the record of care. In this area there is a section dedicated to the consultation of specific health records made available to the patients' parents directly by physicians, one for possible input of data, and still another where parents can manage the "Patient Summary" of their children (authorization/concealment of individual items).

3.3.2 Applications, Tools and Services

The web interface contains several tools and applications as figure 3.9 shows. Each tool has been developed with the support and the supervision of the NICU medical staff "G.Salesi" hospital in Ancona.

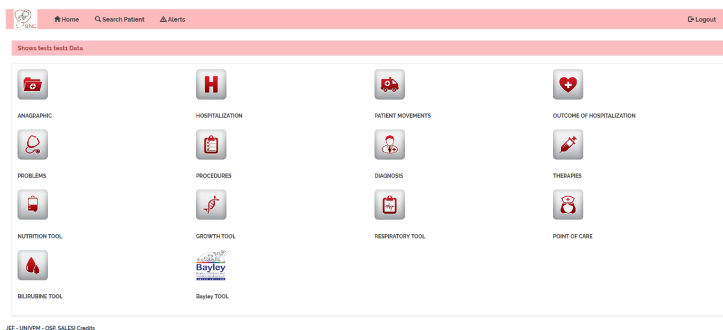


Figure 3.9: *SINC home*.

These applications interact with the DB through the SINC Web Services, supporting the physician in his professional activity, encouraging the improvement of his clinical practice and facilitating the implementation of certain care functions.

They are available to adapt clinical data of a single patient through algorithms that will be described in the next chapter, in the wake of the most recent evidence-based medicine (EBM) documents intended for diseases, including production at the "point of care" of clinical recommendations contextualized to the specific clinical case.

There are also systems for access to self-audit, that have been articulated into several functions, accompanied by benchmarking activities, to ensure and improve data collection quality.

Another important function is to allow an automatic data backup and disaster recovery. These are two aspects very important for physicians, in fact for disciplinary management and confidentiality of medical data, there are data saving procedures with allocated frequencies to avoid the risk of loss of the same data.

The electronic online platform automatically makes frequent backups, allowing full restoration of the database in real time, decreasing risks and responsibilities for the physicians. In addition, for initiatives of tele-diagnosis, tele-consultation, and tele-monitoring, the project offers the possibility to automatically insert reports, data and consultancies (always through web services). This occurs in well-defined locations of the patient record of the DB in the cloud, thus completing a “transparent” mode for the activities of a physician engaged in a professional service.

3.3.2.1 Clinical Tools

As said, SINC platform will consist of several tools, some of which are already fully developed and functioning, others being developed such as those relating to diseases and problems, diagnoses and therapies.

In this section the functionalities of the implemented tools of the platform, accessible from the SINC portal, are briefly described.

In the next chapter the focus will be on three of these tools, which have seen the application of decisional algorithms and computer vision techniques applied with the aim of helping physicians in everyday clinical practice.

3.3.2.1.1 Anagraphic Tool

The “Anagraphic Tool” represents the storage in which the main patient information is summarized. It is structured on several fields, not all of which are mandatory, in order to allow a mapping as precise as possible of the information relevant for infants management.

An independent personal database has been created, with encrypted sensitive data, which has been developed in a very simplified way. However, it will be linked to the Public Health Corporation personal database.

In particular, it will be connected with the ARCA (“Anagrafe Centralizzata Regionale Assistiti”), which is the set of personal data relating to all citizens who use health services at ASUR (“Azienda Sanitaria Unica Regionale”), the local health authority of Marche Region, and at Marche Region Hospital Corporations and certified by the Ministry of Economy and Finance.

In this way it will be possible to benefit from all the functionalities of the ARCA, that performs the function of an Enterprise Master Patient Index (EMPI). In fact, it solves the problem of unambiguous patient identification and allows the patient's clinical history to be linked to a known demographic position. The ARCA-EMPI platform also acts as a centralized system for the management of reference dictionaries for personal data (e.g. the coding of municipalities, nationalities, local health authorities, regions and so on), and it is responsible for obtaining from the appropriate sources a series of regional catalogues and for making them accessible at a centralized level by means of special services (e.g. health care services, drugs and medical devices, affiliated doctors, healthcare facilities and so on).

The tool will also be linked to the medical record used in the Gynaecology and Obstetrics clinic ward of "G. Salesi" hospital in order to create a transversal link that allows information about the infant's mother to be obtained quickly and directly.

Immediately after birth, the newborn infant is registered on the platform. In this way he is given a unique code which will be used throughout the hospital stay. Afterwards the medical staff members can retrieve the page related to the infant and fill in the missing data. The module, in fact, allows the historicization of changes to the patient data in order to support the concept of temporary patients recording.

The required information is distributed on different web pages. In particular, there are a patient's registry (figure 3.10), where, in addition to data relating to the newborn, essential information on parents is requested, and a registry totally dedicated to infant's mother information. This is a very detailed part where not only the personal data are recorded, but also a lot of information related to pregnancy, delivery, possible complications of delivery, possible infections contracted by the mother during pregnancy and the tests carried out. It is possible to extract personal data from the SINC DBaaS for statistical and directional processing.

3.3.2.1.2 Growth Tool

The "Growth Tool" permits to insert and archive data on the patient's growth during hospital staying (see figure 3.11). The data required are: weight, length, and head circumference, with a frequency that depends on the parameter: weight is measured once a day, while the other indicators are measured once a week. On the basis of these frequencies, which can be modified if authorized, a reminder is sent to the medical staff to remind them of the need to take the measurement.

During the insertion phase of the measurements, algorithms have been developed that compare the value inserted with the previous one with several

Figure 3.10: SINC “Anagraphic Tool” - Patient’s registry.

Figure 3.11: SINC “Growth Tool” interface - Patient’s growth data.

warning levels. If, e.g. in the case of weight, the new entered measurement exceeds the previous weight by a value equal to 5%, the person entering the data is informed with an alert; if it exceeds by a value of 7%, he is asked to repeat the measurement.

Moreover, other growth-related information such as tibia length, forearm length, skin folds and many others, can be entered and displayed on another web page.

Afterwards, historical data and a whole series of parameters and indicators extracted from the real time analysis of these data can be displayed (see figure 3.12), such as the growth rate with respect to the last measurement, the growth speed in the last 3 days or in the last 7 days; the nadir value and the recovery value. The nadir value for weight, for example, is calculated as the lowest weight achieved by the infant (the infant suffers a drop in body weight after birth), followed by 3 consecutive increasing measurements; while the value of recovery is the weight of the first day on which it exceeds the birth weight, always followed by 3 consecutive increasing measurements.

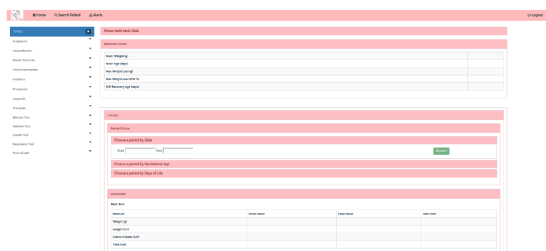


Figure 3.12: SINC “Growth Tool” interface - Patient’s growth parameters.

On another web page (see figure 3.13), all these measurements are graphically compared with the World Health Organization (WHO) Growth Standard Curves [84]. These curves can be of two types, z-scores and percentiles, and depend on the patient’s gender and hours of life. The values are also compared with the z-scores curves modified according to the characteristics of the parents in accordance with “The Generation R Study” work [85].

In fact, identification of growth patterns within the normal range requires comparison with prescriptive standards based on growth of babies classified as healthy. Additionally, standards can be used to monitor and assess the effectiveness of interventions and avoid ill-effects, such as overnutrition. Thus, growth charts permits to follow infant’s progress over time and compare it to the growth of a healthy child of a comparable build and to detect failure to thrive.

3.3.2.1.3 Nutrition Tool

The feeding of the premature infant is extremely important because it ensures that the infant has all the essential substances to complete its development.

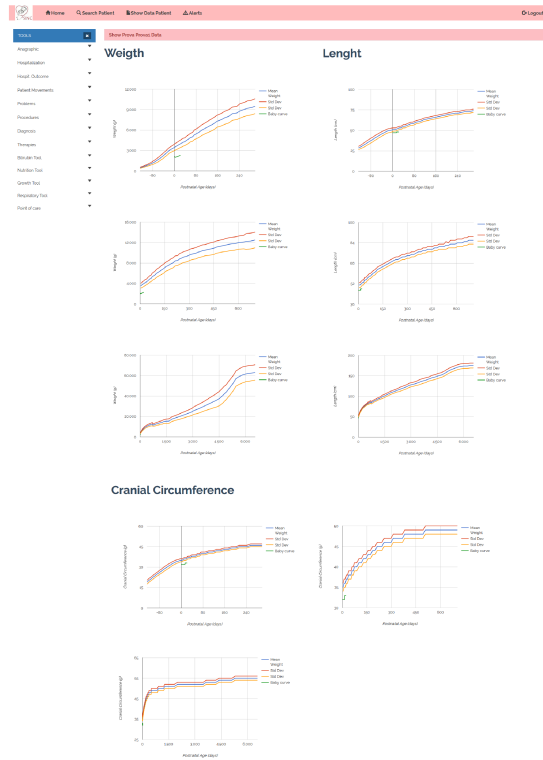


Figure 3.13: SINC “Growth Tool” interface - Patient’s growth graphs.

Generally, the nutrition of the preterm infant may be enteral (with gastric tube or bottle) or parenteral (with intravenous administration).

Enteral nutrition (EN) consists of feeding the baby with breast milk (which is however enriched with fortifying breast milk to increase especially the intake of protein, fat, calcium, phosphorus and sodium) or, alternatively, milk in a specific formula for preterm infants. This type of nutrition is generally indicated for infants where the mechanism of sucking-deglutition is present (infants with a GA between 30 and 32 weeks).

For infants under 30-32 weeks of GA gavage nutrition is generally necessary, which is feeding breast milk through a gastric tube.

When it is not possible to administer the basic nutrients (glucose, amino acids, lipids, electrolytes, minerals, vitamins and trace elements) through the enteral pathway, that is to say through the gastrointestinal tract, parenteral nutrition is used, and this occurs especially in very premature infants weighing less than 1000 g.

Parenteral nutrition (PN) is an intravenous diet in infants who are too young

to feed themselves with the breast milk or bottle. The baby is then fed thanks to special bags containing nutrients and drugs products. Bags may be ready or prepared by the hospital pharmacy.

The composition of the solutions to be administered to infants is determined by specialists using computer programs that can calculate, based on precise parameters, the amount and quality of nutrients to be given [86, 87].

Because of fetal growth being more rapid than infant growth, the extremely preterm infant has extraordinarily high nutrient requirements and thanks to parenteral nutrition it is possible to cover nutritional needs from the first minutes of life in a very premature infant. However, when the infant is stable it is extremely important to introduce enteral nutrition that can be started with a minimum milk content, commonly called “minimal enteral feeding”, to stimulate the maturation of the intestinal mucosa.

In SINC DBaaS a table with all 98 nutritional ingredients (both for EN and for PN) used in Marche Region Hospitals has been created. Among these, it is then possible to use those that are used in the “G. Salesi” Hospital pharmacy because each one uses different ingredients.

An algorithm has been implemented in the “Nutrition Tool” (see figure 3.14) which, on the basis of data taken from the “Anagrahic” and “Growth” tools for a certain infant (life days, GA at birth, current GA, weight and so on) and on the basis of nutritional schemes created by the head physician of NICU of “G. Salesi” Hospital together with specialists of the sector, advises the total amount of fluids to be administered to the infant with EN, when possible, with PN, or with a mix of the two.

The algorithm, then, by removing from the total daily fluids, the amount of liquids administered with EN and drugs, automatically prescribes the bag for parenteral nutrition.

The doctor is instructed to choose what type of PN to administer (central or peripheral venous catheters) and whether to use one of the pre-packaged bags or not. If the choice is made on bags that are not pre-packaged, but prepared by the hospital pharmacy, the physician is guided by the algorithm in the choice of ingredients to be administered and of their quantity in order to respect the energy requirements and the molarity corresponding to the particular conditions of the infant at the time of administration.

Since the ingredients in most cases are found in compounds, an algorithm for compensating the ingredients in the bag had to be implemented.

All data from the tool are saved in the SINC DBaaS and they can be correlated with those of “Anagrahic” and “Growth” tools, with those coming from follow-ups studies (see next paragraph) and in the future also with those coming from other SINC tools, such as those that will concern diseases, diagnoses and therapies in order to perform randomised and prospective studies that cor-

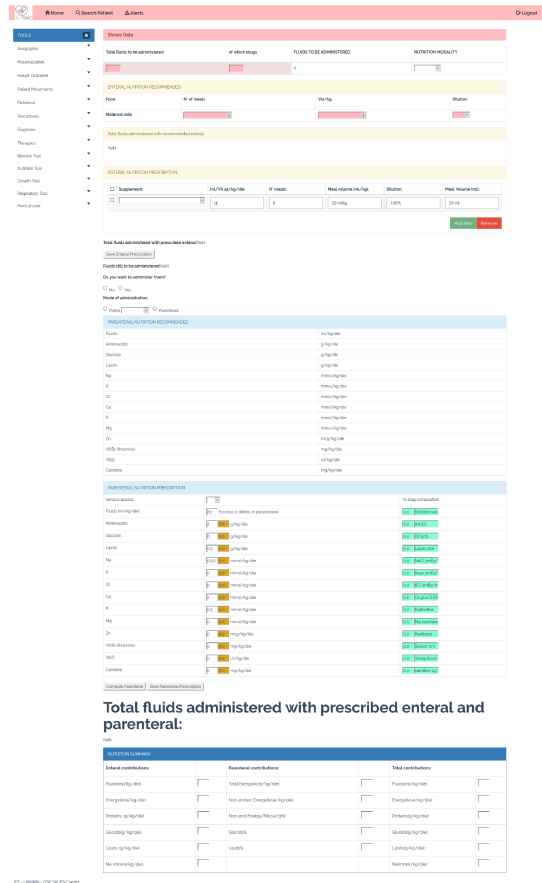


Figure 3.14: SINC “Nutrition Tool” interface - Patient’s nutrition administration.

relate nutrition modalities (EN, PN) and the specific nutritional intakes with long-term outcomes.

3.3.2.1.4 Bayley Tool

The medical care provided to preterm infants has been progressively flanked by methods of psychological care and assistance both in the Neonatal Intensive Care wards and after discharge, in order to monitor the development of these children and improve their quality of life even after their resignation. Preterm births, in fact, even when they do not have neurological damage, may present minor medical problems and sequelae, such as motor, relational, cognitive, linguistic, learning and behaviour problems.

Therefore, many doctors and scholars deal with the neurological, physical and psychological development of preterm born children, through evaluation

and screening tools to be used in the follow-up of these children to improve their evolutionary path.

Among the evaluation and screening tools used in follow-ups at “G.Salesi” Hospital there is the Bayley test.

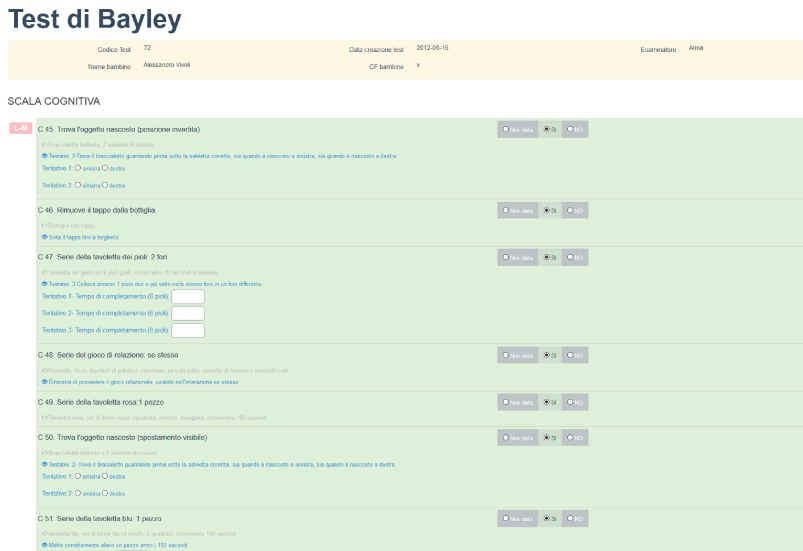


Figure 3.15: SINC “Bayley Tool” - Automated Bayley test interface.

The Bayley Scales of Infant and Toddler Development (Bayley-III is the current version) is a standard series of measurements originally developed by psychologist Nancy Bayley used primarily to assess the development of infants and toddlers, ages 1–42 months [88]. This measure consists of a series of developmental play tasks and takes between 45-60 minutes to administer [89] and derives a developmental quotient (DQ).

Raw scores of successfully completed items are converted to scale scores and to composite scores. These scores are used to determine the child’s performance compared with averages taken from typically developing children of their age (in months).

The most recent edition, the Bayley-III has 5 main subtests, 3 with direct administration (cognitive, language and motor) and 2 addressed to parents (social-emotional and adaptive behaviour).

- The Cognitive Scale (Cog) evaluates the development of motor sense, exploration, manipulation, memory, the relationship between objects and the formation of concepts. It includes items such as attention to familiar and unfamiliar objects, looking for a fallen object, and pretend to play with them.

- The Language Scale (Lang) taps understanding and expression of language, for example, recognition of objects and people, following directions, and naming objects and pictures. It is divided into two subscales:
 - Receptive Communication (RC), which examines preverbal behaviour, vocabulary development and verbal comprehension;
 - Expressive Communication (EC), which assesses communication, vocabulary development and morphosynthetic vocabulary development.
- The Motor Scale (Mot) assesses gross and fine motor skills such as grasping, sitting, stacking blocks, and climbing stairs. It is divided into two subscales:
 - Fine-motor (FM), which examines the manipulation of objects, taking and responding to tactile information;
 - Gross-motor (GM), which evaluates posture, dynamic movement, balance and coarse-motor planning.

There are two additional Bayley-II Scales depend on parental report, including:

- The Social-Emotional scale, which asks caregivers about such behaviors as ease of calming, social responsiveness, and imitation play. It analyses the child's mastery of his or her emotional function, communication needs and ability to relate with others.
- The Adaptive Behavior scale which asks about adaptations to the demands of daily life, including communication, self-control, following rules, and getting along with others. It evaluates the subjects' daily functional abilities.

The Bayley-III Cognitive and Language scales are good predictors of preschool mental test performance. These scores are largely used for screening, helping to identify the need for further observation and intervention, as infants who score very low are at risk for future developmental problems [90, 91, 92].

In the “Bayley Tool” these tests have been automated, as it is possible to see from the web interface of the tool in figure 3.15. The caregiver has no longer to write down the results of the items and then make the necessary calculations to get the score, he can quickly scroll through questions on the tablet and take advantage of the automatic grading done by the implemented algorithm.

In this way, besides avoiding calculation errors, it is possible to immediately visualize patient's score at an individual level and above all it is possible to examine the results on question level to learn, for example, which item is more difficult for children, at what age and so on.

Scores and responses to individual items are saved in the SINC DBaaS and can be downloaded and used for further analysis.

Chapter 3 A new infrastructure for neonatal care

In each tool, an automatic reporting mechanism has been set up that generates reports in pdf format that can be used as medical reports to be delivered to the parents of patients, to be entered in the ward medical record and sent to the regional EHR, with which the SINC platform will be linked using the ARCA-EMPI.

Chapter 4

Decision-Making Tools

4.1 Bilirubin Tool

Jaundice is the yellow colouring of the skin, sclera and gums caused by bilirubin deposition. In newborns, sclera and gums are difficult to see and therefore the yellow colouring of the skin is used to define the newborn jaundice, while they may be more useful in coloured babies. The assessment of skin jaundice should be made in a well illuminated environment and on compressed skin to remove neonatal erythema. However, it is important to remember that the cephalocaudal progression of jaundice can be used as an indication of the evolution and gravity of jaundice, but it does not have a significant correlation with the level of bilirubinaemia [93, 94].

Bilirubin is a yellow pigment derived from the catabolism of haemoglobin. It is continuously formed in both foetus and newborn babies and is transported in the blood associated with albumin because it is a non-polar compound. In the foetus bilirubin is eliminated from the placenta, while in the newborn it must be conjugated by the liver and eliminated through the bile. However, infant's liver is not able to eliminate the amount of bilirubin produced in the first days of life and for this reason bilirubinaemia increases and causes physiological hyperbilirubinaemia.

Physiological jaundice is an event that affects more than 60% of healthy term infants and generally has the following characteristics [95]:

- it appears after the first 24 hours of life;
- it reaches the maximum intensity between the 3rd and 5th day of life in term infants and in the 7th day in preterm infants;
- bilirubinaemia rarely exceeds 12-13 *mg/dl* (205-222 $\mu\text{mol/l}$);
- the increase in bilirubinaemia is $<0.5 \text{ mg/dl/hour}$ ($8.5 \mu\text{mol/l/hour}$);
- Asian, Hispanic and South American populations may have higher bilirubinaemia;
- it is no longer evident after 14 days of life;
- it disappears without any treatment.

Pathological jaundice differs from physiological one because of, generally, it

presents the following characteristics:

- it appears in the first 24 hours of life;
- bilirubinaemia often exceeds 15 mg/dl ($259 \text{ } \mu\text{mol/l}$);
- the increase in bilirubinaemia is $>5 \text{ mg/day}$;
- it can last beyond the first 14 days of life in term infants and beyond the first 21 days of life in preterm infants;
- it always requires treatment (usually with phototherapy).

As said, the reliability of jaundice visual assessment is limited and so at least one measure of bilirubin must be taken for each newborn baby. As explained in chapter 3, there are two ways to measure bilirubin: TcB, can be used as a first measure because it is less invasive but less reliable, and TSB, that it is always necessary to do when bilirubin values are high and in any case before taking any therapeutic decision.

Jaundice can become dangerous, when the serum concentration of un-conjugated bilirubin becomes so high that it causes damage to central nervous system structures [96].

The risk of neurological damage from bilirubin depends, first of all, on the serum concentration of total bilirubin: the higher it is, the greater is the possibility that free bilirubin can enter the brain cells. In healthy term infants, the level of bilirubinaemia may become dangerous in presence of risk cofactors when it is $>350 \text{ } \mu\text{mol/l}$ (20.5 mg/dl), while for preterm infants it is dangerous at $> 255 \text{ } \mu\text{mol/l}$ (15 mg/dl). The gestational and postnatal age (PA) must also be considered: the lower they are, the greater is the possibility of damage, as the higher the permeability of blood-brain barrier. There are also other factors that favour the permeability of the blood-brain barrier (e.g. severe aptitude, hypothermia, respiratory failure, acidosis, hypoglycemia, haemolysis, sepsis, meningitis, neurological pathology and drugs), which must therefore be taken into account.

Another factor to consider is haemolytic disease of the newborn, caused by the transplacental passage of maternal antibodies against the red blood cells of the fetus/neonate; the haemolysis that results in anaemia and hyperbilirubinaemia in the fetus and newborn.

The most important causes of feto-neonatal haemolysis are Rh isoimmunisation disease [97], caused by anti-D antibodies produced by Rh negative mothers against the Rh positive red blood cells of the fetus (it may occur when the mother is Rh negative and the Rh positive fetus) and ABO haemolytic disease [98], which occurs when the mother is a group 0 and the fetus is a group A or B.

If not diagnosed and treated in time, acute bilirubin encephalopathy (ABE), also known as Kernicterus, can cause central deafness, mental retardation and athetoid cerebral palsy or severe hypotonia and may also lead to death [99, 100].

Prevention of ABE is achieved by avoiding high levels of bilirubinaemia with the following strategies [101, 102]:

- early feeding (better breasts) to reduce weight loss, dehydration and the entero-hepatic bilirubin circle;
- early detection of critical bilirubinaemia values;
- adequate treatment with phototherapy;
- treatment with immunoglobulins in case of Rh or ABO haemolytic diseases [103], even if their efficacy is debated;
- blood exchange transfusion (BET) when indicated.

The main remedy for solving neonatal jaundice is phototherapy (PT), a curative technique based on the use of light. Light of a certain wavelength is able to induce in bilirubin an isomerisation that transforms unconjugated bilirubin into hydrosoluble compounds (lumirubin and photobilirubin) that are excreted with bile without the need for liver conjugation [104]. During treatment bilirubinaemia decreases quite rapidly (4-8 *mg/dl* every 24 hours). This reduction depends on the light spectrum used (e.g.: blue light is more effective than white light), the radiance (between 10 and 40 $\mu W/cm^2/nm$), the skin surface exposed to light (preferable supine position) and the distance between the lamp and the newborn skin (between 20 and 40 *cm*). During the treatment, which must be continuous and non-intermittent, baby must be placed naked (the diaper is allowed) at a distance ≤ 40 *cm* from the lamp with eyes covered to avoid damaging the retina.

Excluding hyperbilirubinaemia cases due to Rh and ABO haemolytic diseases, the need for BET is very limited [105, 106]. In particular, it is necessary in the case of hyperbilirubinaemia that does not respond to the treatment with intensive PT to avoid cases of ABE. A newborn infant showing clinical signs of ABE should undergo urgent BET intervention. Intensive PT must always be started while waiting. The BET must be carried out after having obtained the informed consent of the parents, in an intensive ward with monitoring during and after the operation and with the possibility of carrying out all necessary resuscitation operations [107].

4.1.1 Related Works

Neonatal hyperbilirubinaemia is the most frequent problem that every neonatologist has to face in daily practice. Approximately 60% of term and 80% of preterm infants have a visible jaundice that causes diagnostic and therapeutic problems. The attitude of neonatologists towards hyperbilirubinaemia has changed considerably in recent years: from an excessive attention to every “yellow” newborn in the period during which RH isoimmunisation prevailed, to a less caution after the disappearance of this pathology and the advent of PT in

the therapeutic scenario, until no longer considering jaundice as a problem in the last decade.

The early discharge of newborns [108], the consideration of infants with a 35-36 weeks GA as comparable to term infants, and the promotion of exclusive breastfeeding [109] have made hyperbilirubinaemia resurfaced as a “problem”.

Hospitalisation for jaundice after early discharge, severe hyperbilirubinaemia with acute neurological symptoms and more frequent cases of nuclear jaundice (kernicterus) with serious chronic outcomes have re-proposed a problem that, although not disappeared, has certainly had a resurgence [110].

For this reason, in the last twenty years numerous studies have been conducted on how to diagnose and treat neonatal pathological jaundice [111, 112, 113] and especially on how to predict and prevent it [114, 115, 101, 116].

In this respect, many studies have been carried out on possible causes [117] and on risk factors and how these are correlated with the onset of hyperbilirubinemia [118, 119, 120].

Moreover, in recent years, numerous studies have been conducted on the correlation between TSB and TcB [121, 122]. As already mentioned, in fact, non-invasive methods are currently available for the dosage of bilirubin in the undercuts, allowing to reduce invasive and painful determinations by sampling blood on the heel [123]. However, several studies show that only in the concentration range of 6 to 12 *mg/dl* (103-205 $\mu\text{mol/l}$) transcutaneous determination provides a reliable estimate of blood concentration in term and late preterm infants [75, 124, 125].

To prevent adverse outcomes resulting from neonatal hyperbilirubinaemia and to support healthcare physicians in neonatal jaundice assessment and quality of care improvement, standardised protocols for the identification and evaluation of hyperbilirubinaemia were established in many countries.

Clinical practice guidelines support clinicians by synthesising up-to-date evidence and suggesting best practices; however, they are underused in practice and not always effective in influencing physician behaviours in patient’s care [126, 127]. Among the reasons is that they are provided to healthcare professionals on a paper-based format and this contributes to decreasing their friendliness.

To facilitate guidelines implementation in everyday practice some evidence-based decision support systems have been developed to automate recommendations such as in [128], in [129] and in [130], where a model is proposed so that, by entering the various information related to a patient, an output advice on the behaviour to be taken in that situation is obtained, based on the guidelines respectively delivered by Spanish [131], American [132] and English [133] international scientific societies.

In [134] Dani et al. showed that also in Italy, as in other countries, the di-

agnostic and therapeutic approach of neonatal hyperbilirubinaemia is not well codified, hence the need felt by the Italian Society of Neonatology (SIN, *Società Italiana di Neonatologia*) to set up a task force for neonatal hyperbilirubinaemia that, based on national and international experiences, elaborated Recommendations in order to standardize the diagnostic and therapeutic approach to neonatal hyperbilirubinaemia in Italy.

The aim of SIN recommendations is to provide Italian neonatologists with a practical means of dealing with the problem of neonatal jaundice in an effective and safe way. For this purpose the guidelines of many international scientific societies have been taken into account, e.g., those of American Academy of Pediatrics [135, 132, 136], NICE for English society [137, 133], Canadian Pediatric Association [138], Netherlands Neonatal Research Network [139], Norwegian Pediatric Society [140], those of the Israeli [141], New Zealand [142] and Australian (Queensland) [143] societies, in addition to the Indian [144], the Spanish [131] and the Swiss [145] guidelines, largely derived from others.

Experiences in the neonatal population of the Lazio Region have also been taken into consideration as an expression of a representative sample of the Italian population, both for the elaboration and the prospective application of hourly nomograms relating to both transcutaneous and serum determination of bilirubin [146, 147, 148]. Most of these guidelines have been developed for infants with a GA \leq 35 weeks and only a few have also indications for infants of a lower GA.

In section 4.1.4 the design and implementation of a web-based decision support tool is described, which automates SIN guidelines and incorporates some valuable advices from NICU neonatologists who have been consulted during the development of the system.

4.1.2 SIN Guidelines

Recommendation 1: Aim of the guidelines

SIN recommendations foresee to avoid the overcoming of a bilirubinaemia equal to 20 mg/dL in the first 96 hours of life and 25 mg/dL after 96 hours of life (the maturation of the blood-brain barrier progresses with PA) in term infants (LoE 2b)¹. Then, SIN guidelines require that the limit is less than 12 mg/dL for preterm infants with a GA \leq 30 weeks and 15 mg/dL for infants with EG 31-36 weeks (LoE 1b). On this basis, bilirubinaemia values have been defined according to the time of life and GA exceeded, which are indicated to start treatment with PT or perform BET.

Recommendation 2: Methods for controlling hyperbilirubinaemia

SIN recommends that every jaundice infant should receive a measurement of

¹Levels of evidence (LoE) are indicated according to the classification shown in table 4.1.

Table 4.1: *Evidence hierarchy from the centre for evidence-based-medicine.*

Level	Definition
1a	Systematic review (with homogeneity) of RCTs
1b	Individual RCT (with narrow confidence interval)
2a	Systematic review (with homogeneity) of cohort studies
2b	Individual cohort study
3a	Systematic review (with homogeneity) of case-control studies
3b	Individual case-control study
4	Case-series (and poor quality cohort and case-control studies)
5	Expert opinion without explicit critical appraisal, or based on physiology, bench research or “first principles”

bilirubinaemia. Transcutaneous determination (TcB) can be used as a first approach to minimise blood samples, but TSB is always necessary for high bilirubinaemia values. In any case, therapeutic decisions should only be made on the basis of TSB value (LoE 1b).

Recommendation 3: Forecasting of severe hyperbilirubinaemia

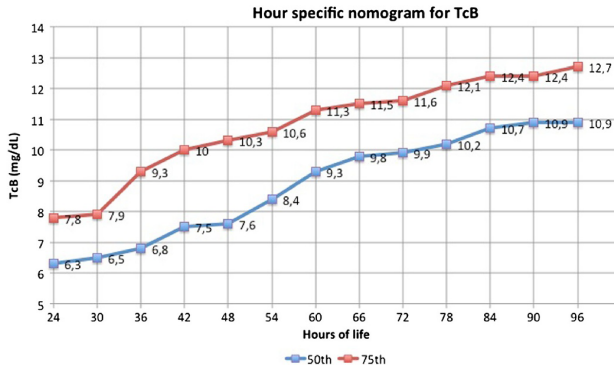
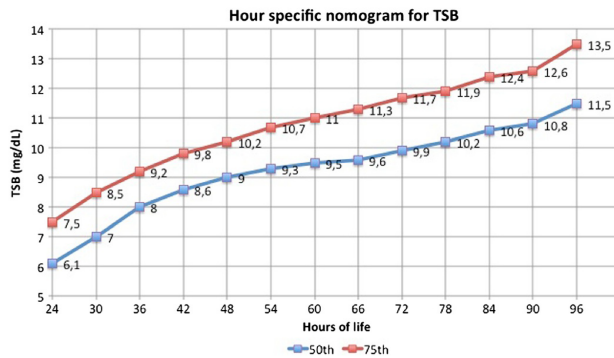
SIN recommends the following procedure for newborn babies with GA \geq 35 weeks [131, 145, 146]:

- All infants with jaundice must undergo TcB measurement.
- If TcB value is higher than the 75° centile given in the nomogram of figure 4.1 TSB must be measured.
- TSB value must be evaluated on the nomogram of figure 4.2 and the follow-up must be programmed as follows:
 - Values of TSB $<$ 50° centile in the first 48 hours or $<$ 75° centile after 48 hours of life are not at risk of clinically relevant hyperbilirubinemia (need for PT) and therefore do not require further control.
 - TSB values $>$ 50° centile in the first 48 hours or $>$ 75° centile after 48 hours of life are at risk of clinically relevant hyperbilirubinemia (need for PT) and require control at 24 or 48 hours respectively after measurement depending on the age of the newborn baby and the possible presence of risk factors (LoE 1b).

For infants with a GA $<$ of 35 weeks there are no predictive nomograms of the risk of developing relevant hyperbilirubinaemia. Therefore, it is recommended that controls should take into account infants GA with reference to the TSB values for which PT treatment is expected to begin (LoE 5).

Recommendation 4: Treatment - Phototherapy

SIN recommends the use of nomograms in which TSB values, indicative of the need to start PT, are expressed in relation to the GA, defining the values for homogeneous groups of GAs: $<$ 30, 30-31, 32-34, 35-37 and $>$ 37 weeks, as it is possible to see in figure 4.3.

Figure 4.1: *TcB hour-specific percentile nomogram.*Figure 4.2: *TSB hour-specific percentile nomogram.*

- Conventional PT equipment using wide spectrum (white light) or high intensity blue light (conventional or LED light) can be used (LoE 1a).
- Fiber optic PT can be used by remembering that it is less effective (LoE 1a).
- If there is no response, conventional lamps can be combined with fibre optics to achieve a more effective treatment (LoE 1a).
- TSB control must be scheduled at 4-8 hours from the start (even less if TSB is < 3 mg/dL from the threshold value to perform BET) and then every 12-24 hours.
- Phototherapy can be stopped after obtaining two values of TSB in reduction, compared to the values at the beginning of treatment, after 6-12 hours (LoE 2a).
- Post-suspension control should be scheduled within 12-24 hours to detect any rebound (LoE 2a).

- During PT, breastfeeding and/or the feeding of milk should never be suspended. Phototherapy may be temporarily discontinued (maximum 30 minutes) to allow breastfeeding and visual contact with the mother and/or operator (LoE 2b).
- Liquid supplementation should only be reserved for cases where weight loss is greater than 5% per day and breastfeeding is not well established (LoE 1b).
- In newborns with haemolytic diseases, PT treatment should be started as soon as the diagnosis is made (LoE 2a).

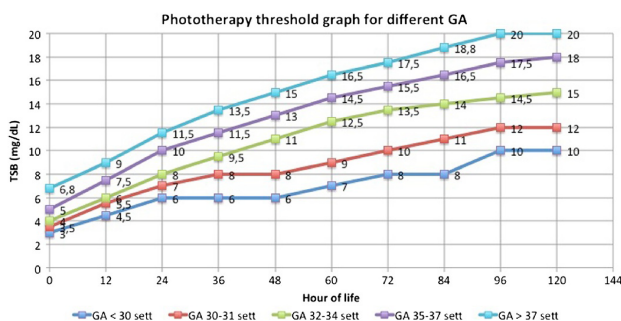


Figure 4.3: Nomogram for PT. Total bilirubin is plotted against PA in hours. The groups of GA are represented with lines of different colours.

Recommendation 5: Treatment - Blood Exchange Transfusion

SIN recommends indicative values for treatment with BET depending on GA and on PA, defining the values for homogeneous groups of GAs (<30, 30-31, 32-34, 35-37 and >37). For each GA group, the reference TSB level for BET is 5-6 mg/dL higher than the indicative TSB level for PT treatment 4.4.

- BET should be performed in NICUs.
- It is preferable to use commercial kits.
- The newborn baby should be monitored for FC, FR, SpO₂, body temperature during and within 12-24 hours after the procedure.
- Particular attention must be paid to metabolic control (hypoglycaemia, hypocalcaemia) and to any post BET haemolytic crises (control of haemoglobinuria and hematocrit).
- TSB must be checked first and at the end of the procedure and then every 4-6 hours until stabilisation.
- After the procedure, intensive PT treatment should be continued.
- A short-term follow-up for late anaemia should be foreseen.
- The feeding must be suspended during and within 6 hours after surgery and may be resumed if there are no complications (always preferable breast or breast milk feeding).

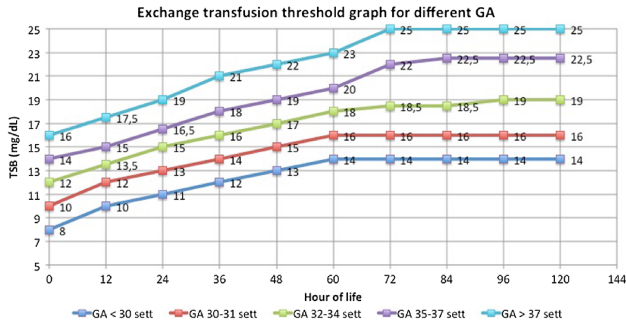


Figure 4.4: Nomogram for BET. Total bilirubin is plotted against PA in hours. The groups of GA are represented with lines of different colours.

In newborns with haemolytic disease BET can be programmed for more conservative levels of bilirubinaemia for Rh isoimmunisation and more conservative levels for ABO, because bilirubinaemia in this pathology rises very rapidly in the first 24-36 hours of life, but then assumes a similar course to the physiological one 4.5. The risk of significant post-exchange transfusion “rebound” in infants with ABO should also be considered (LoE 5).

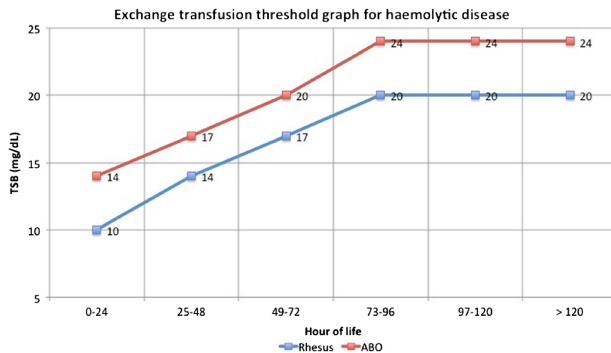


Figure 4.5: Nomogram for BET in case of haemolytic disease. Total bilirubin is plotted against PA in hours.

4.1.3 Scenario

The clinical practice of measuring bilirubin for the diagnosis and treatment of neonatal jaundice is carried out in three different wards at “G. Salesi” Hospital: the NICU, where, as already mentioned, infants of any degree of prematurity and severity are treated, the Neonatal Pathology, where mid-risk infants are hospitalized and the Pediatric Nursery, where care is provided for healthy or

low-risk term infants. The treatment of PT, however, is carried out only in the NICU, the only hospital ward equipped with PT lamps.

Usually if jaundice is not visible and if there are no particular risk factors, such as haemolytic disease, in term infants, the first TcB is carried out within 48 hours, while in preterms infants control is carried out within 24 hours. If the value of TcB is less than 12mg/dL , they proceed with the regular checks, up to the discharge, if it is more than 12mg/dL , they make the TSB and compare it with the curves of the centils and with those relating to PT and BET in the most serious cases, corresponding to the GA of the newborn baby.

If the newborn infant has anemia, the first measurement is taken immediately and depending on the values of the measurement, on the type of anaemia, on GA and on PA, checks are carried out every 4,6 or 12 hours. For comparisons with the corresponding curves, in this case, the curve related to the previous GA group is taken into account, to have a more cautious attitude. Even if the newborn baby has other risk factors, less severe, controls can be programmed more frequently, but in this case the comparison is made on the basis of SIN guidelines.

In particular, measured TcB and TSB values are written down by nurses on a spreadsheet and only later transcribed on the PC. Nurses proceed to the comparison of the measured TcB/TSB value with standard values established by SIN guidelines: the TcB/TSB value is visually compared with the correct curve selected depending on percentile or on GA and on measurement time compared to birth hour. From this purely visual comparison and, therefore very subjective, they decide if the value of TcB/TSB is in the physiological range or not. If it is, they continue with measurements taken at regular intervals, depending on GA and on the presence of risk factors, until discharge. Otherwise, if it is not, in case of TCB measurement, they proceed with the measurement of TSB, and in case of a TSB measurement beyond the limit, nurses must promptly inform physicians who will order to perform therapies such as PT or BET in more serious cases.

Since it is transcribed on PC only later, the TcB value has to be compared with the correspondent curve of the guidelines only visually through a paper chart. For this reason, this comparison is very subjective and prone to error.

The aim was therefore to standardise, first of all, the treatment protocols of the three departments, which showed disparities, and then to create a valid model for all the birthplaces of Marche region.

Another objective was to automatically collect data from all the instruments used for the measurement of serum and transcutaneous bilirubin that are located in the three hospital wards, namely 2 sieric bilirubinometers and 3 transcutaneous ones, in a single DB. Through the interconnection of the instruments, described in chapter 3, in fact, the values of the measurement are

shown in the tool interface in an automatic and instantaneous way and are then processed by the algorithm to extract useful information on jaundice diagnosis.

Thus, the automatic transmission of the measured values will eliminate drawbacks due to manual transcription and it will give the possibility of making comparisons with the standard curves of the guidelines in a direct, automatic and objective way and without the possibility of making mistakes.

Moreover, in the nursery measurements are not even transcribed from paper to EMR with the problem that if the newborn gets sick or gets worse and has to be moved to the NICU, they have to be recovered and transcribed on the PC in order to have the historical patient's bilirubin values. Furthermore, when infants are sent from the nest to PT at the NICU, on their return, nurses of the Pediatric Nursery do not have access to bilirubin values related to the period of PT. The use of a single database, which also includes the personal data of the patient, through the integration with EMR data, has also solved this problem.

4.1.4 Data Analysis: Bilirubin Decision-Making Algorithm

The “Bilirubin Tool” and, in particular, the algorithm have been designed and developed after several interviews with 2 neonatologists and a nurse acting as domain experts. With them the structure of the problem was modelled as a workflow diagram 4.6, identifying decisions to be made, the sequence in which they would arise, and the information available at each decision-making time, as well as all the uncertain events. It is implemented in JavaScript for client side and in PHP for server side.

The developed decision-making algorithm consists in an automated DSS for guideline based care to facilitate the implementation of clinical practice guidelines for neonatal jaundice. It is an evidence based CDSS which, generally, automates SIN guidelines, but also adds physicians' expertise at some critical points.

Decision nodes involve the temporal axis of the model: first, to establish measurements reminders and, then, to decide the treatment (PT, exchange transfusion, or simply observation) depending on some risk factors and on the results of any measurement tests carried out. Decisions about treatments are repeated as many times as necessary until the problem is over, i.e., the infant is discharged unless he has other health problems.

Clinical inputs of the system, apart from SIN guidelines rules and recommendations that form the knowledge base, are GA and PA, coming from “Anagraphic Tool”, birth weight and the current one, coming from “Growth Tool”, bilirubin measurements coming from bilirubinometers and transcutaneous ones (combined in the same DB table), bilirubin levels curves recommended from SIN guidelines and some risk factors.

The risk factors that the algorithm takes into account, on the advice of experienced physicians, are in addition to those covered by the guidelines and considered primary factors, i.e. the presence of Rh isoimmunisation and ABO haemolytic disease, assessed by the Coombs test results, manually inserted by nurses or physicians, some secondary factors, i.e. familiarity with PT, breast-feeding, always manually entered as a response to an initial questionnaire, and a weight loss $\geq 10\%$, automatically calculated by the algorithm as the difference between infant's birth weight and current weight.

SIN guidelines do not specify how risk factors are to be taken into consideration except in the curves of critical bilirubin values for BET (4.5). On the contrary, the algorithm, if one of the primary risk factors is present, takes for the comparison of TcB and TSB measurements the values corresponding to the group of GAs preceding the actual one of the infant and reduces the time between checks; while if one of the secondary risk factors is present, it only reduces the time between bilirubin value checks.

Immediately after the infant's patient data registration on the "Anagraphic Tool" and the mandatory compilation of risk factors, the algorithm starts a countdown to program TcB measurement after 24 hours if there are no risk factors or after 6 hours if there are risk factors (even secondary ones). In any case, the physician may decide to reduce these time intervals between the bilirubin measurement checks depending on the particular case, by modifying a field in the interface of the tool and justifying its motivation in a note field. The algorithm takes into account the new predetermined range.

The countdown results in a reminder for nurses to do the bilirubin measurement and, when this is not done on time, in a warning (need for immediate measurement).

As soon as the DB receives a new measure of bilirubin from the instrumentations depending on the type (TcB or TSB) and time order, a series of actions are triggered, which are translated into a series of if-else cycles controlled by the various inputs described above.

If the infant has a GA \geq of 35 weeks, if TcB value is higher than the 75^o percentile given in the related SIN guidelines nomograms (4.1), depending on infant's PA, TSB must be measured, that results in a TSB measurement warning, otherwise another TcB measurement is required after the predetermined time interval, that results in a TcB measurement reminder.

If the infant has a GA $<$ of 35 weeks, the same nomogram is followed, but independently from PA if it exceeds 11 *mg/dL*, the TSB is required. This is because in the guidelines the critical value is 12 *mg/dL*, but according to physicians' experience in this range of values the transcutaneous bilirubinometer has a great variability, so as a precaution they have decided to set the limit at 11 *mg/dL*.

Then, if TSB value, in the first 48 hours, is $< 50^{\circ}$ centile or, after 48 hours of life, is $< 75^{\circ}$ centile given in the related SIN guidelines nomogram (4.2), depending on infant's GA and PA, further controls are not required other than the final TSB measurement before discharge, while if TSB value is $> 50^{\circ}$ centile in the first 48 hours or $> 75^{\circ}$ centile after 48 hours, the TSB value has to be compared with the SIN guidelines nomograms related to PT (4.3), depending on infant's GA and PA.

If TSB value is lower than that of the monogram for PT related to the infant's GA and PA, then a TSB check must be carried out again after the predetermined time interval, that results in a TSB measurement reminder; otherwise, if it is higher, but lower than that of the monogram for BET (4.4), related to the infant's GA and PA, the PT should start as soon as possible ad it results in a PT acceptance request sent by email to physician in charge because only physicians can give the consent to begin the therapy.

After the physician has accepted, also by sending an unlock code via email, PT is started. Then, TSB control must be scheduled at 4 hours from the start (even less if TSB is $< 3 \text{ mg/dL}$ from the threshold value to perform BET) and then every 12-24 hours depending on whether secondary risk factors are present or not. If the PT has been started for more than 72 hours and the value is not yet below the threshold, the exposure or power of the lamps must be increased. Treatment can be stopped after obtaining two values of TSB in reduction, compared to the values at the beginning of treatment. Post-suspension control should be scheduled within 12-24 hours to detect any rebound.

If TSB value is higher than that of the monogram for BET related to the infant's GA and PA, SIN guidelines are followed: before the start of the procedure PT is immediately initiated after physician's consent; TSB must be checked first and at the end of the procedure and then every 4 hours until stabilisation; after the procedure intensive PT treatment should be continued until stabilisation.

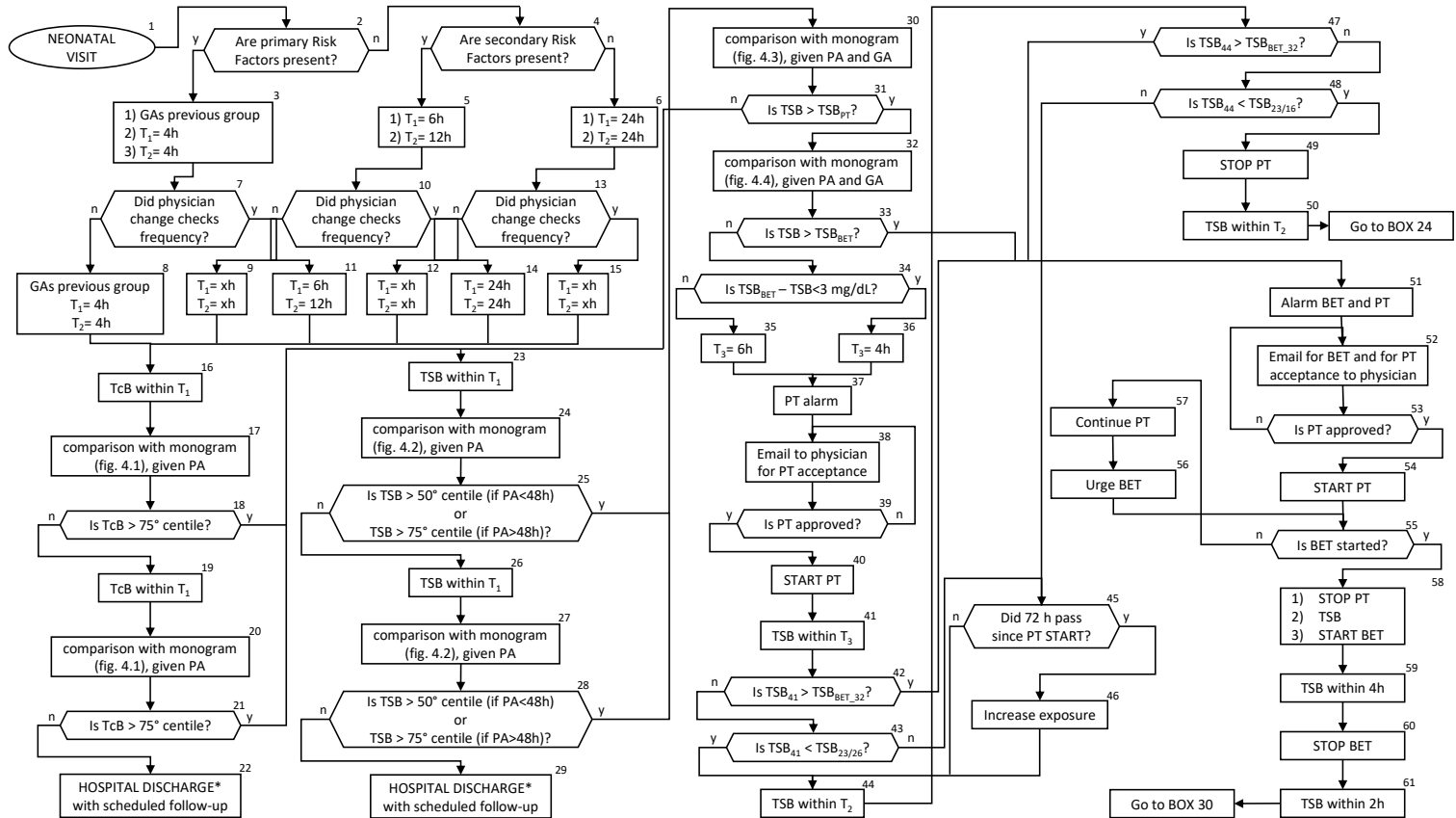


Figure 4.6: Bilirubin Decision-Making workflow diagram.

4.2 Activities Monitoring Tools

In this section a novel non-contact and non-invasive RGB-D imaging method to estimate infants' respiratory rate and movements is presented. In section 4.7 the physical architecture is described, then in section 4.2.2 and 4.2.3 respectively, the methods and algorithms used to analyse data extracted from depth images acquired from the RGB-D camera are described.

4.2.1 The physical architecture

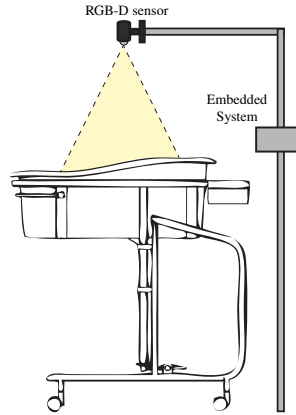


Figure 4.7: Representation of the configuration scheme of the system.

Figure 4.7 shows the configuration scheme of the system. It consists of two main components:

1. *Single Board Computer*: is a complete computer built on a single circuit board, with microprocessor(s), memory, input/output (I/O) and other features required for a functional computer. Single-board computers were made as demonstration or development systems, for the use as embedded computer controllers [149].
2. *RGB-D sensor*: is composed by an infrared sensor, an RGB sensor and some microphones. It is able to provide in output a RGB representation of the scene and it also allows to reconstruct a depth map of the same. In the depth map the value of each pixel codifies the distance of each element in a 3D scene.

The architecture design is based on the choice of hardware and software components. In order to satisfy both functional and non-functional requirements, an

embedded board, such as a CubieBoard2², has been used, since it is sufficiently small and suited to manage all algorithms. Asus Xtion Pro live has been chosen as depth sensor because it has a low cost, it has smaller dimensions than Microsoft Kinect, and the power supply is provided only by the USB port: it does not need an external power. Moreover, it is easy to install over the crib. The Cubieboard2 is a SoC based on ARM Cortex-A7 Dual-Core processor running on 1 GHz, and on ARM Mali 400MP2GPU, containing 1 GB of DDR3 memory and 4 GB of internal NAND flash. On that, a version of Debian OS (CubianX) is installed because compatible with the hardware and easy to setup the drivers of depth sensor (OpenNI2), the vision libraries (OpenCV), and the Qt Framework (Qt5).

4.2.2 Respiration Tool

The respiratory rate is defined as the number of breaths taken by an individual over a minute. Every single respiratory cycle is composed of an inspiratory phase, during which the chest wall expands itself, and an expiratory phase, during which the chest wall goes back to the previous state.

The respiratory rate of an adult at rest is 12 – 20 breaths per minute [150]. In the newborn and throughout the first year of age, the respiratory rate is about 40 breaths per minute. In preterm infants it is higher, about 40 – 50 per minute, and irregular.

As said before, preterm birth affects the anatomical and functional development of all organs, inversely with GA and the degree of immaturity is primarily in the respiratory tract.

The rhythm of the breath is usually irregular for the immaturity of the respiratory centers. Periodic breathing (Cheyne-Stokes rhythm) is frequently encountered, characterized by recurrent periods of apnoea (about 5-10 s) within periods with close breaths.

Respiratory Distress Syndrome (RDS) is one of the most frequent lung diseases in premature births. It is a surfactant deficiency disease, which designates lung immaturity from a biochemical and structural point of view. Normally, RDS can occur from 3 to 6 hours after birth and in the most serious cases at birth, while in the lighter forms it appears after 12-18 hours.

The following terminology is used in a standardised manner to describe the severity of respiratory distress:

- absent: haemoglobin saturation exceeds 85% and respiratory rate is below 60 cycles/minute;
- moderate: haemoglobin saturation is below 85% and the respiratory rate is above 60 cycles/minute;

²<http://cubieboard.org/model/cb2/>

- severe: the patient is in apnoea, gasping (agonal respiration, not effective, with very low frequency) or intubated.

Thus, a respiratory rate greater than 60 breaths per minute creates alert. Even if the infant has an apnoea, i.e., breathing stops for more than 10 seconds, it means that there is a respiratory problem.

For all these reasons it is necessary to continuously monitor the respiratory rate in preterm infants.

For disease assessment hemogasanalytic parameters, such as Ph, PaCO₂ and PaO₂, are also used. Furthermore, it is very useful to quantify the severity of signs and symptoms of RDS using the respiratory score according to Silverman, where each of the parameters taken into consideration is given a maximum score of 2; a total score of 10 identifies an infant with an important respiratory failure.

One of these parameters is the thoraco-abdominal balance, a typical oscillation between thorax and abdomen given by the lack of coordination between diaphragm and intercostal muscles in conditions of intense fatigue. In the absence of RDS pathology, the upper chest portion and abdomen expand simultaneously. On the contrary, when the disease is present, a wavy movement is visible, so the chest falls back while the abdomen expands.

RDS is treated with artificial ventilation and exogenous surfactant, natural (cattle or pig) or synthetic.

4.2.2.1 Related Works

The two most widely used methods for evaluating the respiratory activity in adults are spirometer and pneumotacography.

Other invasive devices are impedance pneumography [151], thoracic impedance [152], respiratory inductance pletysmography [153], photoplethysmography [154], strain gauges [155], thermistor [156], magnetometers [157] and acoustic monitoring [158].

However the measurement of the respiratory rate in all these techniques needs the direct contact with the monitored people and it may cause interference in their normal activity breath.

For this reason, in the last years some non-contact respiratory measurement methods were investigated, such as Doppler radar [159], microwave sensors [160, 161], infrared temperature sensors [162], thermal imaging [163], structured light pletysmography [164] and optoelectronic pletysmography [165, 166].

Most recently, the RGB-D camera is used to detect the respiratory rate [167, 168, 169, 170] but in literature, there is a little number of works describing this technique, which, however, is used only for adults.

Generally, the respiratory activity of hospitalized infants is monitored using the thoracic impedance technique. In literature, it is possible to find that some of the methods previously cited are adapted and tested also on newborns

and preterm infants, such as respiratory inductance pletysmography [171], impedance plethysmography [172], structured light plethysmography [173] and optoelectronic plethysmography [166].

In the neonatal intensive care unit (NICU) of the Women’s and Children’s Hospital “G. Salesi” in Ancona, where these babies are taken into care, the respiratory activity of preterm infants is continuously monitored using a patient monitor, used as benchmark, obtaining the respiratory rate through the ECG electrodes by impedance pneumography.

In this section, a novel contribution for monitoring the respiratory rate of preterm infants is described, developing a low cost embedded video system that measures preterm infant respiratory rate without any physical contact. Respiratory rate is derived by calculating morphological chest wall motions using a depth camera positioned above the infant lying on the infant warmer. The advantage of the proposed method is that it is contact-less, non-invasive and suitable to be used in an indoor environment with poor lighting, as might be rooms in the neonatal intensive care unit.

4.2.2.2 Data Analysis: Respiratory Rate Algorithm

In this section, main steps of the algorithm that analyses the respiratory rate of preterm infants are described.

The subjects under examination are 3 preterm infants (males) recovered in the NICU. Their GA ranged from 32 and 34 weeks, with a mean age of 33^{+3} weeks of age and the weight is between 1400 g and 1800 g, as shown in table 4.2. In order to evaluate the performances of the proposed algorithm, five tests, lasting 30 seconds each one, for each subject were performed.

Table 4.2: *Infants’ characteristics (Gestational Age and Weight).*

ID Acquisition	Gestational Age (<i>weeks^{+days}</i>)	Weight (g)
1	32^{+3}	1420
2	33^{+3}	1618
3	34^{+2}	1762
Mean	33^{+3}	1600

The depth sensor has been placed perpendicularly above the infant lying on the crib at a distance of 70 cm, normally directed to the subject skin. Other tests have been performed putting it in a slightly inclined position, however this different position does not affect the measurement. For the analysis of the respiratory rate, the measurement points have been chosen in the thoraco-abdominal area, considering where the possibility to detect the movements due to inspiration and expiration acts is greater and at the same time where it is

possible to work on an available part of the skin surface of the infant, that is wearing a diaper and has sensors attached to the body. The mechanical movements of this area due to inspiration and expiration acts cause the variation of the depth signal acquired.

The method for the analysis of respiratory rate is based on the depth sensor. The idea is to analyse the time trend of different points in the thoraco-abdominal surface area of the subject monitored, present in the depth frame. The particular configuration of the system facilitates the monitoring of the respiratory rate. A graphical interface has been created in *C++*, which allows viewing video streams (RGB and depth) from the sensor.

The algorithm includes a first step where the user can choose to analyse different strategic points. These, along with the depth values and the timestamps, are exported to a .csv file. Then, for each frame, the average value of depth of the chosen points is calculated. After this first analysis, a filter (fourth-order Butterworth low-pass filter) is applied to raw data so collected to remove the unwanted noise components due to the cardiac activity and to the motion artefacts. Then a find-peak function is used to detect the respiratory signal peaks and the time elapsed between two successive peaks is calculated, which is the instantaneous respiration period (RR). Finally for each performed test, the RR period obtained from the RGB-D sensor is compared with that derived from the patient monitor, used as reference.

4.2.3 Movement Tool

Every year there are more than 15 million worldwide preterm births and the number of cases continues to rise [6]. Preterm infants are babies born between the 22nd and 36th week of gestation that often have health problems because of preterm birth affects the anatomical and functional development of all organs, inversely with GA.

One of the biggest problems concerns the functional integrity of the neonate's central nervous system (CNS). Preterm infants, in fact, are at higher risk of developing adverse neurodevelopmental outcomes and correlated motor impairments than infants born at term [174]. Cerebral palsy (CP) is a permanent disorder in the development of movement and posture and is one of the major disabilities that affects up to 18% of infants who are born extremely preterm [175]. The total rate of neurological impairments, developmental delays and other motor coordination disorders due to less severe category of minor neurological dysfunctions is up to 45% [176].

For the moment, there are no standardized clinical guidelines to assess the risk of later disabilities and predict motor impairment in high risk infants. Neuroimaging results, such as MRI and clinical neurological examination, in-

egrated with infant's clinical history, are used to identify infants at highest risk through different clinical assessments and experience of healthcare professionals. These sophisticated brain imaging techniques can provide additional information for conditions like CP [177], but these approaches are not yet suited for early diagnosis. CP diagnosis generally cannot be made definitively until a child is at least 3-4 years-old [175].

However, in order to limit the consequences of CP or other minor neurological dysfunctions, physiotherapy should start as soon as possible, meaning that infants at risk have to be identified from the earliest possible age. Though the major injury cannot be completely repaired, in fact, with an early identification follow-ups after discharge can be planned in a more focused way in order to provide specific interventions and information for parents about infant's prognosis.

In last years, it was found that the spontaneous motility of preterm infants during their first weeks of life has an important clinical significance. The study of the early motor repertoire in preterm infants is an important predictor of nervous system dysfunctions and neuromotor impairments in high risk infants [178] and it can be considered as an essential step to optimise therapeutic approaches [179].

Prechtl proposed a new method to study infant nervous system by evaluating the quality of movement patterns in infants. In [180], authors introduced the term General Movements (GMs) to describe whole-body movements that have varying speed, amplitude and sequence and in [181] they developed a qualitative approach to assess infants' motor integrity based on the observation of spontaneous motor movements.

GMs can be observed in newborns and young infants until the 20th week post term. In preterm infants (until the 4th week post term) GMs are called Writhing Movements (WMs); they seem to be more proximal and have small to moderate amplitude and slow to moderate speed. To the 6th-8th week post term GMs are called Fidgety Movements (FMs); they appear more distal, circular, with a moderate speed, a smaller amplitude, a constant fluency and are characterized by variable limbs acceleration in all directions. The transition from WMs to FMs indicates a changing maturational stage, whereas the absence of FMs in infants at the 9th-20th week post term is proved to be a marker for later disability and CP [182]. Also the presence of the cramped synchronized general movements (CSGMs), in which infant's limbs are rigid and move almost simultaneously during preterm and term age, have high predictive value for CP development, if observed persistently during a certain number of weeks [183].

The quality of GMs is evaluated by trained observers meaning that GMs assessment (GMA) is based on visual observation by physicians and, thereby,

that the outcome measures are not standardized and influenced by examiner's subjective interpretation. The GMA technique is time-consuming, depends on examiner's experience and shows a considerable intra and inter-observer variability [184]. For these reasons, an objective (observer-independent) method, that automates the process of assessing the quality of infant GMs, would be preferable. Computer-based analysis of GMs could be a useful tool to support the physician in his medical decisions.

Nowadays, the advanced motion capture technologies have made possible the quantitative analysis of movement and the classification of "normal" and "at risk" movements based on objective criteria. However, the utility of these methods is often limited by the need for complex equipment and instrumentation for advanced analyses and for highly experienced personnel who is required [185]. Instead, an ideal system for analysing infants movements in a clinical environment, as might be the Neonatal Intensive Care Unit (NICU) where this solution is tested, has to provide the following characteristics: the system has to be cheap, easy to install, non-invasive and user-friendly and has to provide in outcome objective, accurate and reliable measures.

In this section, a novel contribution for preterm infant's movements analysis is described, by providing a low-cost video-based system that achieves all previous requirements by using a depth sensor positioned above the infant lying on the infant warmer. The advantage of the proposed method is that it is contactless, non-invasive, easy to install and suitable to be used in an indoor environment with poor lighting, as might be rooms in the NICU.

The aim is to provide a 3D motion analysis system that is able to extract some important features from the sequence of depth images collected by RGB-D sensor, which serve as quantitative and qualitative indicators of infant's movements. These indicators can be used to objectively and quantitatively study infant's movements during his development. In that way, it will be possible to see the change of movements type during the time, the transition from WMs to FMs, the absence of FMs or the presence of abnormalities in movement as CSGMs, the improvements after physiotherapy. The work is mainly focused on the statistical method reporting only preliminary test results conducted in the experimental phase on a preterm infant hospitalized in the NICU of the Women's and Children's Hospital "G. Salesi" in Ancona (Italy). The goal is to extract a set of parameters from statistical analysis of depth data, collected from the RGB-D sensor of the video-based system installed over the crib, which support clinician in quantifying movements, e.g. with information about movements percentage, velocity, acceleration and activity sequences.

The project opens also to future evolutions in the direction of infants' classification in "healthy" and "at risk" classes.

4.2.3.1 Related Works

The clinical importance of the early detection of neuromotor impairments in high risk infants has led to an increasing interest in the use of automated movement recognition technologies being applied in this field. Over last years, several researchers tried to overcome GMA subjectivity by attempting to automatically analyse GMs. Different methods of data acquisition (e.g. optical or magnetic tracking, acceleration measurements, image processing) have been studied. However, these approaches are often based on complex equipment and used methods are not always suitable for a clinical environment. In [186] automated movement recognition for clinical movement assessment in high risk infants are divided in two main categories: video-based assessment and assessment through direct movement sensing.

Video-based movement assessment systems can be divided into three-dimensional (3D) motion capture systems, based on special markers that should be attached to the limbs being tracked, and systems that use traditional colour (RGB) sensors.

A first 3D motion capture approach was performed by Meinecke et al. in [185]. Based on a 3D motion analysis system, the aim of this study is to develop a methodology in the direction of an objective and quantitative description of GMs of infants within the first month of life. The measurement procedure allows the spatial detection and quantification of full body movements for long-term control with very high 3D tracking accuracy and resolution (both spatial and temporal), but at a considerable price and setup effort.

With a similar setup, in [187, 188] Kanemaru and colleagues analysed infants' GMs in order to investigate the relationship between the jerkiness in spontaneous movements at term age and the development of CP at 3 years of age.

However, 3D motion analysis of the whole body is a demanding task, especially in the case of very small infants. Infant's movements must not be impeded by cumbersome measurement setups, because the aim is to provide the basis for the application of quantitative methods in clinical routine.

Systems that use standard video cameras, e.g. webcams and RGB sensors, are also used for markerless infants' motion capture. These systems are a more affordable alternative to 3D motion capture systems and require a less set up effort, allowing their applications in research and clinical settings. However, these approaches have lower spatial and temporal resolution and less accurate tracking than 3D motion systems, which limit the level of analysis detail .

Adde and co-workers used a video-based analysis system for quantitative and qualitative assessments of infants' GMs [189]. They developed the General Movement Toolbox (GMT) by modifying some modules of the Musical Gesture Toolbox (MGT), a software collection for performing video analysis of music-

related movements in musicians and dancers [190]. By using the so called “motiongrams” for quantifying changes in the infant’s movements, the GMT is able to detect FMs as described in the GMA.

More recent studies have successfully applied accelerometers to preterm infants to measure spontaneous movements [191, 192]. In [193] authors tested the use of wireless accelerometers in an NICU and compared accelerometers data to the GMA in order to investigate whether accelerometry, combined with machine learning techniques, could accurately identify CSGMs. As in the case of traditional cameras, the use of accelerometers provides low spatial resolution, occasional data losses and relative movement capture only.

In [194] authors used another approach in the movement sensing assessment class by tracking body segments of upper and lower limbs during GMs with a magnetic tracking system compared with traditional GMA through video analyses. Despite the increasing popularity of depth sensors, these have not yet been used extensively for movement analysis in infants. This contrasts with other clinical applications, e.g. gait analysis [195], rehabilitation monitoring [196], postural control assessment [197], or monitoring of musculoskeletal disorders [198]. Although its great potential in human action recognition [199] and in general movement analysis, depth sensors use is not largely explored with regards to preterm infants’ GMA. This may have happened because the provided body tracking functionality of Kinect sensor does not work reliably for humans smaller than one meter, which makes it unsuitable for tracking infants.

In [200] authors started to develop a 3D motion analysis system based on the use of Kinect sensor by providing the development of a markerless body pose estimator in single depth images for infants as the first step towards this goal. The advantages of this kind of solution is that the use of depth sensors provides high spatial resolution with a marker-less, non-invasive, low-cost and privacy preserving motion capture unlike 3D motion capture studied until now. For these reasons, the attention is focused on this approach by continuing the work started in [201].

4.2.3.2 Data Analysis

This section describes proposed Computer Vision (CV) algorithms used for infants’ movements detection (paragraph 4.2.3.2.1) and extremities tracking (paragraph 4.2.3.2.3) and some algorithms used for the analysis of these movements with the aim of processing data and transform them in important indicators useful for physicians in clinical decision-making (paragraph 4.2.3.2.2).

The pattern observed for the analysis of movements is shown in figure 4.8.

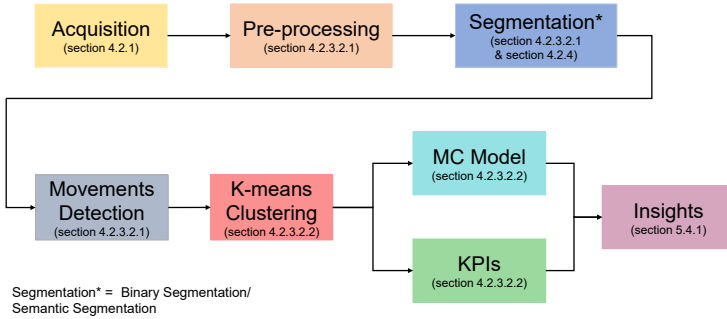


Figure 4.8: Followed pattern for preterm infants' movements analysis.

4.2.3.2.1 Acquisition and Movements Detection Algorithm

As said, the system hardware architecture consists of an RGB-D sensor placed perpendicularly above the infant, lying in a supine position on the crib, at a distance of 70 cm, normally directed to the subject. The entire sensor is composed by an RGB sensor and an infrared sensor, that provides a depth map.

An acquisition framework, based on vision techniques, has been developed, which can detect infant's movements in real time. The main tasks of this framework are:

- frame acquisition;
- noise filtering;
- infant's segmentation;
- motion analysis.

An algorithm is proposed which can detect infant's movements in real time and it is based on vision techniques. Initially, the user selects a region of interest in the GUI where it is possible to visualize the infant. This procedure is used to filter the noise produced by the edges of the crib, creating zero pixels in the depth image. After this stage, the process of acquiring depth stream begins. The frames are stored in a vector so it is possible a subtraction operation between the first and the last frame. The size of the vector has been experimentally defined. Subsequently, an image filtering is performed: all points that, at the time of the acquisition have zero value (pixel where depth is not defined) are filtered. After filtering, the image is segmented using a threshold value, so as to further discriminate positive signals that indicate

moving of limbs, by false positives due to background noise. At this point, the segmented image contains some blobs (movement blobs) that represent an area of pixels where the variations of the depth values between subsequent frames due to infant's movements of the baby exceed a certain threshold. These regions are identified and filtered depending on the area. The centres of mass are extracted from the blobs and are tracked for the duration of the movement. The detail of the algorithm is shown in Algorithm 1.

```

input : Depth image  $d(x, y)$ 
input : Number of frame delay  $N_{fdelay}$ 
output: Vector of points  $points$ 

while  $sensor.isOpen()$  do
  if  $d_{list.size()} > N_{fdelay}$  then
     $d_{diff} \leftarrow d_{list.last()} - d_{list.first}();$ 
     $d_{list.pop\_back}();$ 
     $d_{fil} \leftarrow filtering(d_{diff});$ 
     $d_{seg} \leftarrow segmentation(d_{fil});$ 
     $contours \leftarrow find\_contours(d_{seg});$ 
     $points \leftarrow moments(contours);$ 
     $tracking(points);$ 
  else
     $skip;$ 
  end
   $d_{list.push\_front}(d(x, y));$ 
end

```

Algorithm 1: Movements Analysis algorithm.

4.2.3.2.2 Data processing

Later, this framework has been customised in order to permit extraction and exportation of depth values and timestamps related to movement blobs [202].

After a preliminary analysis, the coordinates of the various instances of the movement blobs (x, y) are plotted and it is easy to observe (from figure 4.9b) that points are distributed in 4 well separated clusters; therefore, K-means algorithm can be used as a clustering method, setting k equal to 4, i.e. the number of the limbs being tracked.

K-means clustering [203] is a commonly used method to automatically partition a dataset into k groups. It proceeds by selecting k initial cluster centres and then iteratively refining them as follows:

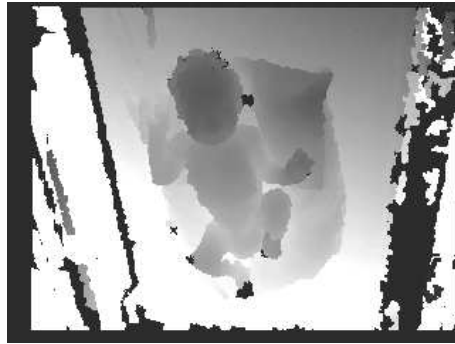
1. Each instance d_i is assigned to its closest cluster centre.
2. Each cluster centre C_j is updated to be the mean of its constituent instances.

The algorithm converges when there is no further change in assignment of instances to clusters.

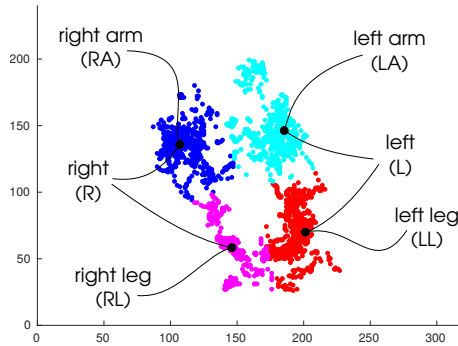
K-means clustering provides in output a ground truth vector that associates to each blob instance (i.e. to each blob timestamp) the cluster value assigned to the corresponding limb:

- right leg (*RL*);
- left leg (*LL*);
- right arm (*RA*);
- left arm (*LA*);

as shown in figure 4.9.



(a) *Depth frame.*



(b) *Clustering result.*

Figure 4.9: In figure 4.9a a depth frame from RGB-D sensor is shown. Figure 4.9b is the result of clustering process; it highlights 4 clusters that correspond to the 4 infant’s limbs.

Considering that each timestamp instance can be associated to multiple clusters because limbs can move simultaneously, this ground truth vector is used as the input of an algorithm that generates the states vector.

Each limb can assume two different states, “in movement” or “not in movement”, and, therefore, considering 4 limbs, the number of possible combinations

is equal to $2^4 = 16$.

At the end of the algorithm in output there are the states vector that associates to each timestamp of the recorded video session a state giving information about which limbs are “in movement” in that moment (timestamp).

KPIs Extraction

Using these preprocessed data and movement blobs position data, the following 10 Key Performance Indicators (KPIs) are derived, each of which describes different characteristics of the infant’s spontaneous movements, of great interest for physicians and already used in other studies [187, 188].

$$M_{\%}^l = \frac{\sum_i t_i^l}{t_{tot}} \quad (4.1)$$

where t_i^l are the time instants during which the l limb (RL , LL , RA , LA) is moving. $M_{\%}^l$ is the percentage of the movement of each limb.

$$M_{\%}^G = \frac{\sum_l \sum_i t_i^l}{t_{tot}} \quad (4.2)$$

is the general movement percentage of all the limbs over the time of a recording session t_{tot} .

$$M_{\%}^s = \frac{\sum_i t_i^s}{t_{tot}} \quad (4.3)$$

where t_i^s are the time instants during which the s state (from 1 to 16) is active. $M_{\%}^s$ is the percentage of movement of each state over the time of a recording session t_{tot} .

$$M_{\%}^{\alpha} = \frac{\sum_i t_i^l}{t_{tot}} \quad \alpha \in \{L, R\}, l \in \alpha \quad (4.4)$$

is the percentage of the movements of each body part, where α indicates, respectively, the right side (R) and the left side (L) of infant’s body.

$$\bar{t}^l = \frac{\sum_i t_i^l}{n^l} \quad (4.5)$$

where n^l indicates the number of movement blobs belonging to the same l limb, which corresponds to the number of times l limb moves. \bar{t}^l is the average time of movement of each limb expressed in seconds.

$$\bar{t}^s = \frac{\sum_i t_i^s}{n^s} \quad (4.6)$$

where n^s indicates the number of movement blobs belonging to the same s state, which corresponds to the number of times states are active. \bar{t}^s is the average time of movement of each state expressed in seconds.

$$\bar{t}^\alpha = \frac{\sum_i t_i^l}{n^\alpha} \quad \alpha \in \{L, R\}, l \in \alpha \quad (4.7)$$

where n^α indicates the number of movement blobs belonging to α body side, which corresponds to the number of times α body side moves. \bar{t}^α is the average time of movement of each body side expressed in seconds.

$$\bar{v}^l = \frac{\sum_i \frac{dp_i^l}{dt_i^l}}{n^l} \quad (4.8)$$

is the average velocity of the movements of each limb calculated on the basis of the position data for the movement blobs of each limb and expressed in cm/s . $3D$ tangential velocities is calculated as $\frac{dp_i^l}{dt_i^l}$, where p is the $3D$ Euclidean distance. Then, the instantaneous velocities is averaged over the number of movement blobs belonging to the same limb, which is referred to as average velocity of each limb.

$$\bar{a}^l = \frac{\sum_i \frac{dv_i^l}{dt_i^l}}{n^l} \quad (4.9)$$

is the average acceleration of the movements of each limb always calculated on the basis of the position data for the movement blobs of each limb and expressed in cm/s^2 . The instantaneous accelerations, obtained by deriving instantaneous velocities, is averaged over the number of movement blobs belonging to the same limb, which is referred to as average acceleration of each limb.

$$\bar{V}^l = \frac{4}{3}\pi r^3 \quad (4.10)$$

is the estimated 95% spheric volume of each limb expressed in m^3 , which corresponds to volume of the 95% bivariate confidence sphere, which is expected to enclose approximately 95% of the $3D$ points inside each cluster.

In order to analyse the results of the experiment, a dataset has been built and it is described in subsection 5.4.1.1. By using this dataset 10 KPIs are calculated for each recording session, shown in table 5.5, that are discussed in subsection 5.4.1.2.

Markov Chain Model

States vector elements value can range from 1 to 16 as shown in figure 4.10.

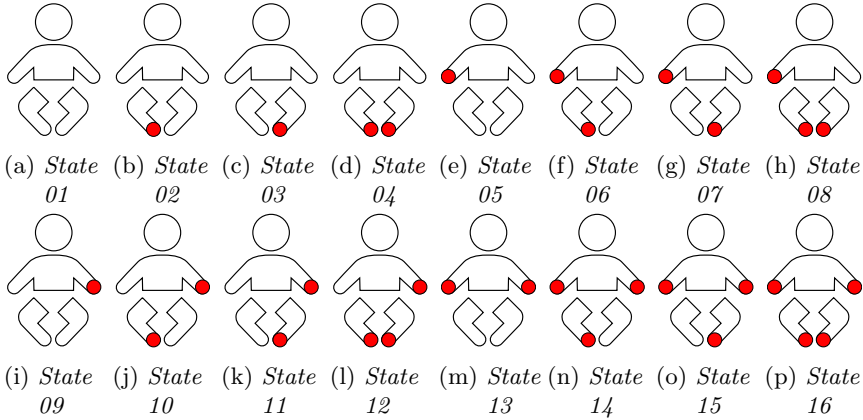


Figure 4.10: *Different movements states in which infant can be in. Red rounds indicate the “in movement” limbs.*

Since there is a temporal sequence of 16 possible combinations (states) in which the infant can be in, infant’s movements sequence can be modelled as a series of transitions states by using Markov Chain (MC).

MC is a natural formalism for modelling users’ behaviours and it is widely used in many applications. The experimental results are modelled with a MC, in particular using a transition matrix, in which the probabilities that infant changes his state are recorded. For example, the transition from state 1 to state 2 records the percentage of occurrences that infant has passed from state 1 to state 2. The MC model is formalised for measuring the movements change in a preterm infant’s GMA between the rounds of the experiment under consideration.

A MC is defined as $M = (S, P)$ and consists of states, i , in a finite set S of size n , and an $n \times n$ transition matrix:

$$P = \{p_{ij} | i, j \in S\}$$

The transition matrix P is row stochastic, i.e. for all states, i , $\sum_j p_{ij} = 1$, and P is assumed to be irreducible and aperiodic, i.e. it exists m such that $P^m > 0$.

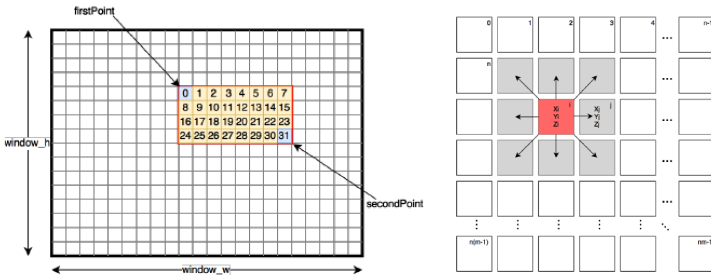
4.2.3.2.3 Extremities Tracking Algorithm

While previous data processing techniques are aimed at determining limb movement indicators, the following application has been developed to focus on limb extremities (hands and feet) and head tracking.

To get the infants’ extremities (hands, feet and head) the longest path approach is used. This approach expects to calculate the maximum distance from the centre of mass of the infant on a portion of the image relative to a limb or

the head. For example, the portion of image that has the edge of the centre of mass and depicts a leg can be used to obtain the position of the tip of the foot [204].

The implementation of this technique expects to transform a portion of a 2D image in a graph structure where a vertex is associated to every pixel. A progressive identification number is assigned to every node by an appropriate enumeration function that transforms the $X - Y$ pixel coordinates in a progressive number. Figure 4.11a shows an example of the labelling of pixel inside the area of the application of the algorithm.



(a) Labelling of graph nodes according to their position in the area of interest. (b) Transformation in a graph structure.

Figure 4.11: Longest path approach steps.

Once created all nodes of the graph, the realization of edges begins, taking in exam a node at a time and scanning by column and then by row. Every node is connected with the edge that ends in a representative node of the adjacent pixel from the examined pixel. A weight is associated to each arch, which represents the distance in millimetres between the points in the 3D space represented by pixels. This value is calculated for every arch, after getting the X , Y and Z values of nodes through the calculation of the Euclidean distance.

To minimize the computational complexity of the creation of the graph, the image given in input to the algorithm is the segmented image. Then, a graph is created, which concerns only the pixels that depict the infant. Figure 4.11b represents a scheme of the transformation of the image in a graph.

Once obtained the graph Dijkstras algorithm is used to identify the node at maximum distance. This algorithm calculates the cost of the shortest path that starts from an initial point to the other nodes.

The initial point is wisely chosen, and, in the case of the legs, a position on the diaper is chosen, obtained shifting to the right the position calculated from the centre of mass. The result of the execution of the algorithm is a vector, indexed by the identifier of the node, containing the minimal cost to reach every node. Scrolling the vector, the node which has the maximum cost is found, i.e.

the one that is located at the maximum distance from the initial node.

To get the path is sufficient to back through the path from the final node until the beginning memorising the identifications of the nodes which are along the path. Applying the function of inverse enumeration, it is possible to get the pixel coordinates that belong to the shortest path of the longer node.

The algorithm is recursively repeated for every portion of the image (feet, hands and head) and for every frame. Finally, the path and the node with maximum distance are drawn over each frame (see section 5.4).

To summarise, infants' extremities detection algorithm follows these steps:

1. For each pixel inside the area of interest, performing of:
 - a. Labelling of the pixel through the enumeration function;
 - b. Creation of a vertex in the indexed graph with the label of the pixel;
2. Scanning from left to right and from top to bottom, for each pixel performing of:
 - a. Computing of the Euclidean distance between the pixel and its neighbour;
 - b. Creation of an arch between the nodes by a weight equals to the computed distance;
3. Dijkstras algorithm application;
4. Scrolling of distances vector to find the node with the maximum distance;
5. Memorisation of crossed nodes identifier along the path by going back through the path until the initial node;
6. Conversion of nodes identifier in absolute coordinates by applying inverse labelling function;
7. Drawing on screen of paths and final points.

4.2.4 Infant Semantic Segmentation

Limitations of the proposed system are due to occlusions caused by external interventions that occur when nurses or physicians put their hands between the depth sensor and the infant to perform their activities.

Another problem may be caused when nurses or clinicians change the position of the infant inside the crib. Such new arrangements may adversely affect clustering goodness.

To avoid these issues, in a first moment only recording sessions in which there are not interactions with nurses or clinicians were analysed, as it is possible to

see later in section 5.4.1. Then to completely resolve these problems semantic segmentation with Convolutional Neural Networks is used.

Semantic segmentation is understanding an image at pixel level i.e, each pixel of the image has to be assigned to an object class. Apart from recognizing the object, it includes the delineation of the boundaries of each object. Therefore, unlike classification, dense pixel-wise predictions from models are needed.

4.2.4.1 Related Works

Semantic segmentation has several use cases such as detecting road signs [205], detecting tumors [206], detecting medical instruments in operations [207], colon crypts segmentation [208], land use and land cover classification [209]. Several applications of segmentation in medicine are listed in [210].

Techniques used in this field, before deep learning took over computer vision, were approaches like Texton Forest and Random Forest based classifiers. Then, as happened with image classification and in many visual recognition tasks [211, 212], Convolutional Neural Networks (CNNs) have had enormous success on segmentation problems [213, 214, 215].

On the argument, there are various semantic segmentation surveys such as the works by Zhu et al. [216] and Garcia et al. [217], where existing methods are summarised and classified, datasets and metrics are discussed, and design choices for future research directions are provided.

4.2.4.2 Convolutional Neural Networks

In this section five different approaches taken from literature and based on CNNs are presented in order to solve the problem of infants' images segmentation. Then, a novel architecture is described.

4.2.4.2.1 U-Nets

While developing a system for biomedical image segmentation, Ronneberger et al. [1] proposed a fully convolutional neural network architecture (figure 4.12) with 23 convolutional layers composed by a contracting path (left side) able to capture context and a symmetric expanding path (right side) that enables precise localization.

The contracting path follows the typical architecture of a convolutional network. It consists of the repeated application of two 3x3 convolutions (unpadded convolutions), each followed by a rectified linear unit (ReLU) and a 2x2 max pooling operation with stride 2 for downsampling. At each downsampling step they double the number of feature channels. Every step in the expansive path consists of an upsampling of the feature map followed by a 2x2 convolution

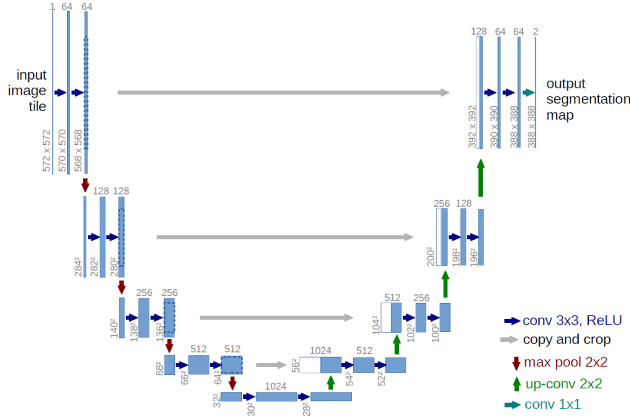


Figure 4.12: *Illustration of the U-Net architecture. Image taken from [1].*

(“up-convolution”) that halves the number of feature channels, a concatenation with the correspondingly cropped feature map from the contracting path, and two 3×3 convolutions, each followed by a ReLU. The cropping is necessary due to the loss of border pixels in every convolution. At the final layer a 1×1 convolution is used to map each 64- component feature vector to the desired number of classes.

In [2] Ravishankar et al. proposed the RS-UNet a cascade of two Fully convolutional networks (FCNs), one for segmentation and one for shape regularization (figure 4.13).

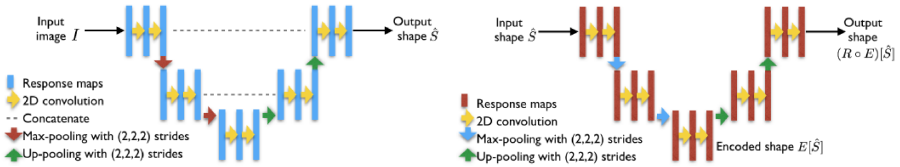


Figure 4.13: *Illustration of the cascade of vanilla U-Net and shape regularization networks. Image taken from [2].*

The segmentation network is the vanilla U-Net architecture, the classic U-Net revisited by removing two levels of max pooling and changing the ReLU activation function with a LeakyReLU. The shape regularization network contains shape encoder and decoder blocks, which project the incomplete shapes into latent representations using compositions of convolutions and non-linear mappings.

Finally, another modified U-Net architecture, with the best performance compared to the others, is proposed in this thesis. The structure remains

largely the same, but some changes were made at the end of each layer. In particular a batch normalization [218] is added after the first ReLU activation function and after each max pooling and upsampling functions (figure 4.14).

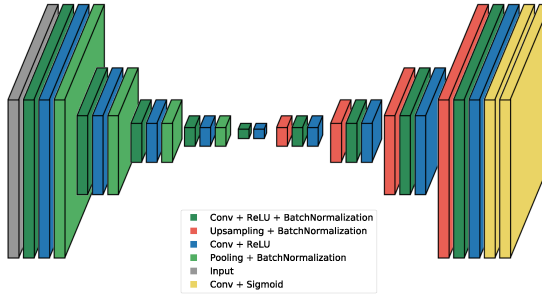


Figure 4.14: *Illustration of implemented modified U-Net architecture.*

4.2.4.2.2 SegNet

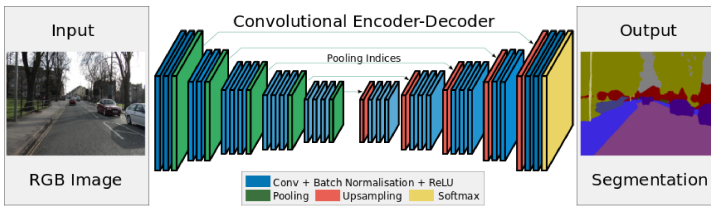


Figure 4.15: *Illustration of the SegNet architecture. Image taken from [3].*

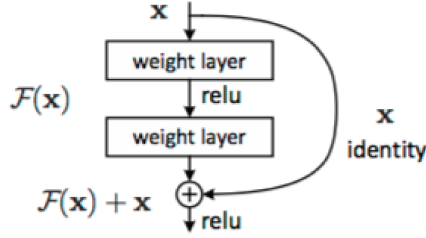
SegNet (figure 4.15) [3] has an encoder-decoder architecture based on the convolutional layers of VGG-16 from the Visual Geometry Group [219, 220], followed by a final pixelwise classification layer.

The encoder is a succession of 13 convolutional layers followed by batch normalization and rectified linear units. Blocks of convolution are followed by a pooling layer of stride 2. The decoder has the same number of convolutions and the same number of blocks. In place of pooling, the decoder performs upsampling using the max pooling indices from the corresponding feature maps in the encoder phase.

The upsampled maps are then convolved with a set of trainable filter banks to produce dense feature maps.

The final decoder output is fed to a multi-class soft-max classifier to predict pixel-wise labels for an output which has the same resolution as the input image.

4.2.4.2.3 ResNet

Figure 4.16: *Residual Unit*. Image taken from [4].

The architecture of Residual Network (ResNet) proposed by He et al. [4] is based on the Plain Network one, which is mainly inspired by the philosophy of VGG nets [221].

The convolutional layers mostly have 3x3 filters and follow two simple design rules: (i) for the same output feature map size, the layers have the same number of filters; and (ii) if the feature map size is halved, the number of filters is doubled so as to preserve the time complexity per layer. Downsampling is performed directly by convolutional layers that have a stride of 2. The network ends with a global average pooling layer and a 1000-way fully-connected layer with softmax. The total number of weighted layers is 34.

After the observation that the performance of neural networks actually gets worse when developed to a very great depth, due to the fact that the gradient vanishes when information back-propagates through many layers, He et al. decided to insert shortcut connections, which turn the network into its counterpart residual version with an architecture referred to as residual units. The residual unit (figure 4.16) performs the following computation:

$$x_{l+1} = ReLU(id(x_l) + f_l(x_l)), \quad (4.11)$$

where x_l denotes the input feature of the l -th residual unit, $id(x_l)$ performs identity mapping, and f_l represents layers of the convolutional transformation of the l -th residual unit.

4.2.4.2.4 FractalNet

As an alternative to ResNet, for building ultra-deep neural networks, Larsson et al. in [5] developed the FractalNet (figure 4.17), which network's structure, connections and layer types, is defined by $f_C(\cdot)$, where C denote the index of the truncated fractal $f_C(\cdot)$. The base case is a network that consists of a single

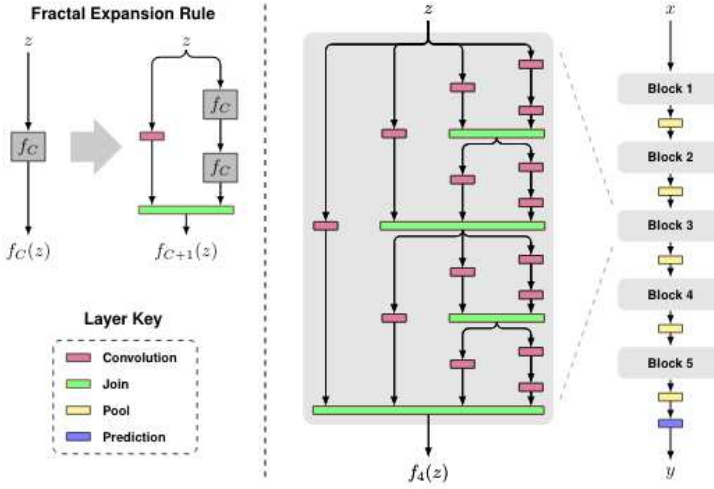


Figure 4.17: Illustration of the FractalNet architecture. Image taken from [5].

convolutional layer:

$$f_1(z) = conv(z), \quad (4.12)$$

and then successive fractals are defined recursively as:

$$f_{C+1}(z) = [(f_C \circ f_C)(z)] \oplus [conv(z)], \quad (4.13)$$

where \circ denotes composition, \oplus is the join operator and C corresponds to the number of columns, or width, of network $f_C(\cdot)$.

If depth, defined to be the number of $conv$ layers on the longest path between input and output, scales as 2^{C-1} , by using $f_C(\cdot)$ as a building block and stacking it with subsequent pooling layers B times, Larsson et al. yielded a total depth of $B \cdot 2^{C-1}$, as in convolutional networks pooling layers are interspersed.

4.2.4.3 Adopted Metrics

To measure the performance of different segmentation approaches, several metrics are proposed in literature.

In this thesis two set of metrics are adopted: the first set measures how much the system is able to separate the infant silhouette from the background, while the second one measures the ability of the system to correctly classify the silhouettes.

The first metric is the Jaccard index, also known as Intersection over Union (IoU), which is used for comparing the similarity and diversity of sample sets.

It measures similarity between finite sample sets, and is defined as the size of the intersection divided by the size of the union of the sample sets:

$$JaccardIndex = \frac{true_{pos}}{true_{pos} + false_{pos} + false_{neg}}, \quad (4.14)$$

where the positive class is the infant silhouette and the negative is the background. It is averaged across all the test images.

The second metric is the Sørensen–Dice Index [222], also known as the Overlap Index, which is used for comparing the similarity of two samples. It is the most used metric in semantic segmentation, and is computed as:

$$DiceIndex = \frac{2 \times true_{pos}}{2 \times true_{pos} + false_{pos} + false_{neg}}, \quad (4.15)$$

where the positive class is always the infant silhouette and the negative is all the rest.

The second set of metrics is composed by the average accuracy, precision, recall and *f1* score averaged across all the test images. Considering that the ability to discriminate the background has been already measured, those metrics are evaluated just on the silhouette pixels. These metrics are computed as:

$$Accuracy = \frac{true_{pos} + true_{neg}}{true_{pos} + true_{neg} + false_{pos} + false_{neg}}, \quad (4.16)$$

$$Precision = \frac{true_{pos}}{true_{pos} + false_{pos}}, \quad (4.17)$$

$$Recall = \frac{true_{pos}}{true_{pos} + false_{neg}}, \quad (4.18)$$

$$F1score = \frac{2 \times Precision \times Recall}{Precision + Recall}. \quad (4.19)$$

Chapter 5

Results and discussion

5.1 SINC cloud-based healthcare architecture evaluation

Table 5.1: *Database Traffic.*

Traffic	Value per hour (MByte)
Received	471
Sent	832

Table 5.2: *Database Connections.*

Connections	Value per hour
Max contemporary connections	578
Failed attempts	0

Table 5.3: *Query Statistics.*

Queries	Value per hour
select	386 <i>k</i>
insert	36
update	27
delete	8

Some initial studies have been conducted by evaluating system performance in order to validate system usability. Some first results have been reached from this system implementation regarding the integration of the patient monitor, the bilirubinometer and the transcutaneous bilirubinometer.

They demonstrate that the solution provides good performance, by improving infants' personal data availability by medical staff members and permitting data sharing.

Table 5.1 and table 5.2 present, respectively, the database performance about traffic and about connections, and table 5.3 shows the overall of the query statistics.

The acquired results can be considered as indicative since the experiments are conducted in a real case scenario where the specific service is utilized in order to transmit and receive medical data.

As mentioned in chapter 3, a web platform is developed, where members of the hospital staff can log in via mobile or stationary devices (e.g., workstation, personal computer, tablet) through an authentication system (SSO Single Sign On) in order to increase the security of shared data.

Each of them has a customised interface depending on their roles and on the operations that they can do.

It is a highly configurable modular platform that can be easily adapted according to needs to be managed. In fact, the platform is created considering the possibility to expand it with new tools as new devices and new functionalities are integrated in the healthcare infrastructure.

The platform permits to browse personal data of the patient's medical record and enter new patient data.

Moreover, the tools described in section 3.3.2.1 and in Chapter 4 were implemented and tested by physicians and nurses of the NICU of the Women's and Children's Hospital "G.Salesi" of Ancona.

5.1.1 The web interface usability test

A web interface usability test was performed.

In a first phase, participants (6 physicians and 4 nurses) were invited to test the system one after the other on a computer desktop in the NICU.

The SINC expert first introduced explained the purpose and procedure of the testing. Participants were assured of their privacy and formal consent was obtained. The hospital ward layout was adapted to ensure proper testing and observation with no influences on comments and suggestions from other member of the hospital staff. A short survey on participant familiarity with technology was asked to every participant before the testing.

The participants was then given the website name and asked to explore the web based SINC system on their own. The SINC expert sat behind the participant and gave no instruction to the participant unless him or her could not proceed after repeated efforts. The participant was also encouraged to make comments during the navigation. Participant behaviours and comments

are recorded using observation metrics and detailed notes. The metrics included 20 tasks to complete on the website (10 on “Bilirubin Tool”, 5 on “Activities Monitoring Tools” and 5 about the other tools), time needed on each task, and if a task was performed without error, with error, or needed assistance.

Results showed a very good usability impact and some comments, mainly on button positioning and icons meanings, are currently used for renew SINC version. On average all usability test were performed with no suggestions. Average time to complete a single task was of about 26 seconds. More than 85% of final usability surveys judged the web application with a very good feeling.

The same set of tests was performed in a second phase using a tablet to prove the effectiveness of the touch interface. Final results confirmed previous results; suggestions were again mainly related to icons meanings and their usability when no text is shown. In the survey 76% of users affirmed that a tablet use is the preferred one in the future of medical data sharing systems.

5.2 Bilirubin Tool

Figure 5.1 shows the web interface of “Bilirubin Tool”. It is obviously connected with data coming from EHR, which can be seen summarised at the top of the web page in a pop-up window.

Physicians or nurses, once selected the involved infant and entered the tool for the first time, are asked, if they have not already done during the registration phase, to fill in the risk factors sheet (figure 5.2), both primary and secondary, which are used by the algorithm described in section 4.1.4 to determine the time intervals between one measurement and another and to decide the curve of which GAs group to take into consideration for the comparison with the measurements coming from the instruments. This time interval is projected as a countdown on the top of the page and is associated with a reminder for nurses to do the bilirubin measurement within the predetermined time or in a warning that represents the need for an immediate measurement.

Once a TcB or a TSB measurement is made, the value is displayed in real time on the PC monitor and it can be viewed with infant’s historical values of bilirubin listed in a table or in a graphical way. Furthermore, it is automatically compared with the corresponding guidelines curve value, depending on the infant’s GA and PA. After the automatic comparison, the system displays again a reminder, a warning or an alarm, if a therapy is required, i.e. phototherapy or BET.

From the graphs it is possible to see the progress of bilirubin values over the time in relation to the curves of the different monograms as shown in figure 5.1. Of course, only the infant’s related GA curve is plotted, or that corresponding

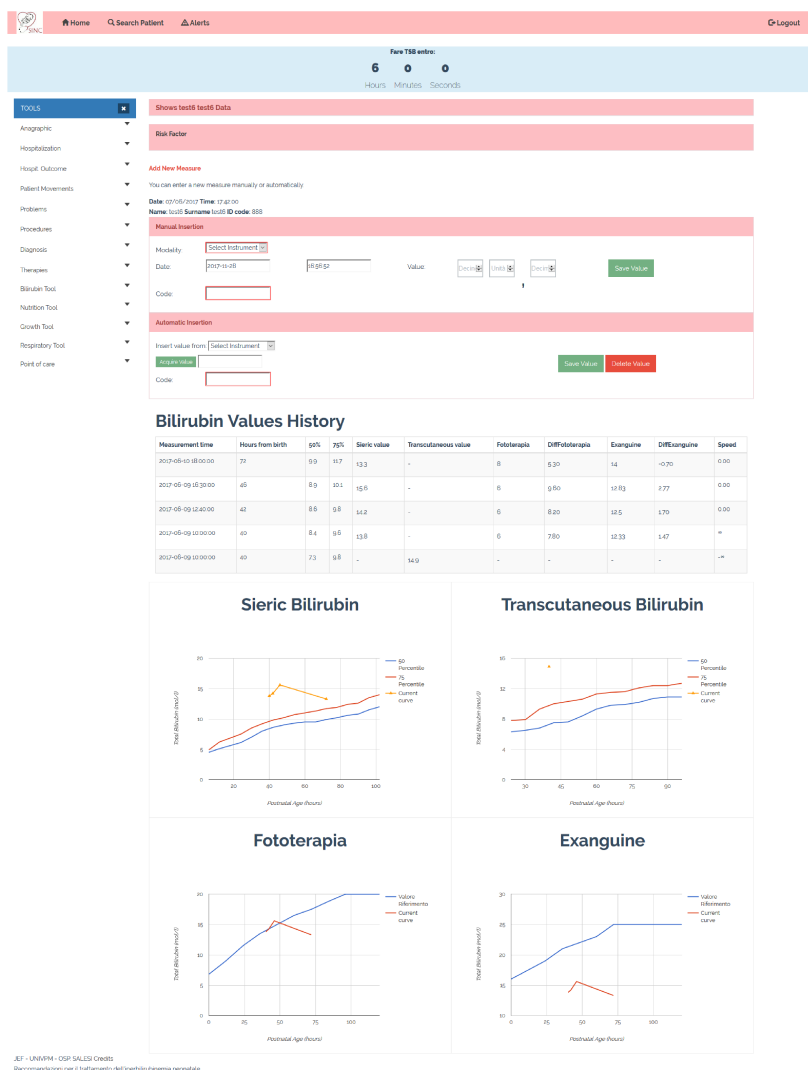


Figure 5.1: SINC “Bilirubin Tool” interface.

to the previous GAs group, when a primary risk factor is present. Also in the tables, besides the value, the numerical difference with the values of the corresponding curves are shown, in this case also with the relative current PA.

In addition, as already mentioned, physicians may change the interval between two consecutive checks of bilirubin measurement, which changes the algorithm countdown control parameters. Doctors, generally, increase the frequency of controls if there is a visible loss of appetite or numbness, factors that have not yet been included in the algorithm because they are difficult to

The screenshot shows the SINC 'Bilirubin Tool' interface. At the top, there is a navigation bar with 'Home', 'Search Patient', 'Alerts', and 'Logout'. Below this is a 'COUNTDOWN' bar. The main content area is titled 'Shows test6 test6 Data'. On the left, there is a 'TOOLS' menu with a list of tools: Anagraphic, Hospitalization, Hospit. Outcome, Patient Movements, Problems, Procedures, Diagnosis, Therapies, Bilirubin Tool, Nutrition Tool, Growth Tool, Respiratory Tool, and Point of care. The 'Bilirubin Tool' is selected. The main content area is titled 'Risk Factor' and is divided into two columns. The left column is titled 'Risk factors from guidelines:' and contains four sections: 'Isimmunization' (radio buttons for Yes/No), 'Maternal Rh' (radio buttons for Positive/Negative), 'Faterly Rh' (radio buttons for Positive/Negative), and 'ABO' (radio buttons for Yes/No). The right column is titled 'Optional risk factors:' and contains three sections: 'Ponderate decline > 10% in 48 h' (radio buttons for Yes/No), 'Familiarity with phototherapy' (radio buttons for Yes/No), and 'Breastfeeding' (radio buttons for Yes/No). A green 'Save Value' button is located below the optional risk factors. Below the form, there is a section for manual measurement with the text 'Add New Measure' and 'You can enter a new measure manually or automatically.' Below this are fields for 'Date: 07/06/2017', 'Time: 17:42:00', 'Name: test6', and 'Surname: test6 ID code: 888'.

Figure 5.2: SINC “Bilirubin Tool” interface - Risk Factors.

quantify with indicators.

In addition, in the interface there is also a section for manual insertion of the measurement, in case measuring instruments not interfaced to the DB should be used, before they are connected. In this case it is necessary to manually enter the type of instrument used (if for a serum or a transcutaneous measurement), the date and time of the measurement, which is used to calculate the current PA, the value of the measurement, for which a check has been set in terms of minimum and maximum allowed values, and the identification code of the healthcare staff member who performed the measurement.

5.2.1 Data Analysis Results

As said, in the previous section the algorithm takes in input the bilirubin values measured each time by the nurses and automatically sent by the measuring instruments to the DB, the bilirubin threshold values of the nomograms of SIN guidelines, data inserted by nurses or physicians about possible risk factors, data coming from the “Anagraphic Tool” and “Growth Tool” and the workflow rules, which derive from SIN guidelines and from the experience of the physicians, and gives in output automatic comparisons of measurements, reminders, warning and alarms.

Each step of the algorithm has been marked with a number, and in the database is saved in addition to a table relating to the measured bilirubin values associated with the children’s code, also a table with, for each child, the step in which the algorithm is located and its timestamp, the number of the

step from which it came, and the value of bilirubin that brought the algorithm in that step. In this way the time sequence of the steps of the algorithm is available, which makes it easier to compare with the actual clinical practice.

In this way it was possible to perform a blind test to evaluate the algorithm goodness. Physicians were asked to carry out their clinical practice in the diagnosis and treatment of hyperbilirubinaemia, following as much as possible the guidelines and noting their actions and decisions for 100 treated children, without being aware of the decisions made at the same time by the algorithm. These annotations were then compared with the time trend of the algorithm described above to see the correspondence and discrepancies with the decisions made by physicians.

It was found that in 75 out of 100 cases there were no discrepancies between the decisions (reminders, warnings and alarms) taken by the algorithm and the actual decisions taken by physicians.

The remaining 25 cases, where differences were found, were carefully analysed with the help of expert physicians and it was found that:

- In 3 cases, the difference between the decisions taken is due to the fact that in comparison between measured bilirubin values and nomograms, in the case of intermediate PA values compared to those present in the nomogram of the guidelines, the algorithm makes a linear interpolation between the two extremes of the range within which the PA is included, while the nurses make an approximate average between these limit values.
- In 15 cases, the difference between the decisions taken is due to the fact that when comparing the value of the first measurement of TcB with the related nomogram, the algorithm takes into account the nomogram of figure 4.1, with in addition the rule that independently from PA if TcB exceeds 11 *mg/dL*, the TSB is required, while nurses often do not consider the nomogram but only apply the last rule of TSB required if TcB is ≥ 11 *mg/dL*.
- In 2 cases jaundice was evident, so a measurement of TSB was immediately carried out, while the algorithm, not being able to recognize the symptoms, required a TcB.
- In 2 cases, the presence of loss of appetite and numbness in the child led the doctor to request a TSB despite the fact that the size of the TcB did not imply it (the values were however at the limit); in 3 cases the presence of loss of appetite and numbness, together with the presence of a strong weight loss and other factors led the doctor to start phototherapy with values lower than the thresholds provided by the nomogram for phototherapy (the values were in any case the values were as follows).

From these results it is evident that in some cases the algorithm is more precise than human decisions, in other cases, however, some deficiencies of the

algorithm are evident, which concern in particular the presence of some symptoms of hyperbilirubinaemia that are noticed by the medical staff, while the algorithm does not consider, such as the colour of the skin tending to yellow, the lack of appetite and numbness. Therefore, consideration is already being given to how these factors can be added to the decision algorithm. The secondary risk factors considered are only familiarity with phototherapy, breastfeeding and a weight loss $\geq 10\%$, while it is important to consider also the loss of appetite, numbness and the colour of the skin. These indicators are difficult to quantify, so they will initially be considered as binary values, then they can be entered as scaled values, for example from 1 to 10. Moreover, for the time being, secondary risk factors are only required at the beginning of the decision-making process, while it is clear how important it is to update these factors over time and take them into account in decisions. For example, weight loss is taken into account when risk factors are recorded, in order to make the decision about the time interval between measurements checks, but for how it has now been structured the algorithm a progressive decrease in weight over time is not considered, even if it can be useful for decision making.

5.2.2 Discussion

As already mentioned, the “Bilirubin Tool” interface and the decision-making algorithm workflow (figure 4.6) have been designed and developed after several interviews with 2 neonatologists and a nurse acting as domain experts.

Very often, unfortunately, it happens that CDSSs, even though they have the potential to help and support physicians and nurses in daily clinical practice, are not used by healthcare professionals, because they are not user-friendly and, indeed, they are seen as tools that make them lose time and sometime as something that remove physician’s importance or dignity at work. For these reasons, involving medical staff in the application design phase was essential to avoid further problems of acceptance of the proposed solution.

After the interviews with doctors the strategic knowledge is outlined in order to delimit the aims of the system, which are to:

- promote and facilitate the use of the guidelines, as studies have demonstrated that guidelines following helps to reduce ABE and kernicterus cases;
- avoid over-precautionary behaviours that lead to an excessive use of phototherapy, which in some cases is resulted to be an unnecessary treatment, and, thus, lead to the NICU overcrowding, as this is the only hospital ward where phototherapy is carried out;
- facilitate the exchange of information between the three hospital wards where bilirubin measures are carried out (NICU, Neonatal Pathology, and

Pediatric Nursery) in order to create a single, standardised treatment protocol;

- create a database to allow future studies to be conducted in order to verify, for example, that following the guidelines actually reduces the number of ABE and kernicterus.

The decision-making algorithm developed and described in section 4.1.4 consists in an evidence-based CDSS which automates SIN guidelines, used as the general rules and the knowledge base of the algorithm, but also adds physicians' expertise at some critical points. In particular, it departs from the guidelines, using instead the observations and experience of physicians, in the choice of time intervals between checks and in the selection of the curve corresponding to the previous GAs group in case of Rh isoimmunisation or ABO haemolytic disease.

As a result, the algorithm provides reminders to remember the bilirubin measurement, warnings to emphasize the need for an immediate measurement, and alarms when a therapy (phototherapy or BET) is required.

A critical point of the algorithm is the inability to automatically recognise some risk factors that are not present from the beginning but may appear over time, e.g., loss of appetite or numbness. For this reason, the doctor is given the possibility to manually vary the frequency of the controls. Even the skin colour information cannot be automatically entered as an algorithm parameter. If jaundice begins to show obvious symptoms, such as yellow skin colour, the doctor immediately performs a TSB measurement. These parameters will be inserted in the update version of the algorithm, always giving the physician the possibility to do it manually.

The strength of the proposed EB-CDSS lies in the simultaneous exploitation of both a physical infrastructure that allows the interconnection of the instrumentation used to make bilirubin measurements that in this way are automatically loaded on the SINC DB and directly visible from the algorithm, completely eliminating the manual collecting laborious work and the resulting possibility of typing and comparison errors, and a web-based platform where there are other tools in addition to Bilirubin Tool, so the system can read directly from the DB some parameters used by the algorithm, e.g., GA, PA, birth weight, current weight. This leads it to be better than any other system proposed in section 4.1.1, where manual entries are provided not only for bilirubin measurements but also for values related to GA, to PA and so on.

In this way, all the objectives presented in section 4.1.3 have been achieved: the system use and process data collected in a single DB from all the instruments used for the measurement of serum and transcutaneous bilirubin that are located in the three hospital wards, namely 2 spheric bilirubinometers and 3 transcutaneous ones, in order extract useful information on jaundice diagnosis,

to facilitate the exchange of information between different wards and to standardise the treatment protocols of neonatal jaundice, by creating a valid model for all the birthplaces of Marche Region.

Another advantage introduced by the system is the reduction of the waiting time necessary for the doctor to accept the request for the start of the phototherapy treatment. While before the nurse had to seek the doctor to receive the consent, now the doctor can accept the request by answering the email that is generated by the system when the step of “phototherapy start request” is reached.

Finally, when the algorithm reaches the last step of “hospital discharge”, a report in pdf format is automatically generated, which can be used as medical report to be delivered to the parents of patients, to be entered in the ward medical record and also sent to the regional EHR. In any case, if the infant remains hospitalized for reasons other than hyperbilirubinemia, routine TcB measurements are continued at regular intervals, which are saved on SINC DBaaS. They are displayed on the Bilirubin Tool interface in the temporal trend of historical bilirubin values and can also be saved in the medical report.

In addition, even after the hospital discharge, the system provides the possibility of entering the scheduled follow-up data. Follow-up measurements can be taken at the “G. Salesi” Hospital or in peripheral hospitals, which are closer to the parents’ residence. Up until now, when parents went to peripheral hospitals, the bilirubin measurement value was lost, while now there is the possibility of setting up an account for peripheral hospitals to allow storage of the new measured bilirubin value. In the same way it will be possible to save the bilirubin values measured by family paediatricians in further follow-ups: it will be sufficient to provide them with an account where they can enter such data.

In conclusion, a web-based decision support tool based on clinical practice guideline was developed and implemented. The tool revealed rapid acceptance, and its use was associated with increased observance of SIN clinical guidelines. Physician evaluations indicated that “Bilirubin Tool” application made the SIN guidelines look easier to use, more practical, and more significant for physicians and nurses, which is a particularly important goal to reach.

5.3 Respiration Tool

An application with a user-friendly interface was realised, which physicians and nurses of the hospital ward can easily use.

Entering the Respiration Tool, they find a graphical interface where they can select the measurement points on the thoraco-abdominal area of the infant (figure 5.3) and then in real time the system displays the path of temporal depth measured by RGB-D camera from which the respiratory signal and the

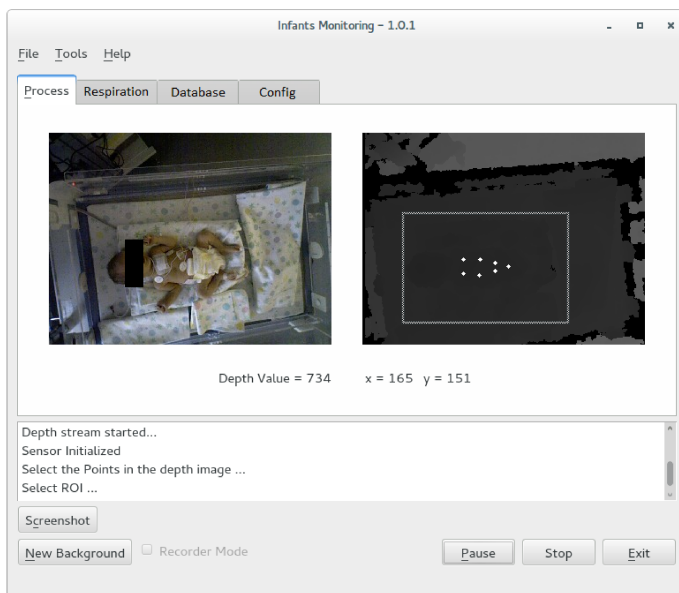


Figure 5.3: Screenshot of interface developed with the Qt Framework while it is running on Cubieboard2.

respiratory rate are derived.

In particular, in “Process” window there is the RGB stream video on the left and the depth stream video on the right, where it is possible to select a region of interest and to monitor the selected points on the infant chest. Then in “Respiration” window it is possible to see the time trend of the acquired depth values of the chest points. Finally, in “Database” window it is possible to see these values and the relative timestamp and by clicking the button “Save Data” it is also possible to save them in a .csv file in the local PC in order to post-process data.

These data are also sent to the SINC DBaaS in order to be stored for further analysis. Saving these data and data extracted from the patient monitor (section 3.2.1) on the same DBaaS allows to compare the respiratory rate obtained with the RGB-D camera with that measured by the gold standard.

5.3.1 Data Analysis Results

Figure 5.4 reports an example of the respiration signal acquired with the RGB-D camera (blue line) with the filtered signal superimposed (red line) on a time window of 10s. The filtered signal is used to detect better the peaks of the respiratory signal and to calculate the mean value of the RR period compared with that obtained from the patient monitor.

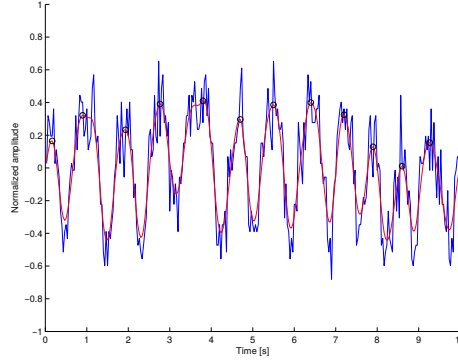


Figure 5.4: Example of respiration signal measured from RGB-D camera (blu line) and of the filtered signal (red line) on a time window of 10s.

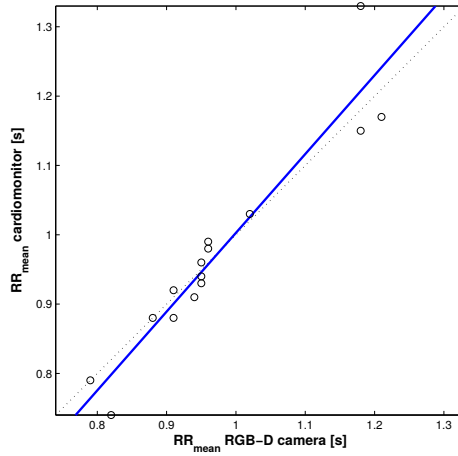


Figure 5.5: Scatter plot and regression line of RR mean values.

Table 5.4: Mean RR values measured by RGB-D camera and patient monitor.

Patient ID	Device	Mean RR values (s)				
		Test 1	Test 2	Test 3	Test 4	Test 5
1	Patient Monitor	0.98	0.91	0.92	0.88	0.96
	RGB-D Camera	0.96	0.94	0.91	0.88	0.95
2	Patient Monitor	1.17	1.33	1.15	1.03	0.99
	RGB-D Camera	1.21	1.18	1.18	1.02	0.96
3	Patient Monitor	0.93	0.94	0.79	0.74	0.88
	RGB-D Camera	0.95	0.95	0.79	0.82	0.91

This comparison is only made possible by the fact that the various instruments are all integrated into the same infrastructure.

The scatter plot and the regression line, reported in figure 5.5, show a good correlation between the measured data with respect to the data derived from the reference instrument. The agreement between the two methods is also confirmed by the Pearson’s correlation coefficient that is equal to 0.95.

Table 5.4 reports the mean values of the RR period measured both from the RGB-D sensor and the patient monitor, for each test and for each patient.

The breathing rate (breaths per minute), mentioned in section 4.2.2, can be easily inferred from the RR period through this simple formula:

$$BR(bpm) = \frac{60}{RR_{period}(s)}. \quad (5.1)$$

Comparing these values with the RDS thresholds, it appears that 2 of the infants under examination had a high respiratory rate, therefore, to be kept under control.

5.3.2 Discussion

The work was mainly focused on the basic hardware and software architecture of the system, including the web interface, and only preliminary tests were conducted in the experimental phase.

Though, experimental results showed that the proposed method can correctly measure the respiratory rate in preterm infants, compared to gold standard, and it can activate an alarm signal when respiratory rate values go out of the physiological range, especially when the respiratory rate is higher than normal values.

The RR_{period} , in fact, is instantly compared with threshold value, that discriminates between the disease absence and its presence.

In the future a machine learning approach will be used to classify infants’ in “healthy” and “at risk” classes, for what concerns RDS. This approach will involve information about thoraco-abdominal balance (section 4.2.2).

In fact, the possibility to select the measurement points on the thoraco-abdominal area from the web interface, described above, allows to study the displacement of the chest and abdomen in a separate way and so to see if there is the wave movement typical of RDS disease.

5.4 Movement Tool

A similar framework is realised for the “Movement Tool” interface (figure 5.6), that permits the real-time visual monitoring of the infant during the acquisition. It displays in real time the RGB stream video on the left and the real-time “colour-map” of the infant movements on the right.

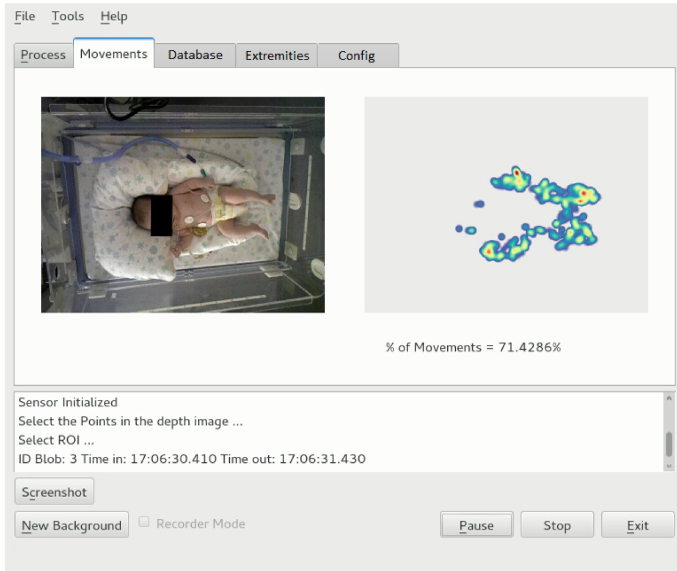


Figure 5.6: “Movement Tool” graphic interface.



Figure 5.7: “Colour-map” of the movements extracted from the software.

The “colour-map” (figure 5.7) is a graphical representation of data where the variations of the values contained in the depth matrix (movement blobs) are represented as colours. In particular, by visualizing the “colour-map” it is possible to get an idea of the amplitude of the movements of the infant and of their duration: the “colour-map” assumes colours that go in a scale from blue to red depending on the duration of a movement blob.

From the graphic interface of the “Movement Tool” it is also possible to see in real time the changing percentage of total movement calculated as the total movement time of the infant (the sum of the timestamps of all movement blobs)

on the duration of the acquisition. This percentage updates automatically every second as the acquisition progresses over time.

By clicking on the “Database” window at the top of the interface it is possible to see the list of movement blobs over the time. Each movement blob is characterized by a unique ID and several timestamps, as the movement has a certain length time. For each timestamp, it is possible to view the x , y and z coordinates of the relative movement blob centre of mass.

These data are sent to the SINC DBaaS in order to be stored for further analysis. By clicking the button “Save Data” it is also possible to save them in a .csv file in the local PC in order to post-process data as shown in section 5.4.1.

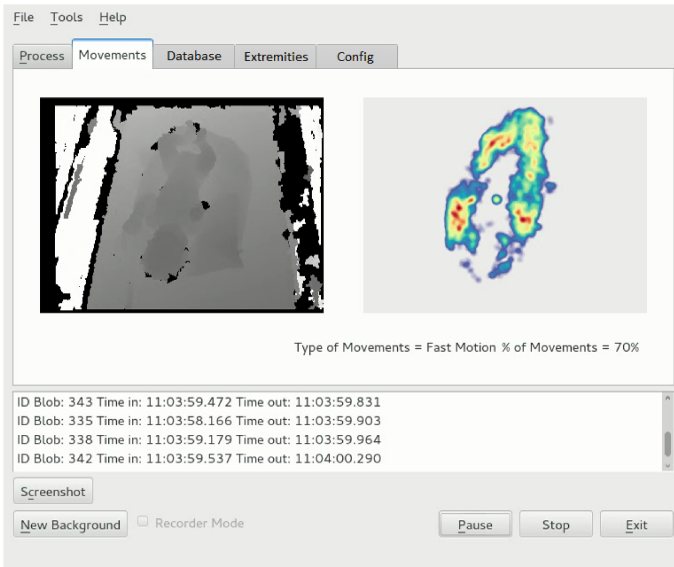


Figure 5.8: “Movement Tool” graphic interface with velocity information.

An upgrade of the just described version of the “Movement Tool” interface permits to visualise the depth stream video on the left, in order to preserve privacy, the “colour-map” on the right, to qualitatively monitor infant’s movements in real time, and, in addition to the total percentage of movements, always displayed, it is possible to see on the monitor if the movement in that instant is fast, slow or absent (figure 5.8).

It was possible to obtain this information by dividing the space covered by a tracked movement blob by the time length of the blob itself at the end of each movement. The velocity thus obtained is instantly compared with 2 thresholds values, one that discriminates between non-movement and movement and one that discriminates between slow and fast movements. These threshold values were determined empirically by showing some test acquisitions to the NICU

physicians. In the future a machine learning approach will be used to classify movements in slow, fast or absent and for this reason a dataset is being built recording infant’s activities characteristics (i.e. crying, sleeping, eating, external activity, slow motion, fast motion) and the relative timestamp during the acquisition.

In figure 5.9 there is a series of interface screenshots extracted from a real time acquisition, which shows the sequence of a fast movement 5.9a, a slow movement 5.9b and then the absence of movement 5.9c. During the acquisition the child has progressively calmed down and consequently it is possible to see the decrease of the total percentage of movements, which is related to the current timestamp.

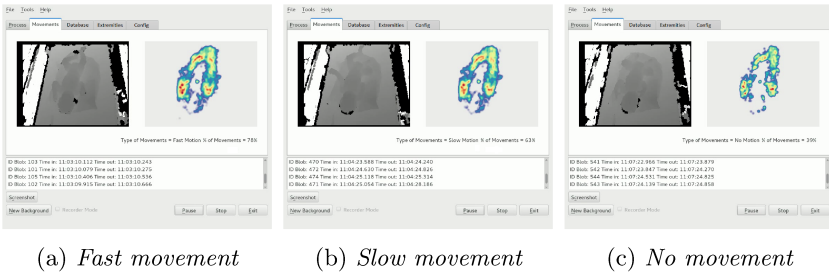


Figure 5.9: “Movement Tool” interface screenshots that represent a sequence of fast movement 5.9a, slow movement 5.9b and the absence of movement 5.9c during a real-time acquisition.

Finally, by clicking on the “Extremities” window it is possible to see the real-time tracking of the body extremities, i.e. hands, feet and head, as shown in figure 5.10. The image on the right is the result of the elaboration described in section 4.2.3.2.3, where the path (in green) and the node with maximum distance (in yellow) are depicted over each frame during the acquisition to track body extremities.

Experimental results showed that the procedure works well when applied on foot and head tracking, less well when applied to hand tracking, because often the infant carries his hands above the body and therefore segmentation does not allow the distinction between extremities (hands) and the rest of the body.

Concerning the computational cost of the entire calculation procedure, a delay with respect to the video stream was noted, due to the fact that the algorithm requires more time than the frame time of the original video. Experimental analysis showed that the problem is the step of edges creation. To implement the graph, Boost Library is used [223], which offers a lot of pre-compiled and optimized functions, but it is unable to ensure sufficient performance to the application scenario. To minimize the time, the algorithm must be applied to the smaller portion of image that contains the limbs under examination.



Figure 5.10: “Movement Tool” graphic interface with extremities tracking.

5.4.1 Data Analysis Results

In this section results related to the data post-processing phase described in section 4.2.3.2.2 are presented. After the exportation of depth values and timestamps related to movement blobs during an acquisition, data were analysed in post-processing in order to extract some important indicators and models useful to describe infant movement characteristics.

5.4.1.1 MIA (Motion Infant Analysis) dataset

MIA dataset¹ consists in the states vector described in section 4.2.3.2.2, along with the corresponding timestamps, derived from depth measurements collected by an RGB-D sensor placed perpendicularly above an infant, lying in a supine position on the crib, at a distance of 70 cm, normally directed to the subject.

The preterm infant under examination is a male hospitalised in the NICU of the Women’s and Children’s Hospital “G.Salesi” of Ancona (Italy) of 37 + 1 weeks of GA, with a GA at birth of 31 + 2 weeks and a weight of 2050 g.

For data collection the time interval between one meal and the following is chosen. During this period, of about 4 hours, the infant can be awake or asleep. This time interval is divided in recording sessions of 300 seconds each

¹<http://vrai.dii.univpm.it/mia-dataset>

one, which allowed to discard those records in which there is an interaction with a nurse or a clinician.

As a result MIA dataset contains a timeline of 16 different states in which the infant under examination was in, for a total period of 35 recording sessions.

5.4.1.2 KPIs and MC Transition Matrix

Data of table 5.5 show the presence of three long periods of inactivity, affecting recording sessions 8, 10–12, 32–33, in which the infant is completely stationary. During the other recording sessions inactivity moments (state 1) alternate with moments during which infant moves one or more limbs (states 2 to 16). These information are also clearly visible in figure 5.11.

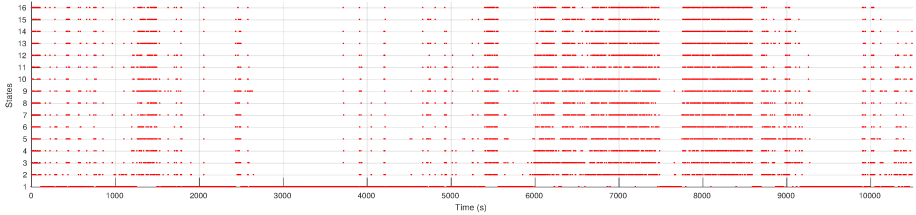


Figure 5.11: *States activation sequence during time.*

Thanks to the $M_{\%}^G$ KPI it is possible to see that the percentage of total infant's movement averaged over 35 recording sessions is equal to 34.14%. In particular, 17.76% is the percentage of movement for RL , 16.91% for LL , 18.05% is the one for RA and 18.67% for LA .

The $M_{\%}^l$ KPI also highlights that over the 35 recording sessions the upper limbs, RA and LA (red-highlighted), move more than lower limbs, RL and LL (yellow-highlighted).

$M_{\%}^G$ KPI says that the right side of the body (RL and RA) and the left one (LL and LA) are characterized by approximately the same percentage of movement over the total recordings, i.e., they move on average for the same time.

Although on average arms move for the same time, thanks to \bar{t}^l KPI, it is clear that LA ($\bar{t}^{LA} = 0,60 s$, red-highlighted) makes longer movements rather than the RA ($\bar{t}^{RA} = 0,51 s$) and also with respect to the legs ($\bar{t}^{RL} = 0,49 s$, $\bar{t}^{LL} = 0,52 s$).

This also influences the average duration of the movements of the left part of the body ($\bar{t}^L = 0,97 s$, red-highlighted), which is greater than that of the right side ($\bar{t}^R = 0,85 s$).

\bar{v}^l KPI gives information about movements average velocity: RL makes jerks and very fast movements ($\bar{v}^{RL} = 21,44 cm/s$, red-highlighted), otherwise RA

makes slower movements ($\bar{v}^{RA} = 13.98 \text{ cm/s}$, yellow-highlighted) than other limbs.

This is confirmed also by \bar{a}^l KPI, greater for *LA* and lower for *RA* ($\bar{a}^{RL} = 100,71 \text{ cm/s}^2$, red-highlighted and $\bar{a}^{RA} = 57,04 \text{ cm/s}^2$, yellow-highlighted).

From \bar{V}^l KPI information about movements amplitude can be obtained: legs, as expected, cover larger volumes (red-highlighted) than the arms as they perform larger movements.

Figure 5.11 shows the activation of each state s during the registration period. From this figure it is clear that infant is stationary for most of the time (state 1) and that remains completely stationary for three long periods of time, as already highlighted in table 5.5. When the infant is moving (states 2 to 16), the state, in which he is in, varies very quickly and for this reason it is difficult to view the state changes in the image.

Table 5.5: Data results and KPIs.

RS	M_G^α				M_L^α				M_α^α				\bar{t}^l [s]				\bar{t}^α [s]				\bar{v}^l [cm/s]				\bar{a}^l [cm/s ²]				V^l [m ³]			
	RL	LL	RA	LA	R	L	RL	LL	RA	LA	R	L	RL	LL	RA	LA	RL	LL	RA	LA	RL	LL	RA	LA	RL	LL	RA	LA				
01	44.86	33.73	23.22	28.80	18.13	40.37	28.55	0.98	0.68	0.65	0.63	2.38	1.00	12.24	32.06	20.70	41.92	39.49	151.25	81.96	217.85	0.16	0.23	0.15	0.30							
02	17.41	4.76	7.31	12.12	7.85	14.01	11.76	0.44	0.65	0.89	0.50	1.00	0.84	24.32	7.76	18.41	27.10	129.82	21.36	74.06	87.71	0.24	0.20	0.18	0.16							
03	10.67	3.98	5.49	4.90	5.79	7.35	8.55	0.45	0.67	0.76	0.73	0.68	1.49	55.74	24.42	10.16	31.05	319.63	91.35	26.83	81.42	0.83	0.24	0.19	0.18							
04	5.14	2.05	2.33	2.19	1.92	4.21	2.77	0.74	1.35	0.70	0.62	0.72	2.00	114.98	8.28	7.01	32.03	561.68	27.82	15.96	154.97	0.83	0.18	0.14	0.22							
05	80.34	28.70	34.89	41.31	49.97	56.74	66.45	0.54	0.54	0.60	0.68	0.80	1.11	26.27	37.89	16.13	32.40	96.59	184.84	64.33	118.84	0.26	0.24	0.18	0.19							
06	14.88	7.49	7.57	3.07	6.43	8.88	11.81	0.85	0.80	0.38	0.80	0.78	1.11	13.75	13.79	7.01	24.49	31.34	65.13	24.40	103.53	0.18	0.14	0.22	0.22							
07	1.27	0.72	0.59	0.27	0.44	0.83	0.77	0.43	0.59	0.80	1.33	0.50	1.15	82.25	12.98	10.33	29.32	587.88	36.94	28.99	86.98	0.32	0.26	0.23	0.23							
08	0	0	0	0	0	0	0	0	0	0	0	0	0	-	-	-	-	-	-	-	-	-	-	-	-	-	-	-				
09	19.37	5.42	6.86	6.30	7.49	10.16	13.25	0.37	0.79	0.55	0.40	0.76	0.80	43.53	21.81	61.80	75.47	182.53	111.65	254.24	373.05	0.30	0.17	0.33	0.33							
10	0	0	0	0	0	0	0	0	0	0	0	0	0	-	-	-	-	-	-	-	-	-	-	-	-	-	-	-				
11	0	0	0	0	0	0	0	0	0	0	0	0	0	-	-	-	-	-	-	-	-	-	-	-	-	-	-	-				
12	0	0	0	0	0	0	0	0	0	0	0	0	0	-	-	-	-	-	-	-	-	-	-	-	-	-	-	-				
13	1.57	0.34	0.53	1.04	0.96	1.12	1.23	0.50	0.52	0.78	2.87	1.11	1.83	8.93	7.13	8.29	7.59	25.85	31.52	27.25	10.84	0.23	0.26	0.13	0.11							
14	5.81	2.31	1.69	2.50	2.22	4.11	3.42	0.48	0.33	0.81	0.46	1.00	0.50	59.58	59.93	28.11	11.17	283.98	299.34	125.53	42.73	0.35	0.32	0.21	0.15							
15	3.17	1.15	1.06	0.98	1.86	1.96	2.48	0.57	0.35	0.49	0.55	0.73	1.06	11.07	78.08	9.31	20.88	24.37	272.43	32.90	46.44	0.25	0.34	0.16	0.22							
16	8.99	1.36	4.25	3.78	4.63	4.64	7.53	0.43	0.64	0.54	0.66	0.60	1.07	7.81	89.04	24.82	65.34	31.38	400.63	79.90	272.34	0.15	0.23	0.23	0.32							
17	8.01	3.75	3.49	2.00	3.43	4.67	5.75	0.47	0.42	0.44	0.75	0.67	0.97	40.65	50.51	79.91	28.17	152.73	187.25	455.00	75.96	0.55	0.26	0.32	0.18							
18	5.54	0.90	3.38	2.33	1.00	3.23	3.87	0.52	0.81	0.75	0.36	0.72	1.24	57.42	30.02	8.29	5.47	327.20	167.98	19.46	20.11	0.13	0.24	0.25	0.26							
19	57.79	26.06	38.37	37.88	27.75	46.41	48.43	0.50	0.62	0.74	0.48	1.15	1.10	10.47	29.97	16.87	8.46	38.00	145.92	57.97	29.34	0.15	0.27	0.23	0.13							
20	4.30	1.09	1.83	0.38	1.55	1.36	3.07	0.44	0.87	0.53	0.49	0.64	1.24	2.83	15.73	4.13	8.32	8.35	23.81	12.70	38.22	0.11	0.31	0.14	0.22							
21	90.00	46.60	58.75	31.50	50.39	59.40	80.25	0.50	0.63	0.45	0.72	0.75	1.65	19.83	13.25	9.61	16.07	91.37	50.61	33.03	70.80	0.24	0.21	0.15	0.17							
22	86.45	25.81	50.50	42.88	39.30	56.26	71.12	0.51	0.76	0.55	0.69	0.77	1.25	8.01	15.83	24.24	15.54	30.27	55.17	98.96	63.74	0.14	0.32	0.37	0.18							
23	93.36	57.20	26.52	41.93	49.04	76.56	63.61	0.72	0.46	0.61	0.57	1.19	0.80	18.79	9.27	9.86	13.09	73.28	38.86	33.85	36.27	0.33	0.14	0.16	0.20							
24	99.45	75.82	59.03	76.68	55.25	95.53	82.38	0.79	0.60	0.74	0.53	2.41	1.02	16.05	9.91	14.92	16.80	62.13	35.41	66.02	62.97	0.21	0.14	0.16	0.22							
25	93.57	54.26	43.75	51.45	66.61	77.39	78.38	0.64	0.52	0.58	0.75	1.08	1.35	17.57	16.26	9.94	16.62	67.55	59.37	40.36	70.22	0.28	0.27	0.15	0.25							
26	14.11	10.89	7.66	7.15	7.59	12.80	11.26	0.77	0.78	0.60	0.49	1.51	1.10	9.32	38.16	9.46	30.45	32.24	191.09	28.59	130.17	0.15	0.32	0.16	0.15							
27	99.46	58.15	49.00	68.74	76.69	88.70	88.30	0.68	0.56	0.70	0.88	1.41	1.45	13.38	16.95	13.97	14.92	46.98	74.50	54.91	56.06	0.30	0.25	0.15	0.16							
28	99.31	65.68	54.54	56.04	66.81	86.08	85.51	0.73	0.62	0.58	0.75	1.53	1.39	18.46	17.11	11.13	10.60	72.30	61.51	40.49	39.15	0.22	0.21	0.14	0.15							
29	63.83	29.94	42.21	35.50	48.82	45.68	59.31	0.48	0.64	0.51	0.72	0.74	1.87	8.02	18.09	7.36	21.22	30.31	67.52	27.82	85.90	0.13	0.21	0.15	0.29							
30	61.15	30.27	17.32	35.64	17.66	51.37	28.07	0.51	0.52	0.73	0.49	1.40	1.79	12.64	13.73	11.79	10.66	42.93	50.41	38.30	44.65	0.39	0.18	0.27	0.14							
31	40.42	5.07	19.32	23.50	11.42	26.28	26.07	0.32	0.56	0.68	0.62	0.67	0.84	10.53	17.44	15.15	13.59	49.04	58.93	66.52	45.18	0.12	0.31	0.67	0.18							
32	0	0	0	0	0	0	0	0	0	0	0	0	0	-	-	-	-	-	-	-	-	-	-	-	-	-	-	-				
33	0	0	0	0	0	0	0	0	0	0	0	0	0	-	-	-	-	-	-	-	-	-	-	-	-	-	-	-				
34	28.65	14.29	11.75	9.13	9.66	19.60	18.48	0.61	0.61	0.51	0.44	0.81	0.82	8.71	10.37	12.07	15.11	27.29	40.34	46.09	48.22	0.16	0.33	0.40	0.14							
35	35.87	23.96	8.48	1.83	12.77	24.52	19.43	1.18	0.49	0.23	1.05	1.23	1.00	17.34	7.74	8.43	11.59	58.18	23.17	39.95	29.56	0.37	0.17	0.15	0.17							
AVG	34.14	17.76	16.91	18.05	18.67	26.58	26.62	0.49	0.52	0.51	0.60	0.85	0.97	21.44	20.67	13.98	18.73	100.71	86.46	57.04	72.66	0.23	0.20	0.18	0.17							

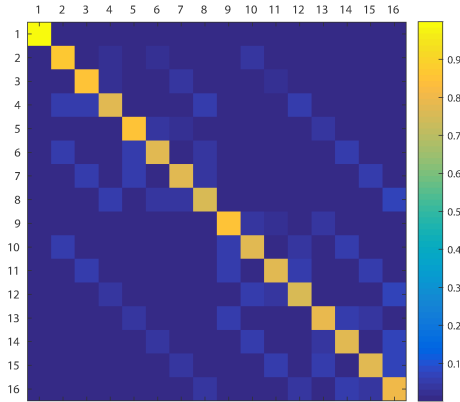


Figure 5.12: *Transition matrix P of infant's movements.*

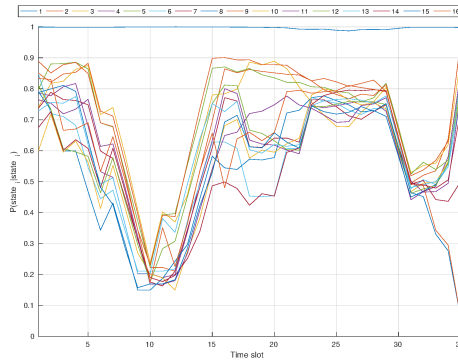


Figure 5.13: *Temporal evolution of $P(i|i)$ probabilities related to each state.*

Figure 5.12, that represents the modelling of the MC transition matrix P of the total recorded period, shows the matrix representation of the probability of transition from one state to another, whose values range from zero to one.

The fact that the probability values along the matrix diagonal are very high means that the probability that in the next instant ($K + 1$) infant remains in the same state of the previous instant is very high. In other words, it is very likely that once infant moves certain limbs, he continues moving those same limbs also in the next instant.

Furthermore, along the matrix diagonal there are some element with more intense colour (higher probability) than others, e.g. elements $P(2, 2)$, $P(3, 3)$, $P(5, 5)$, $P(9, 9)$, in which infant moves only one limb, meaning that the probability that he continues to move only the same limb is high.

The highest probability value is the element $P(1, 1)$ because of the infant is stationary for 65, 86% of the total time, and, therefore, the probability that he remains in state 1 is very high.

Other elements (not along the diagonal) with significantly higher values are due to the addition in the next state of the movement of a single other limb in addition to those already moved in the previous state. An example of these cases can be seen in element $P(4, 8)$, that describes the probability of a transition from state 4, in which infant moves legs, to state 8, in which he moves legs and *RA*.

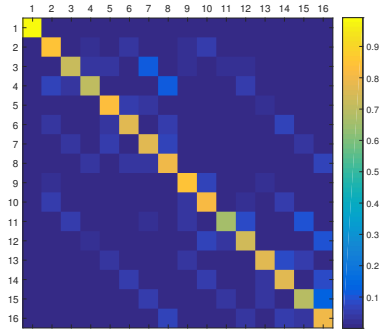
The transition matrix is calculated for each recording session and then the diagonal element values are plotted for each session in figure 5.13. In this graph, there are three areas where the probability of remaining on the same state decreases for all the diagonal elements except that one related to the state 1 (which corresponds to infant inactivity). These areas correspond with recording sessions mentioned before, in which the infant is stationary (8, 10–12, 32 – 33). Confirming what has just been said, during the recording sessions in which he moves, the probability of all the diagonal elements increases except inactivity probability (state 1), that decreases.

Figure 5.14 shows different models of MC transition matrix during several time periods of the day. Studying the evolution of the motor behaviour of the infants will be possible by analysing such models over time.

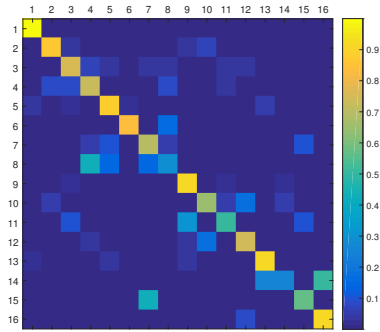
Thereby, models can be used to study infants movements, their behaviour over time and in particular the sequences of movements.

The sequence in which infants move their limbs is predictive of certain pathologies. For example, the simultaneous movement of all limbs is associated with CSGMs, while the movement of one limb after the other is associated with normal movement.

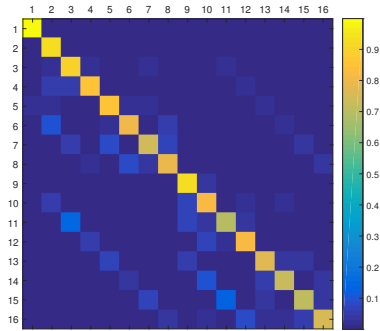
Thus, the classification of infants based on these CM transition matrix models could be helpful in classifying them in “healthy” and “at risk” classes.



(a) Transition matrix during the morning.



(b) Transition matrix after a meal.



(c) Transition matrix during the evening.

Figure 5.14: Transition matrix P of infant's movements during different periods of the day.

5.4.2 Discussion

In this subsection discussion and some possible future developments are presented.

In this section, a novel video-based system for preterm infant's movement detection and analysis is presented by using a non-invasive depth sensor placed over the infant lying on the infant warmer.

An algorithm is developed, able to detect infant's movements in real-time from depth stream and to extract some important features from the sequence of depth images collected by RGB-D sensor.

Some important indicators are derived, which can be used by clinicians to objectively study infant's movements during his development.

By using the information included in KPIs it will be possible to quantify the change in infant's limbs movements during the time and the improvements after physiotherapy, to observe the presence of the physiological transition from WMs to FMs, the absence of FMs or the presence of abnormal movements.

KPIs give information about movements percentage, velocity, acceleration, amplitude and volume, about activities sequences and symmetries in movement.

E.g., $M_{\%}^s$ KPI, when $s = 16$, tells about the percentage time during which the infant moves all the limbs simultaneously and it can give information about the presence of abnormal movements as CSGMs.

Recent studies indicate that infants with an abnormal persistence of GMs between the different stages of transformation (Writhing and Fidgety) present a high risk (70%-80%) of developing CP. Some studies report that the permanent presence of abnormal GMs in the fidgety phase, which implies a total absence of elegance and complexity of movements, predicts a CP with an accuracy between 85% and 98%. More recent studies indicate that infants with abnormal GMs in the fidgety phase who do not develop CP may develop other problems, such as minor neurological disorders, attentive deficits, hyperactivity, aggressive behaviour or cognitive problems [224].

The work is mainly focused on the statistical method reporting only preliminary test results, but, currently, more extensive studies with more infants are in process.

The project, indeed, opens to future evolutions in the direction of infants' classification in "healthy" and "at risk" classes. Based on this set of parameters, the aim is to develop scores to resemble GMA as a support for clinician in CP diagnosis, in order to increase the number of early detections of movement disorders, so that treatment can be started as soon as possible.

Limitations of the proposed system are due to occlusions caused by external interventions that occur when nurses or physicians put their hands between the

depth sensor and the infant to perform their activities.

Another problem may be caused when nurses or clinicians change the position of the infant inside the crib. Such new arrangements may adversely affect clustering goodness.

To avoid these issues, only recording sessions in which there are not interactions with nurses or clinicians are considered in the data processing phase. Then, to completely resolve these problems semantic segmentation with Convolutional Neural Networks is used improving the quality of limbs tracking.

Results of image semantic segmentation approach to extract preterm infant's silhouette from depth image are presented in next section.

5.5 Semantic Segmentation

This section presents the results obtained from the implementation of the different CNNs architectures described in subsection 4.2.4.

For training neural networks the dataset, generally, is splitted into three parts: training, validation, and test. When training the neural networks, here proposed, a common approach was followed in order to better highlight comparisons between the different architectures. Thus, in the following experiments, 70%, 10% and 20% of dataset are chosen respectively for train, test and validation.

Each CNN architecture was trained with two types of depth images, respectively of 16 bit (original depth image) and 8 bit (scaled depth image), since the dataset is composed of tuples consisting of three images for each frame, the original depth image, the scaled depth image and the ground truth, as explained in the next paragraph.

An update rule based on iterations over training was used to learn model parameters, and the best model was generally chosen by evaluating a secondary stopping criterion on a held out validation set. Once this is complete, the best model was also evaluated over the never before seen test set. In addition, several combinations of hyperparameters were tested: a learning rate of 0.001 and an Adam optimization algorithm were used.

5.5.1 PIDS (Preterm Infants' Depth Silhouette) Dataset

In order to locate the silhouette of preterm infants lying on the crib under the RGB-D sensor placed perpendicularly above the infant warmer at a distance of 70cm, normally directed to the subject, by the use of semantic segmentation, PIDS (Preterm Infants' Depth Silhouette) Dataset is built.

The sensor used captures depth and colour images, both with dimensions of 320x240 pixels, at a rate up to approximately 30 fps and illuminates the

scene/objects with structured light based on infrared patterns.

Subjects under acquisition are 9 preterm infants hospitalised in the NICU of the Women’s and Children’s Hospital “G.Salesi” of Ancona (Italy). Their GA at the time of acquisition ranged from 32 and 34 weeks, with a mean age of 33^{+3} weeks and the weight is between 1400 g and 1800 g, as shown in table 5.6.

Table 5.6: *PIDS Dataset infants characteristics (Gestational Age and Weight).*

ID Acquisition	Gestational Age (<i>weeks⁺days</i>)	Weight (<i>g</i>)
1	32^{+3}	1420
2	33^{+3}	1618
3	34^{+2}	1762
4	37^{+1}	2050
5	35^{+4}	1800
6	34^{+4}	1625
7	36^{+5}	1970
8	36^{+3}	1890
11	35^{+5}	1770
16	33^{+2}	1655
Mean	34^{+6}	1756

As mentioned above the dataset is composed of tuples, instances identified by a unique timestamp, and each of them consists of three images:

- a 16 bit depth image, the original image acquired by depth sensor;
- a 8 bit depth image, obtained after a preprocessing phase aimed at scaling the original corresponding 16 bit depth one in order to obtain an image where the infant silhouette is highlighted by improving contrast and brightness;
- the corresponding ground truth, that consists of the infant silhouette (white) on an homogeneous background (black).

The ground truth was manually labelled by 6 human annotators, with the help of the timestamp corresponding RGB image, that has been acquired for the sole purpose of facilitating the labelling and thus the creation of the dataset, but that is not part of the dataset itself.

Figure 5.15 shows an example of a dataset instance that includes the three images described above.

The dataset is divided into two folders:

- positive, which contains 1710 positive instances, i. e. 1710 tuples of the 3 images above described in which the infant is in the crib (5.15);
- negative, which contains 1800 negative instances, i. e. 1800 tuples of the 3 images above described in which the infant is not in the crib and therefore it is not the infant’s silhouette in the image. Here the ground

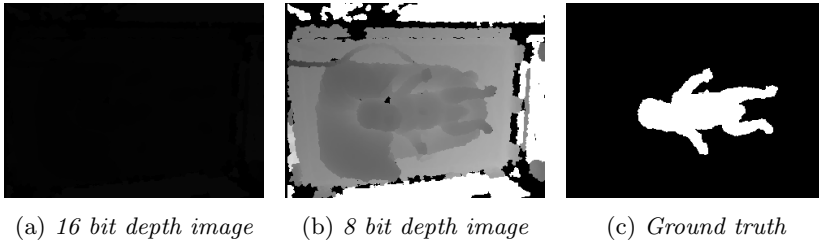


Figure 5.15: Example of a PIDS Dataset positive instance. It consists of 16 bit original depth image (5.15a), 8 bit scaled depth image (5.15b) and the corresponding ground truth (5.15c).

truth consists of a completely black mask (5.16).

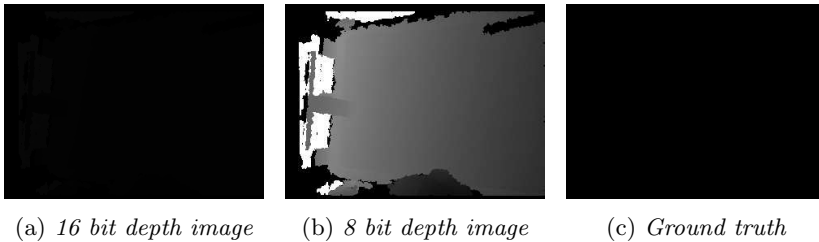


Figure 5.16: Example of a PIDS Dataset negative instance. It consists of 3 images where the infant is not present in the frame: a 16 bit original depth image (5.16a), a 8 bit scaled depth image (5.16b) and the corresponding ground truth (5.16c), a completely black mask.

Positive instances also include the so-called partial instances (5.17) where the infant is only partially visible because it is partially framed, because it is covered by the hands of health workers or because it is partially covered by a sheet. In this case the acquired RGB image (5.17d) was very useful for correctly labelling the corresponding depth image.

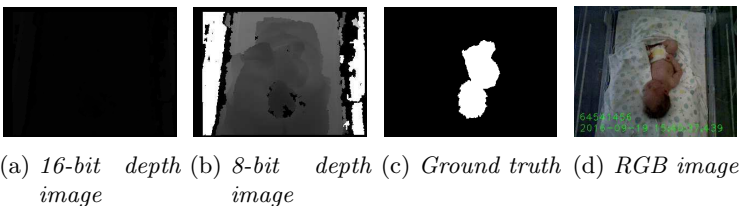


Figure 5.17: Example of a PIDS Dataset partial instance. It consists of 3 images where the infant is partially visible in the frame: a 16 bit original depth image (5.17a), a 8 bit scaled depth image (5.17b) and the corresponding ground truth (5.17c). Figure 5.17d is the corresponding RGB image used to facilitate ground truth annotation.

The infant is generally in a central and horizontal position with respect to the framing, but sometimes when nurses change sheets, diapers or during meals, the infant is moved to a vertical or lateral position with respect to the framing. The same happens when the depth camera is moved. For this reason, these special cases have also been included in the dataset (figures 5.18, 5.19).

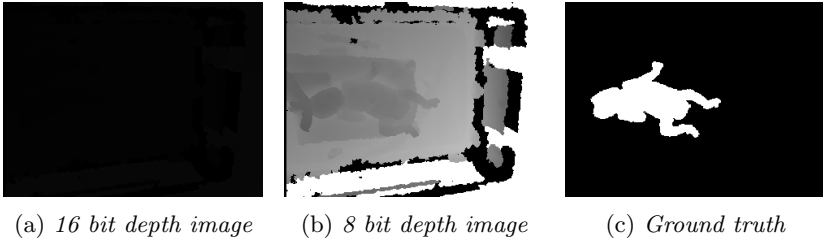


Figure 5.18: *Example of a PIDS Dataset decentralised infant's instance.*

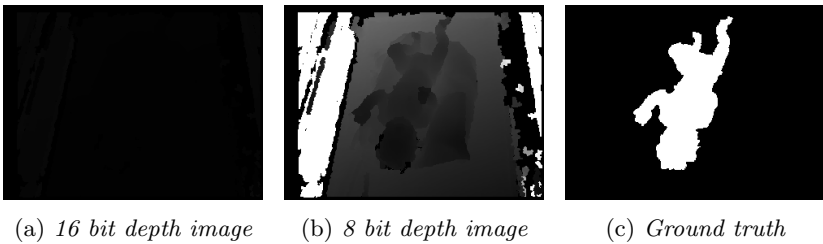


Figure 5.19: *Example of a PIDS Dataset vertically positioned infant's instance.*

The total 17 acquisition sessions (see table 5.7) forming PIDS Dataset have been performed over a 28-months period of time. Acquisitions were made in an indoor scenario (NICU) where the illumination conditions are not constant: some acquisitions were made with natural light entering the windows, others with artificial light. Moreover, natural light varies in function of the different hours of the day and it also depends on weather conditions.

The use of depth sensor makes it possible to make acquisitions even during the night when lights are very low. It is evident from figure 5.20d that it would be difficult to perform segmentation using RGB images, and this is not one of the worst cases.

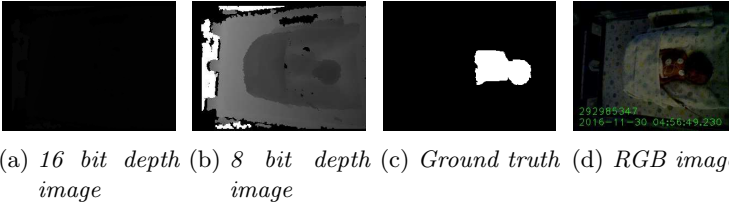


Figure 5.20: Example of a PIDS Dataset instance acquired when lights are very low.

Table 5.7: PIDS Dataset acquisition sessions and relative instances.

ID Acquisition	# of Positive Instances	# of Negative Instances
1	149	-
2	274	-
3	734	-
4	34	-
5	46	-
6	300	-
7	112	-
8	29	-
9	-	383
10	-	537
11	25	-
12	-	79
13	-	468
14	-	63
15	-	66
16	7	-
17	-	204
TOT	1710	1800

5.5.2 Data Analysis Results

5.5.2.1 Quantitative Evaluation

The performances of the different CNNs architectures described in 4.2.4.2 are evaluated on the dataset splitted in train, test and validation sets, respectively formed by the 70%, 10% and 20% of entire dataset, as said above.

Each CNN architecture was trained with the two types of depth images of each dataset instance, the 16 bit and the 8 bit image.

When training the neural networks, a common approach was followed in order to better highlight comparisons between the different architectures. Thus, each network was trained with a learning process of 200 epochs, which approximately corresponds to the achievement of convergence, as is possible to visually see

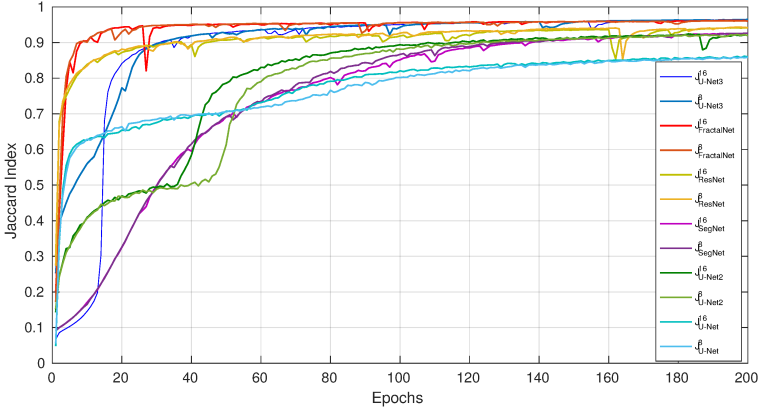


Figure 5.21: Jaccard index trends over the 200 epochs for each CNN architecture.

Table 5.8: Jaccard and Dice indices of different CNN architectures.

Net	Bit	Jaccard Train	Jaccard Validation	Dice Train	Dice Validation
U-Net [1]	8	0.859001	0.862817	0.924153	0.926358
	16	0.861923	0.864808	0.925842	0.927503
U-Net2 [2]	8	0.922663	0.941277	0.959776	0.969750
	16	0.924417	0.941705	0.960724	0.969977
U-Net3	8	0.964909	0.944524	0.982141	0.971471
	16	0.964385	0.943941	0.981869	0.971162
SegNet [3]	8	0.926655	0.901882	0.961931	0.948410
	16	0.926333	0.897216	0.961758	0.945824
ResNet [4]	8	0.943468	0.924655	0.970912	0.960853
	16	0.941735	0.927212	0.969994	0.962232
Fractal [5]	8	0.961119	0.952994	0.980174	0.975931
	16	0.962137	0.951963	0.980703	0.975390

from the images below.

Then the epoch with the best result on train and validation sets is selected as the final model and the corresponding indexes are reported in the following tables.

Table 5.8 shows Jaccard and Dice indices calculated on train and validation set respectively.

Considering the value of Jaccard and Dice indices calculated on the train set, which is the most significant one, it is possible to see that the network that wins over the others is the U-Net3, the one implemented in this thesis work. The U-Net3 8-bit version greatly outperforms all the concurrents with a value of Jaccard index of 0,964909 and a Dice Index of 0,982141. The performance

Table 5.9: *Semantic segmentation results of different ConvNet architectures.*

Net	Bit	Accuracy	Precision	Recall	F1-Score
U-Net [1]	8	0.984514	0.926640	0.951217	0.904518
	16	0.984581	0.928222	0.951852	0.907175
U-Net2 [2]	8	0.986978	0.966541	0.965419	0.967820
	16	0.987042	0.967384	0.966019	0.968877
U-Net3	8	0.988792	0.989633	0.988389	0.990899
	16	0.988799	0.988496	0.987339	0.989663
SegNet [3]	8	0.987432	0.965309	0.962212	0.968493
	16	0.987445	0.965120	0.962161	0.968151
ResNet [4]	8	0.988122	0.974488	0.972054	0.976957
	16	0.988048	0.973575	0.971580	0.975608
FractalNet [5]	8	0.988575	0.989374	0.986805	0.992015
	16	0.988583	0.990059	0.988008	0.992142

of the FractalNet is also very good, as in the 8-bit version it obtains the best results on validation test and in the 16-bit version it is second only to the U-Net3 on train set results. Immediately after there is the ResNet.

In table 5.9 are reported the results in terms of accuracy, precision, recall and F1-score.

Also from this table it is possible to see that in general the best network is the 8-bit version U-Net3, which has the highest values of precision and recall compared to all other networks and very high values of accuracy and F1-score. The highest accuracy value belongs to the 16-bit version U-Net3, while that of F1-score to the 16-bit version of the FractalNet, which is still performing well and, as before, is followed by the ResNet in terms of results.

In conclusion, considering all the metrics as a whole, it is possible to say that the best CNN architecture for PIDS Dataset is the 8-bit version of U-Net3, followed by FractalNet and ResNet, i. e. the deepest networks.

In figure 5.21 is shown for each CNN the trend of Jaccard index during the fit process. It is possible to see that the FractalNet and the ResNet immediately reach high values after a few epochs. Instead, the U-Net3 increases its value more slowly, but converges at high values as the FractalNet. On the contrary, it is easy to see that the performances of the classic U-Net are below all other networks.

In a similar way, in table 5.10, for each network is shown the Jaccard index trend along the 200 epochs.

5.5.2.2 Qualitative Evaluation

The segmented images can also be evaluated from a qualitative point of view. In fact, a good annotation is not just an annotation that reaches high scores on all the metrics, but above all an annotation that looks nice and closely matches the borders of infant silhouettes.

The achievement of this visual matching is not captured by the discussed metrics. Thus, the segmented images can be qualitatively evaluated in order to see which of the various networks is more prone to reach the objective.

In this light, in table 5.11 the predicted images obtained from the various networks are reported, compared with the ground truth at the top. As a first thing, it is clearly visible that the classic U-Net achieves not very good performances, as resulted from the analysis of the metrics. This is justified by the nature of the network born with the aim of segmenting cells into biomedical images, with shapes that are more compact, circular and less articulated than an infant's silhouette.

The ResNet reaches good results on metrics, but from visual inspection it is visible that the annotations have a not so high quality, as the SegNet.

Finally, also from qualitative observations, it is clear that the best CNN is the U-Net3 (8 and 16-bit versions) which manages to fairly faithfully reproduce the infant's silhouette. The net partly continues to maintain this tendency towards rounding that allows it to blunt the figure and make it more smoothed and less fragmented than the FractalNet predicted image and so more similar to the label.

5.5.3 Discussion

In this subsection some important advantages and limitations of semantic segmentation approach are highlighted.

A novel dataset containing 10530 depth images has been created, of which a third are 16 bit depth images, the original images acquired by depth sensor, a third are 8 bit depth images, obtained after a pre-processing phase aimed at scaling the original corresponding 16 bit depth ones in order to obtain an image where the infant silhouette is highlighted, and the remaining third consists of ground truth corresponding images. It contains 1710 positive triplets in which the infant is in the crib and 1800 negative triplets in which the infant is not in the crib.

6 different CNNs have been tested on this new dataset with good quantitative and qualitative results. The use of CNNs greatly improves the detection of the infant's silhouette with respect to simple binary segmentation.

Experimental results demonstrate the effectiveness and suitability of the new implemented U-Net, obtained by modifying the classic U-Net, that achieves

high accuracy and performs better than all other tested networks.

Semantic segmentation has been used to solve the problem of occlusions that occur by healthcare staff members: hands that are placed between the sensor and the infant during clinical practice, if at the height of the infant, can, in fact, be exchanged for the infant himself, when threshold segmentation is used. Hand movements can thus be mistaken for infant's movements.

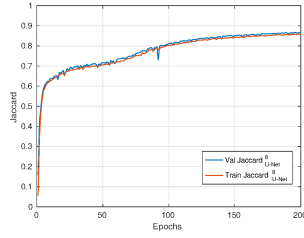
To avoid this issue, initially, the time interval of the acquisition studied in order to analyse data processing was divided in recording sessions of 300 seconds each one, which permits to discard those records in which there are interactions with a nurse or a clinician.

Using semantic segmentation it will be possible to apply the algorithm for motion detection without interruption, even during procedures by nurses and doctors.

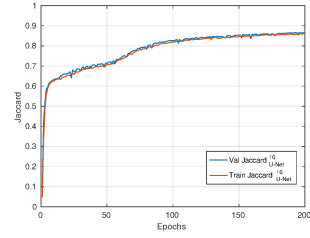
The high computational calculation due to the use of neural networks, made it necessary to use a PC with higher characteristics than those of the Cubieboard used in the architecture described above. Networks were trained on a PC desktop with a NVIDIA GTX 970 GPU, but also for the application of the real-time prediction model during the acquisition it was necessary to use something more powerful than the Cubieboard. In particular, the Asus Vivo-Mini PC UN42-M026M was used in order to try to keep as much as possible the characteristics of the system not to be bulky.

Table 5.10: *Jaccard Index results.*
8 bit

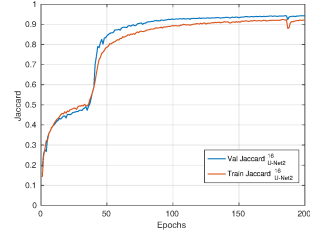
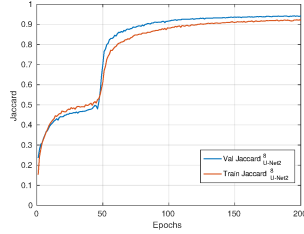
U-Net



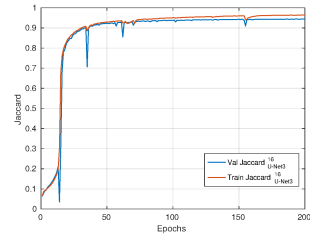
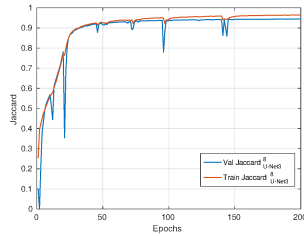
16 bit



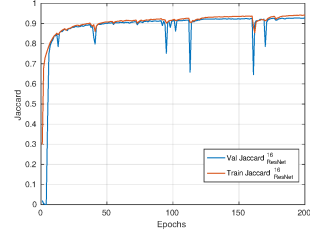
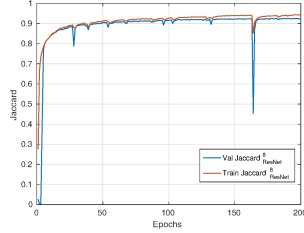
U-Net2



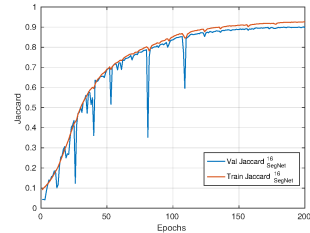
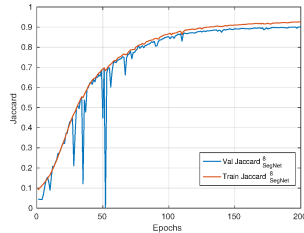
U-Net3



ResNet



SegNet



FractalNet

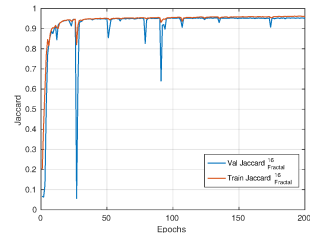
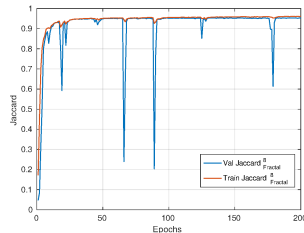
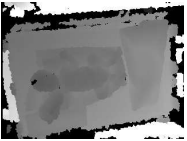
















Table 5.11: *Qualitative result of prediction.*

	8-bit	16-bit	Label
			
U-Net [1]			
U-Net2 [2]			
U-Net3			
SegNet [3]			
ResNet [4]			
FractalNet [5]			

Chapter 6

Conclusions and Future Works

6.1 Discussion

This thesis has presented an efficient cloud-based health infrastructure that permits the automation of the processes of data collection, transmission, storage, processing and availability for the personnel of the NICU of “Women’s and Children’s Hospital G. Salesi” of Ancona.

A solid foundation for building a device network has been developed to allow data sharing between medical devices, as well as the communication in real-time with EMR data.

This allows physicians to have a general idea about patient’s health conditions and to not neglect any important detail for the patient’s care and to support them in medical decisions.

Moreover, the automatic transmission of the measured values from devices to the cloud storage eliminates the drawbacks of manual collection work and the consequent possibility of typing errors.

The infrastructure has been tested by connecting 4 different types of instruments with a single DB connected to the EMR of the hospital ward. The 4 different types of medical instruments, patient-monitors, bilirubinometers, transcutaneous bilirubinometers and RGB-D vision systems, and the related communication protocols used to interconnect them to the DB have been described in detail.

Thus, in addition to connecting medical instruments already present in the department, a new device has been created, which deserves some consideration. It is a medical imaging method to estimate preterm infant’s respiratory rate and movement indicators with a non invasive embedded RGB-D sensor. It is low-cost, not bulky and easy to install in the hospital environment where the experimental phase was carried out and where it is going to be used in daily clinical practice. Affordability, installability and practicability are important characteristics required to all new systems installed in the NICU. It is non-contact and non-invasive. This ensures the decrease of the discomfort procured to the baby, reducing the number of transducers applied on the infant skin and

also the risk incurred whenever the infant comes into contact with external objects, as is the case of marker-based capture systems and sensor-based approaches. This aspect is of major importance especially in this case, in which infants have a very small accessible body surface area and a very sensitive skin. Moreover, the use of depth data makes the system suitable to be used in an indoor environment with poor lighting, as might be rooms in the NICU and it allows the preservation of privacy, unlike RGB cameras. Future developments may involve the use of new, more performing, structured-light sensors or of time-of-flight (ToF) sensors that supply depth images of better quality and are less affected by the presence of sunlight. In any way, experimental results showed that the system can automatically measure preterm infant's respiratory rate and some movement indicators, activating an alarm signal when respiratory rate values go out of the physiological range or when the infant remains stationary for a long time.

The infrastructure here created can provide the scalability necessary to support the adding of all medical devices that surround the neonatal crib for monitoring, diagnosis and treatment of different diseases, which is the next target. The idea is to obtain a single tailored display for each neonatal crib, where the clinician can access all patient's data, e.g., he can visualise his medical records, all device data in real time, historical values, and where he can change device settings and set up new vital signs or new alarm values.

Data availability and accessibility, guaranteed from the web interface through Web services and ensured by strong authorization for only medical staff, facilitates the process of data delivery and visualisation.

In particular, a modular platform has been created, equipped with many tools that allow to visualize the patient's personal data, the data coming from the instruments and therefore the historical values of the vital parameters measured by these instruments with user-friendly dashboards, graphs and tables.

NICU medical staff have remote access to the cloud database, both with the PC within the ward and in a more innovative way with mobile devices (smartphones and tablets) to view patient data, and have the ability to perform a continuous backup of their data.

The DB is also made available for "transversal" interoperability with other colleagues who need continuity of care for the same patient, such as, for example, with colleagues from peripheral hospitals and family paediatricians in the case of bilirubin, and for "vertical" interoperability with other databases and NHS operators.

This is guaranteed by a maximum security of data, encrypted, and access, controlled and strictly allowed only to those who have the necessary authorizations and differentiated according to the figure of the personnel. The web-platform, in fact, guarantees, subject to prior authorization, differentiated ac-

cess to the data depending on the figure that makes the log-in. Also infants' parents can access it with the possibility to view the infant's clinical history and the reports of the various tools. In the future, parents will not only be able to view the infant's medical record, but also to communicate with doctors and carry out tele-consulting through the platform itself, actively participating in the process of caring for their child.

The device integration in the infrastructure made also possible to elaborate collected data in real time with specific algorithms to assist physicians with clinical decision-making for improved healthcare in the view of Clinical Decision Support Systems.

The decision-making algorithms developed within this work collect and use data coming from the connected instruments, and therefore the values of the various biomedical parameters and signals measured by these instruments such as, heart rate, respiratory rate, TSB, TcB, movement indicators and so on, as well as infant's personal data and growth data, inserted in the appropriate tools of the web-platform during the registration and hospitalization phase of the infant from NICU personnel, and EMR data of the hospital ward. Then they elaborate this set of data and bring out from it useful information to monitor infants breathing and movement, to prescribe the recipes of bags for parenteral nutrition, to provide follow-ups and to diagnose neonatal jaundice as well as to decide a possible therapy to treat it.

6.2 Thesis contributions

The main contributions of this Thesis can be summarized as follows:

- Design and implementation of SINC cloud-based healthcare infrastructure that allows the developing and the deploying of the process automation of data collection, storage, processing and distribution through a medical device network that uses cloud computing in the NICU of the "Women's and Children's Hospital G.Salesi" in Ancona.
- Integration and interfacing with SINC cloud-based infrastructure of three different type of instruments (patient monitors, bilirubinometers, and transcutaneous bilirubinometers) located in the NICU, through medical communication protocols used to enable the communication and data transfer between these infant's monitoring devices and the unique database of the architecture.
- Development and interconnection with SINC infrastructure of a new device that is a novel non-contact and non-invasive RGB-D system that

consists in an RGB-D camera and in an embedded board, where the algorithms used to extract and analyse data from the depth images acquired by the camera are run in real-time.

- Design and development of an end-user web interface based on specifications given by healthcare staff and medical guidelines, which works as an application on Mobile Devices and Desktop Workstations, where medical staff members can access all available information. The propose web-platform exceeds the characteristics of a simple EMR, thanks to the development of innovative clinical tools, each of which has particular functionalities useful to make faster and easier physicians' clinical daily practice and to improve patient care:
 - "Anagraphic Tool"
 - "Growth Tool"
 - "Nutrition Tool"
 - "Bayley Tool"
 - "Bilirubin Tool"
 - "Respiration Tool"
 - "Movement Tool"
- Design and implementation of decision-making systems that, based on clinical guidelines, on physicians' expertise, on EMR data entered by medical staff in the different SINC tools, on computer vision techniques and on machine learning algorithms, are able to analyse and process data extracted from different devices. They provide in output advices, warnings, alarms, insights and important indicators, that can support physicians in the prediction or diagnosis of diseases such as neonatal jaundice or motor disabilities, or in the monitoring of physiological and developmental parameters and problems, such as respiratory rate, growth parameters and nutrition.
- Design and implementation of several CNNs for semantic segmentation of preterm infants' silhouette from depth images. Four different types of CNNs, i.e. U-Net, SegNet, FractalNet, and ResNet, have been trained through a manually annotated dataset.
- Creation of two datasets:
 - MIA dataset;
 - PIDS dataset.

6.3 Future Works

In the future, the possibility to share data and, especially, healthcare protocols, here investigated, will play a key role in the regional distribution of Neonatal Units.

In fact, the method used in this thesis work, based on a flexible and extensible infrastructure, is appropriate for the creation of a network that will include all the regional Neonatal Units and it will be used within SINC regional project.

The possibility of linking SINC DB to the regional ARCA-EMPI and the fact that every medical report delivered from the platform tools can be sent to the regional EHR shows that the work, described in this thesis, is focused towards the direction of the creation of a single regional model.

In this way, the system will facilitate the function of tele-consultation between specialists, enabling more effective collaboration between the peripheral structures and the central one, e.g., to better evaluate the conditions of a patient for which a transfer is requested or simply to unify healthcare protocols.

For example, it will facilitate the infant's transfer between the different hospitals, which can take place after having already made an initial analysis of the patient's vital signals by the reception peripheral centre, or vice versa, facilitate the continuity of monitoring once the infant is transferred from the central structure ("G. Salesi" Hospital) to a hospital closer to the residence of the parents, ending there the last days of hospitalization.

Moreover, the sharing of care protocols in the regional distribution of neonatologies will allow the achievement of a standardization of care, obtaining an important improvement in the services offered to citizens and proposing throughout the Region the same quality and efficiency that the NICU of "G. Salesi" Hospital demonstrates by covering the first places at EU level.

The interdisciplinary approach, the updating in the field of research and clinical research, the evolutionary perspective will provide those who work with these infants with a fundamental reference model to design courses of care and support for the development of the child and his family through a multidisciplinary assistance that continues for several years after the discharge and involves, in addition to neonatologists and psychologists, different professional figures: the family paediatrician, the child neuropsychiatrist, the physiatrist, the physiotherapist, the speech therapist and the educator.

Appendices

Appendix A

Table 1: *U-Net Indexes results.*

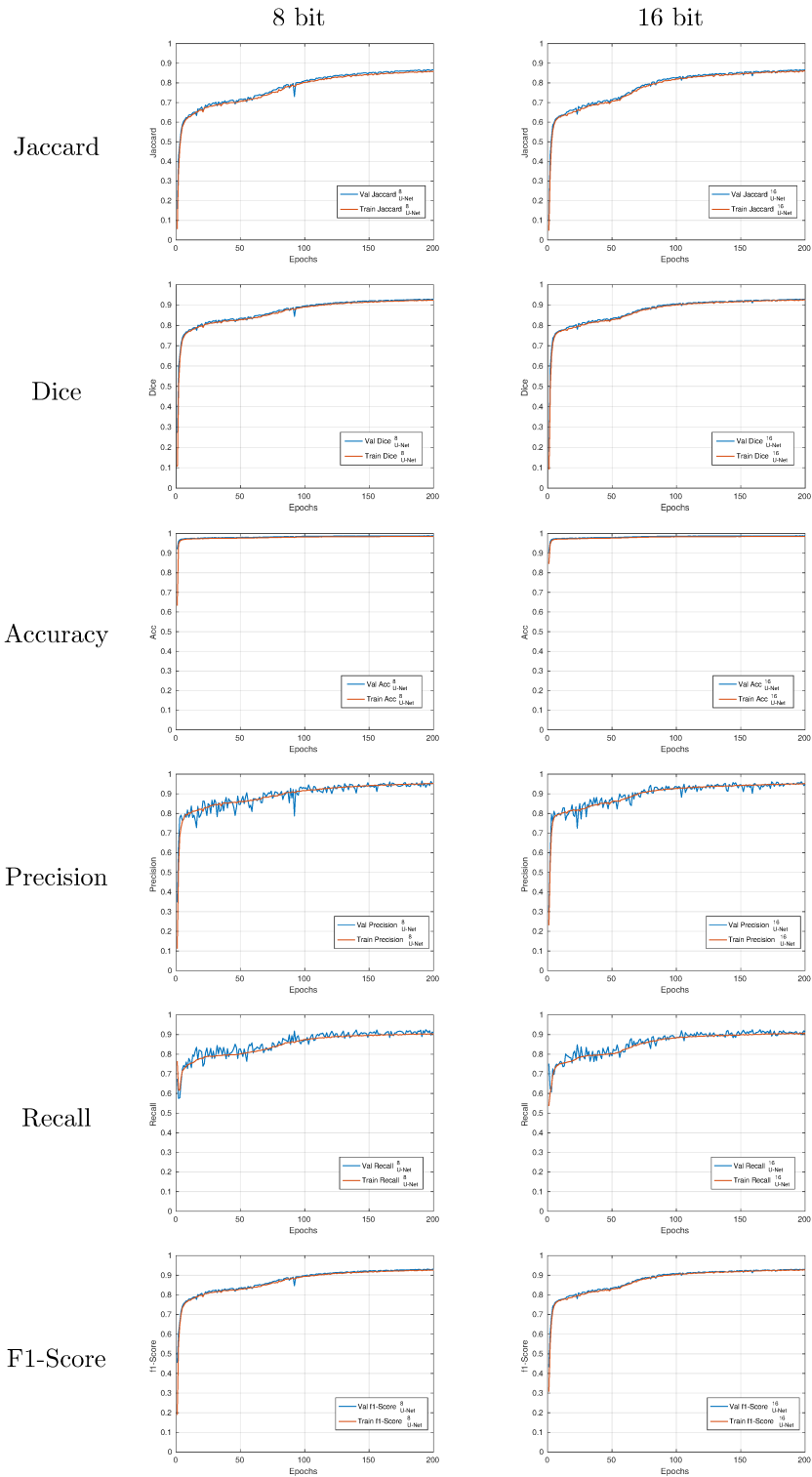
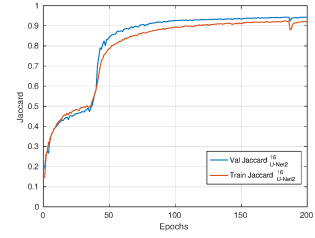
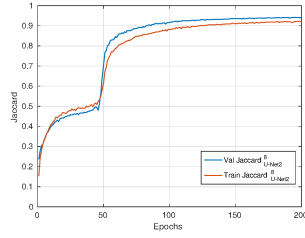


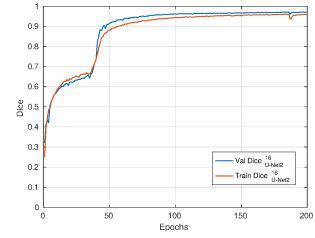
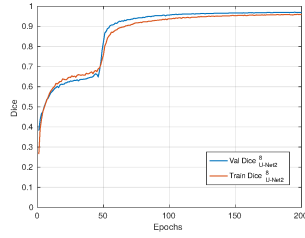
Table 2: *U-Net2 Indexes results.*
8 bit

16 bit

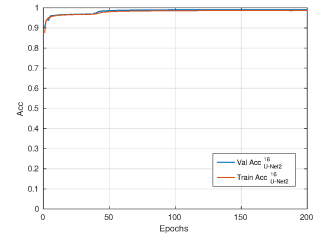
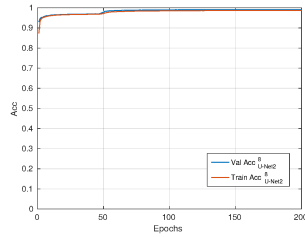
Jaccard



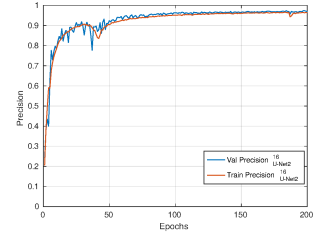
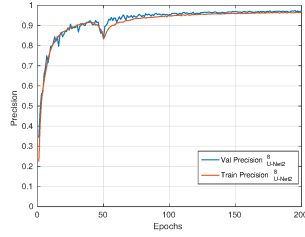
Dice



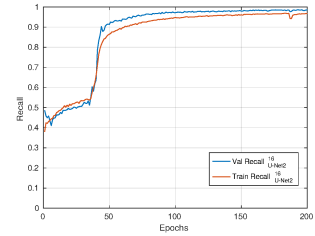
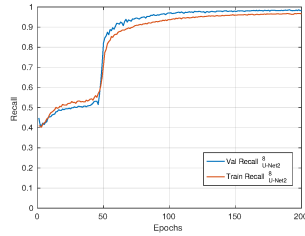
Accuracy



Precision



Recall



F1-Score

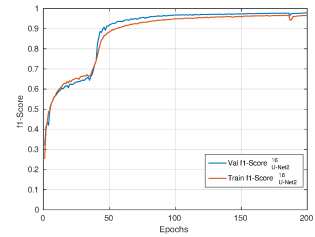
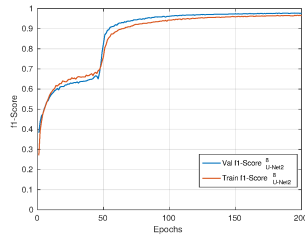


Table 3: *U-Net3* Indexes results.

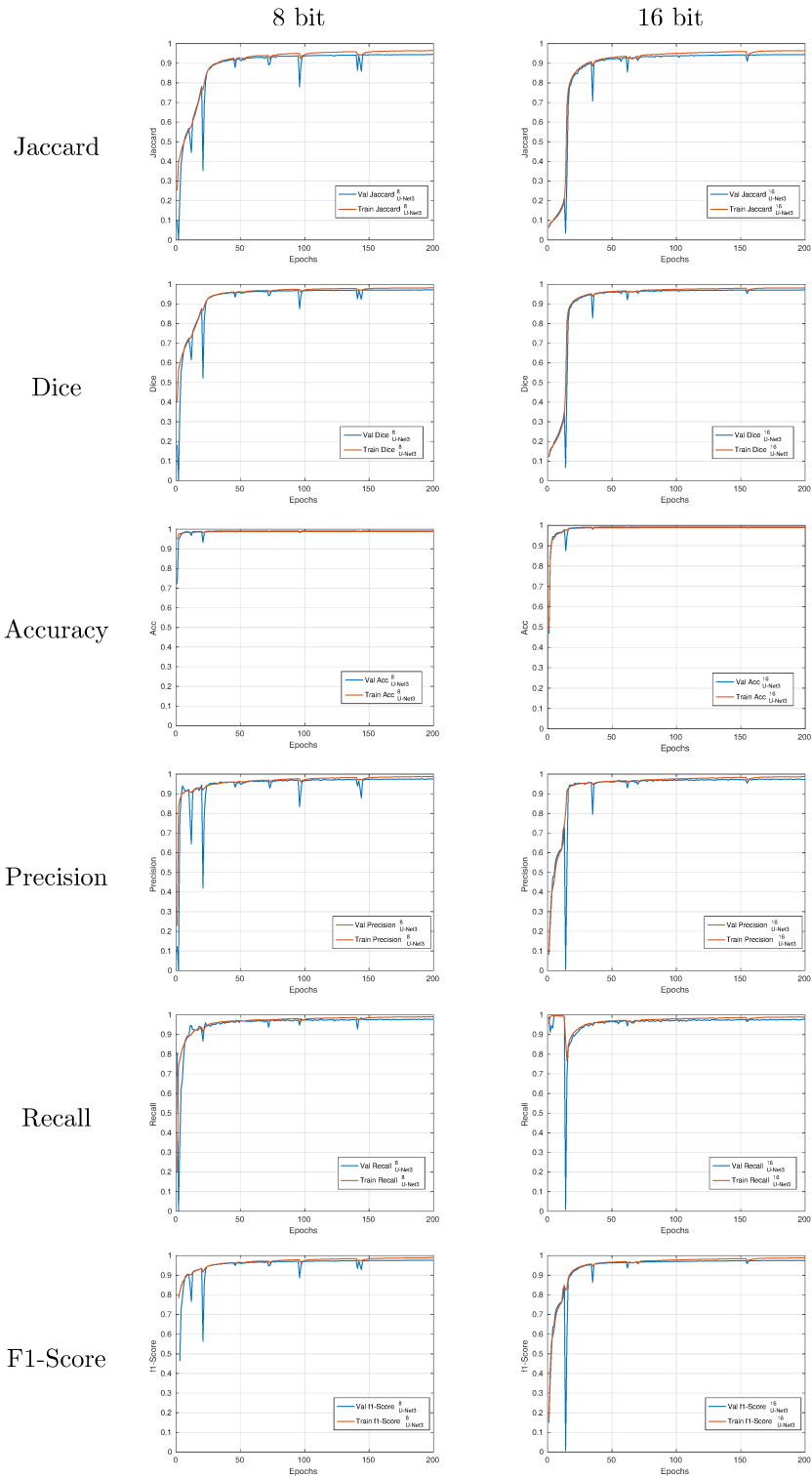


Table 4: *ResNet Indexes results.*

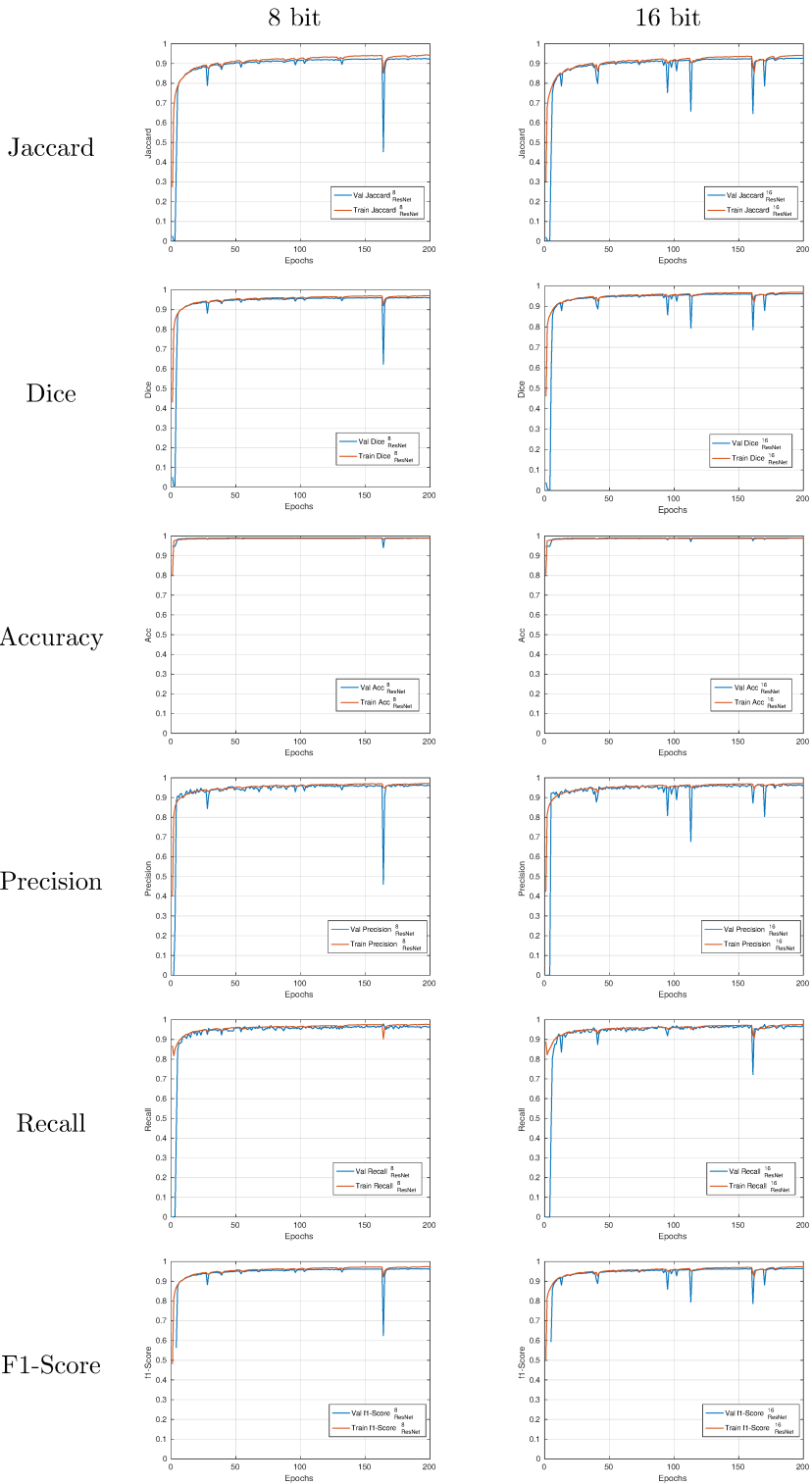
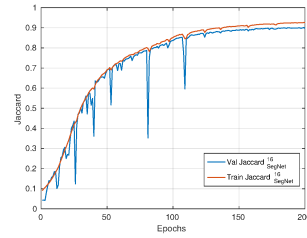
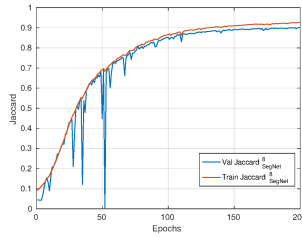


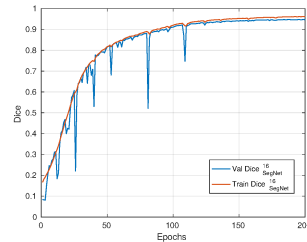
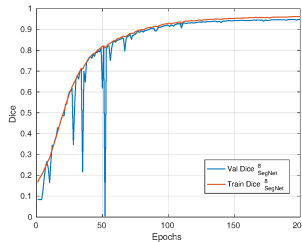
Table 5: *SegNet Indexes results.*
8 bit

16 bit

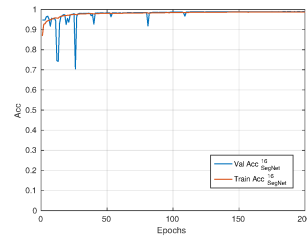
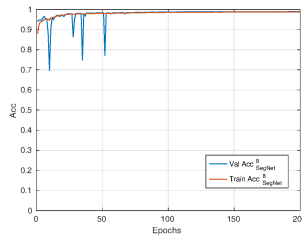
Jaccard



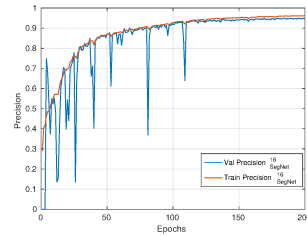
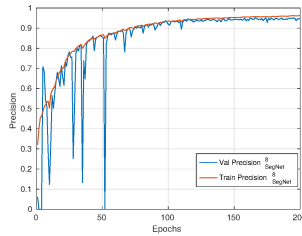
Dice



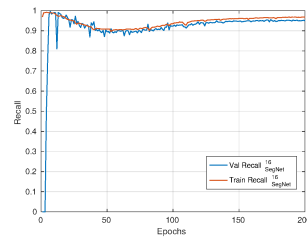
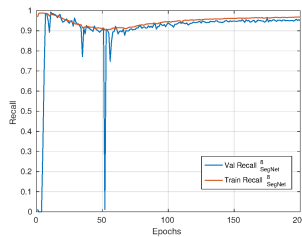
Accuracy



Precision



Recall



F1-Score

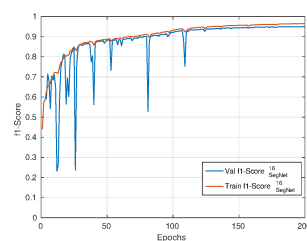
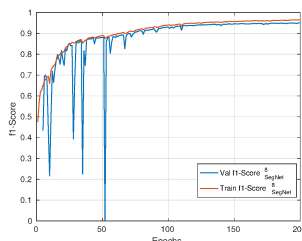
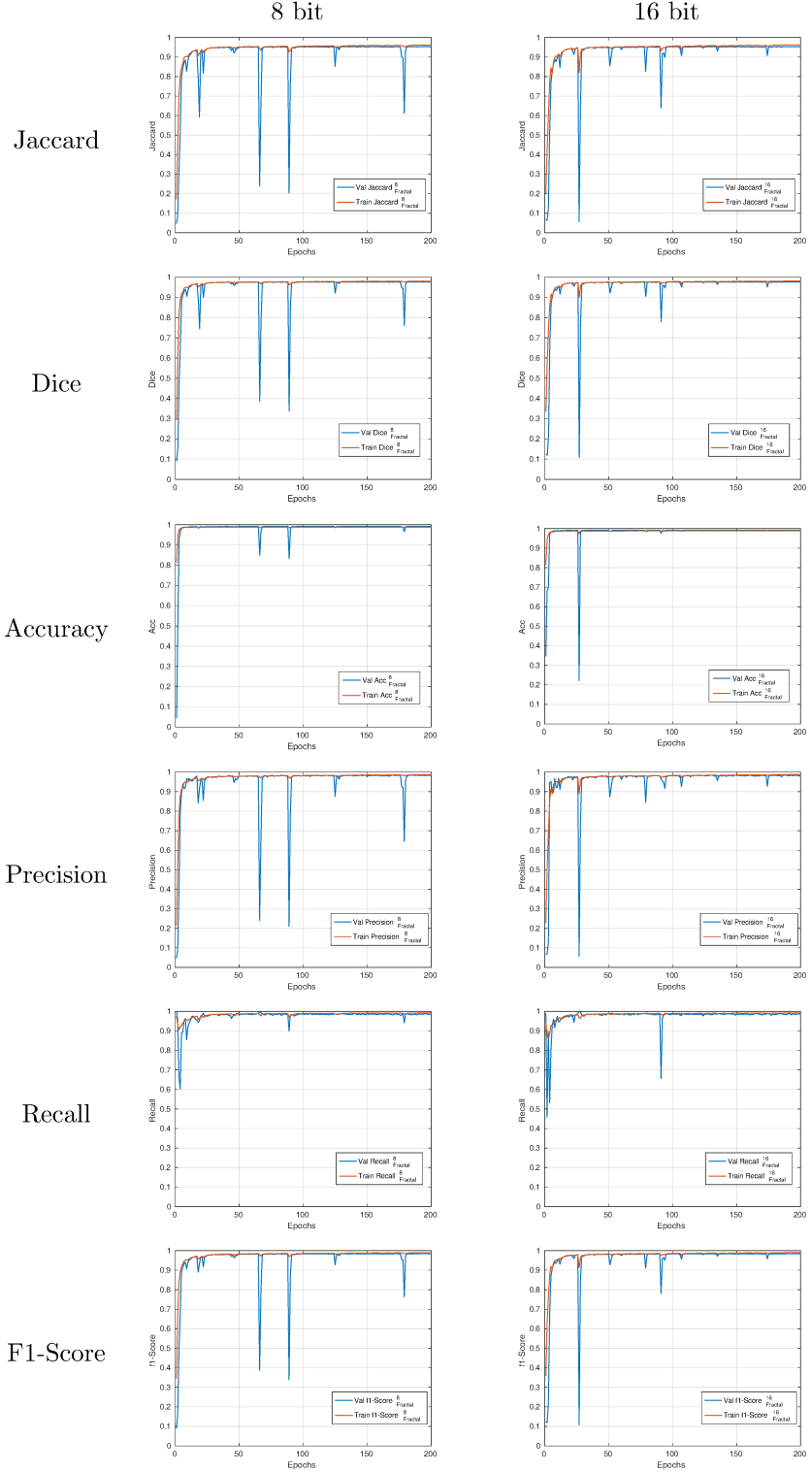


Table 6: *FractalNet Indexes results.*



Bibliography

- [1] O. Ronneberger, P. Fischer, and T. Brox, “U-net: Convolutional networks for biomedical image segmentation,” in *International Conference on Medical Image Computing and Computer-Assisted Intervention*. Springer, 2015, pp. 234–241.
- [2] H. Ravishankar, R. Venkataramani, S. Thiruvankadam, P. Sudhakar, and V. Vaidya, “Learning and incorporating shape models for semantic segmentation,” in *International Conference on Medical Image Computing and Computer-Assisted Intervention*. Springer, 2017, pp. 203–211.
- [3] V. Badrinarayanan, A. Kendall, and R. Cipolla, “Segnet: A deep convolutional encoder-decoder architecture for image segmentation,” *arXiv preprint arXiv:1511.00561*, 2015.
- [4] K. He, X. Zhang, S. Ren, and J. Sun, “Deep residual learning for image recognition,” in *Proceedings of the IEEE conference on computer vision and pattern recognition*, 2016, pp. 770–778.
- [5] G. Larsson, M. Maire, and G. Shakhnarovich, “Fractalnet: Ultra-deep neural networks without residuals,” *arXiv preprint arXiv:1605.07648*, 2016.
- [6] W. H. Organization *et al.*, “Born too soon: the global action report on preterm birth,” 2012.
- [7] E. R. Millett, J. K. Quint, B. L. De Stavola, L. Smeeth, and S. L. Thomas, “Improved incidence estimates from linked versus stand-alone electronic health records,” *Journal of Clinical Epidemiology*, 2016.
- [8] M. K. Obenshain, “Application of data mining techniques to healthcare data,” *Infection Control & Hospital Epidemiology*, vol. 25, no. 08, pp. 690–695, 2004.
- [9] S. Tsumoto and S. Hirano, “Data mining in hospital information system for hospital management,” in *2009 ICME International Conference on Complex Medical Engineering*, 2009.
- [10] M. N. Almunawar and M. Anshari, “Health information systems (his): concept and technology,” *arXiv preprint arXiv:1203.3923*, 2012.

Bibliography

- [11] R. Haux, “Health information systems—past, present, future,” *International journal of medical informatics*, vol. 75, no. 3, pp. 268–281, 2006.
- [12] S.-H. Lee, J. H. Song, J.-H. Ye, H. J. Lee, B.-K. Yi, and I. K. Kim, “Soa-based integrated pervasive personal health management system using phds,” in *Pervasive Computing Technologies for Healthcare (PervasiveHealth)*, 2010 4th International Conference on-NO PERMISSIONS. IEEE, 2010, pp. 1–4.
- [13] P. Kulkarni and Y. Ozturk, “mphasis: Mobile patient healthcare and sensor information system,” *Journal of Network and Computer Applications*, vol. 34, no. 1, pp. 402–417, 2011.
- [14] J.-T. Hsu, S.-H. Hsieh, C.-C. Lo, C.-H. Hsu, P.-H. Cheng, S.-J. Chen, and F.-P. Lai, “Ubiquitous mobile personal health system based on cloud computing,” in *TENCON 2011-2011 IEEE Region 10 Conference*. IEEE, 2011, pp. 1387–1390.
- [15] J. Biswas, J. Maniyeri, K. Gopalakrishnan, L. Shue, P. J. Eugene, H. N. Palit, F. Y. Siang, L. L. Seng, and L. Xiaorong, “Processing of wearable sensor data on the cloud—a step towards scaling of continuous monitoring of health and well-being,” in *Engineering in Medicine and Biology Society (EMBC), 2010 Annual International Conference of the IEEE*. IEEE, 2010, pp. 3860–3863.
- [16] Z. Rashid, U. Farooq, J.-K. Jang, and S.-H. Park, “Cloud computing aware ubiquitous health care system,” in *E-Health and Bioengineering Conference (EHB), 2011*. IEEE, 2011, pp. 1–4.
- [17] N. Botts, B. Thoms, A. Noamani, and T. A. Horan, “Cloud computing architectures for the underserved: Public health cyberinfrastructures through a network of healthatms,” in *System Sciences (HICSS), 2010 43rd Hawaii International Conference on*. IEEE, 2010, pp. 1–10.
- [18] Q. Huang, L. Ye, M. Yu, F. Wu, and R. Liang, “Medical information integration based cloud computing,” in *Network Computing and Information Security (NCIS), 2011 International Conference on*, vol. 1. IEEE, 2011, pp. 79–83.
- [19] Z. Chang, S. Mei, Z. Gu, J. Gu, L. Xia, S. Liang, and J. Lin, “Realization of integration and working procedure on digital hospital information system,” *Computer Standards & Interfaces*, vol. 25, no. 5, pp. 529–537, 2003.

- [20] C. O. Rolim, F. L. Koch, C. B. Westphall, J. Werner, A. Fracalossi, and G. S. Salvador, "A cloud computing solution for patient's data collection in health care institutions," in *eHealth, Telemedicine, and Social Medicine, 2010. ETELEMED'10. Second International Conference on*. IEEE, 2010, pp. 95–99.
- [21] E. Frontoni, M. Baldi, P. Zingaretti, V. Landro, and P. Misericordia, "Security issues for data sharing and service interoperability in ehealth systems: the nu. sa. test bed," in *Security Technology (ICCST), 2014 International Carnahan Conference on*. IEEE, 2014, pp. 1–6.
- [22] R. Zhang and L. Liu, "Security models and requirements for healthcare application clouds," in *Cloud Computing (CLOUD), 2010 IEEE 3rd International Conference on*. IEEE, 2010, pp. 268–275.
- [23] L. Rossi, A. Belli, A. De Santis, C. Diamantini, E. Frontoni, E. Gambi, L. Palma, L. Pernini, P. Pierleoni, D. Potena *et al.*, "Interoperability issues among smart home technological frameworks," in *Mechatronic and Embedded Systems and Applications (MESA), 2014 IEEE/ASME 10th International Conference on*. IEEE, 2014, pp. 1–7.
- [24] B. Orgun and J. Vu, "HI7 ontology and mobile agents for interoperability in heterogeneous medical information systems," *Computers in biology and medicine*, vol. 36, no. 7, pp. 817–836, 2006.
- [25] M. Deng, M. Nalin, M. Petković, I. Baroni, and A. Marco, "Towards trustworthy health platform cloud," in *Secure Data Management*. Springer, 2012, pp. 162–175.
- [26] C. He, X. Jin, Z. Zhao, and T. Xiang, "A cloud computing solution for hospital information system," in *Intelligent Computing and Intelligent Systems (ICIS), 2010 IEEE International Conference on*, vol. 2. IEEE, 2010, pp. 517–520.
- [27] A. L. King, S. Procter, D. Andresen, J. Hatchliff, S. Warren, W. Spees, R. P. Jetley, P. L. Jones, and S. Weininger, "An open test bed for medical device integration and coordination." in *ICSE Companion*, 2009, pp. 141–151.
- [28] J. Roukema, R. K. Los, S. E. Bleeker, A. M. van Ginneken, J. van der Lei, and H. A. Moll, "Paper versus computer: feasibility of an electronic medical record in general pediatrics," *Pediatrics*, vol. 117, no. 1, pp. 15–21, 2006.

Bibliography

- [29] R. Hillestad, J. Bigelow, A. Bower, F. Girosi, R. Meili, R. Scoville, and R. Taylor, “Can electronic medical record systems transform health care? potential health benefits, savings, and costs,” *Health affairs*, vol. 24, no. 5, pp. 1103–1117, 2005.
- [30] S. M. Retchin and R. P. Wenzel, “Electronic medical record systems at academic health centers: advantages and implementation issues.” *Academic Medicine*, vol. 74, no. 5, pp. 493–8, 1999.
- [31] D. J. Brailer, “Interoperability: the key to the future health care system,” *Health affairs*, vol. 24, p. W5, 2005.
- [32] J. L. Habib and D. B. Trends, “Ehrs, meaningful use, and a model emr,” *Drug Benefit Trends*, vol. 22, 2010.
- [33] P. Kierkegaard, “Electronic health record: Wiring europe’s healthcare,” *Computer law & security review*, vol. 27, no. 5, pp. 503–515, 2011.
- [34] ISO/TC 20514 Health Informatics, “Health Informatics – Electronic Health Record – Definition, Scope, and Context,” 2005.
- [35] K. Häyrynen, K. Saranto, and P. Nykänen, “Definition, structure, content, use and impacts of electronic health records: a review of the research literature,” *International journal of medical informatics*, vol. 77, no. 5, pp. 291–304, 2008.
- [36] S. V. Jardim, “The electronic health record and its contribution to health-care information systems interoperability,” *Procedia Technology*, vol. 9, pp. 940–948, 2013.
- [37] S. Garde, P. Knaup, E. J. Hovenga, and S. Heard, “Towards semantic interoperability for electronic health records–domain knowledge governance for open ehr archetypes,” *Methods of information in medicine*, vol. 46, no. 3, pp. 332–343, 2007.
- [38] F. M. Bowens, P. A. Frye, and W. A. Jones, “Health information technology: integration of clinical workflow into meaningful use of electronic health records,” *Perspectives in Health Information Management/AHIMA, American Health Information Management Association*, vol. 7, no. Fall, 2010.
- [39] “HiMMS Analytics, Electronic Medical Record Adoption Model,” <http://www.himssanalytics.org/emram>.
- [40] “HiMMS Analytics, Electronic Medical Record Adoption Model Score Distribution - European Countries,” <http://www.himss.eu/healthcare-providers/emram>.

- [41] J. J. Cimino, J. M. Teich, V. L. Patel, and J. Zhang, “What is wrong with emr?” *Panel proposal for AMIA*, vol. 99, 1999.
- [42] I. Valdes, D. Kibbe, G. Tolleson, M. Kunik, and L. Petersen, “Barriers to proliferation of electronic medical records,” *Journal of Innovation in Health Informatics*, vol. 12, no. 1, pp. 3–9, 2004.
- [43] H. Yan, R. Gardner, and R. Baier, “Beyond the focus group: understanding physicians’ barriers to electronic medical records,” *The Joint Commission Journal on Quality and Patient Safety*, vol. 38, no. 4, pp. 184–AP1, 2012.
- [44] A. Boonstra and M. Broekhuis, “Barriers to the acceptance of electronic medical records by physicians from systematic review to taxonomy and interventions,” *BMC health services research*, vol. 10, no. 1, p. 231, 2010.
- [45] P. Guarda, *Fascicolo sanitario elettronico e protezione dei dati personali*. Trento: Università degli Studi di Trento, 2011, vol. 94.
- [46] “Agenzia per l’Italia Digitale (AgID),” <http://www.agid.gov.it/>.
- [47] “LINEE GUIDA FSE - Framework dei servizi di integrazione con l’infrastruttura FSE di Regione Marche,” 2015.
- [48] A. Baker, “Crossing the quality chasm: a new health system for the 21st century,” *BMJ: British Medical Journal*, vol. 323, no. 7322, p. 1192, 2001.
- [49] D. L. Sackett, W. M. Rosenberg, J. M. Gray, R. B. Haynes, and W. S. Richardson, “Evidence based medicine: what it is and what it isn’t,” 1996.
- [50] J. A. Osheroff *et al.*, “Improving outcomes with clinical decision support: an implementer’s guide.” Himss, 2012.
- [51] T. Schecke, M. Langen, H.-J. Popp, G. Rau, H. Käsmacher, and G. Kalf, “Knowledge-based decision support for patient monitoring in cardioanesthesia,” *International journal of clinical monitoring and computing*, vol. 9, no. 1, pp. 1–11, 1992.
- [52] J. Warren, G. Beliakov, and B. Van Der Zwaag, “Fuzzy logic in clinical practice decision support systems,” in *System Sciences, 2000. Proceedings of the 33rd Annual Hawaii International Conference on*. IEEE, 2000, pp. 10–pp.
- [53] J. C. Prather, D. F. Lobach, L. K. Goodwin, J. W. Hales, M. L. Hage, and W. E. Hammond, “Medical data mining: knowledge discovery in a clinical

- data warehouse.” in *Proceedings of the AMIA annual fall symposium*. American Medical Informatics Association, 1997, p. 101.
- [54] R. E. Bolinger, S. Price, and J. L. Kyner, “Use of a computerized clinical decision system in a diabetic clinic,” in *Proceedings of the ACM annual conference*. ACM, 1973, pp. 362–364.
- [55] C. Catley and M. Frize, “A prototype xml-based implementation of an integrated’intelligent’neonatal intensive care unit,” in *Information Technology Applications in Biomedicine, 2003. 4th International IEEE EMBS Special Topic Conference on*. IEEE, 2003, pp. 322–325.
- [56] C. Catley, M. Frize, C. Walker, and L. StGermain, “Integrating clinical alerts into an xml-based health care framework for the neonatal intensive care unit,” in *Engineering in Medicine and Biology Society, 2003. Proceedings of the 25th Annual International Conference of the IEEE*, vol. 2. IEEE, 2003, pp. 1276–1279.
- [57] M. Frize, L. Yang, R. C. Walker, and A. M. O’Connor, “Conceptual framework of knowledge management for ethical decision-making support in neonatal intensive care,” *IEEE Transactions on Information Technology in Biomedicine*, vol. 9, no. 2, pp. 205–215, 2005.
- [58] C. Catley, D. C. Petriu, and M. Frize, “Software performance engineering of a web service-based clinical decision support infrastructure.” in *WOSP*, vol. 4, 2004, pp. 130–138.
- [59] “MarketsandMarkets,” <https://www.marketsandmarkets.com/>.
- [60] E. G. Liberati, L. Galuppo, M. Gorli, M. Maraldi, F. Ruggiero, M. Capobussi, R. Banzi, K. Kwag, G. Scaratti, O. Nanni *et al.*, “Barriere e facilitatori all’implementazione dei sistemi di supporto decisionale computerizzati in ospedale: uno studio “grounded theory”,” *Recenti Progressi in Medicina*, vol. 106, no. 4, pp. 180–191, 2015.
- [61] S. Corrao, V. Arcoraci, S. Arnone, L. Calvo, R. Scaglione, C. Di Bernardo, R. Lagalla, A. P. Caputi, and G. Licata, “Evidence-based knowledge management: an approach to effectively promote good health-care decision-making in the information era,” *Internal and emergency medicine*, vol. 4, no. 2, pp. 99–106, 2009.
- [62] F. Pesce, M. Diciolla, G. Binetti, D. Naso, V. C. Ostuni, T. Di Noia, A. M. Vågane, R. Bjørneklett, H. Suzuki, Y. Tomino *et al.*, “Clinical decision support system for end-stage kidney disease risk estimation in iga nephropathy patients,” *Nephrology Dialysis Transplantation*, vol. 31, no. 1, pp. 80–86, 2015.

- [63] M. Capobussi, R. Banzi, L. Moja, S. Bonovas, M. González-Lorenzo, E. Liberati, F. H. Polo, O. Nanni, M. Mangia, and F. Ruggiero, “Computerized decision support systems: Ebm at the bedside,” *Recenti progressi in medicina*, vol. 107, no. 11, pp. 589–591, 2016.
- [64] A. Cenci, D. Liciotti, I. Ercoli, P. Zingaretti, and V. P. Carnielli, “A cloud-based healthcare infrastructure for medical device integration: The bilirubinometer case study,” in *Mechatronic and Embedded Systems and Applications (MESA), 2016 12th IEEE/ASME International Conference on*. IEEE, 2016, pp. 1–6.
- [65] J. Rao and X. Su, “A survey of automated web service composition methods,” in *Semantic Web Services and Web Process Composition*. Springer, 2004, pp. 43–54.
- [66] H. Hacigümüs, B. Iyer, and S. Mehrotra, “Providing database as a service,” in *Data Engineering, 2002. Proceedings. 18th International Conference on*. IEEE, 2002, pp. 29–38.
- [67] *Datascope Passport 2 - Passport 2 LT User Manual*, http://www.frankshospitalworkshop.com/equipment/ecg_service_manuals.html, Datascope Patient Monitoring, USA, 1945.
- [68] “Ginevri One Beam,” <http://www.ginevri.com/Prodotti.aspx?id=20&l=en-US>.
- [69] J. M. Kirk, “Neonatal jaundice: a critical review of the role and practice of bilirubin analysis,” *Annals of clinical biochemistry*, vol. 45, no. 5, pp. 452–462, 2008.
- [70] J. Dai, D. M. Parry, and J. Krahn, “Transcutaneous bilirubinometry: its role in the assessment of neonatal jaundice,” *Clinical biochemistry*, vol. 30, no. 1, pp. 1–9, 1997.
- [71] L. D. Lilien, V. J. Harris, R. S. Ramamurthy, and R. S. Pildes, “Neonatal osteomyelitis of the calcaneus: complication of heel puncture,” *The Journal of pediatrics*, vol. 88, no. 3, pp. 478–480, 1976.
- [72] I. Yamanouchi, Y. Yamauchi, and I. Igarashi, “Transcutaneous bilirubinometry: preliminary studies of noninvasive transcutaneous bilirubin meter in the okayama national hospital,” *Pediatrics*, vol. 65, no. 2, pp. 195–202, 1980.
- [73] S. Yasuda, S. Itoh, K. Isobe, M. Yonetani, H. Nakamura, M. Nakamura, Y. Yamauchi, and A. Yamanishi, “New transcutaneous jaundice device

Bibliography

- with two optical paths,” *Journal of perinatal medicine*, vol. 31, no. 1, pp. 81–88, 2003.
- [74] R. Tayaba, D. Gribetz, I. Gribetz, and I. R. Holzman, “Noninvasive estimation of serum bilirubin,” *Pediatrics*, vol. 102, no. 3, pp. e28–e28, 1998.
- [75] F. F. Rubaltelli, G. R. Gourley, N. Loskamp, N. Modi, M. Roth-Kleiner, A. Sender, and P. Vert, “Transcutaneous bilirubin measurement: a multicenter evaluation of a new device,” *Pediatrics*, vol. 107, no. 6, pp. 1264–1271, 2001.
- [76] D. De Luca, E. Zecca, M. Corsello, E. Tiberi, C. Semeraro, and C. Romagnoli, “Attempt to improve transcutaneous bilirubinometry: a double-blind study of medick bilimed versus respironics bilicheck,” *Archives of Disease in Childhood-Fetal and Neonatal Edition*, vol. 93, no. 2, pp. F135–F139, 2008.
- [77] G. Bertini, S. Pratesi, E. Cosenza, and C. Dani, “Transcutaneous bilirubin measurement: Evaluation of bilitestTM,” *Neonatology*, vol. 93, no. 2, pp. 101–105, 2008.
- [78] J. R. Petersen, A. O. Okorodudu, A. A. Mohammad, A. Fernando, and K. E. Shattuck, “Association of transcutaneous bilirubin testing in hospital with decreased readmission rate for hyperbilirubinemia,” *Clinical chemistry*, vol. 51, no. 3, pp. 540–544, 2005.
- [79] M. J. Maisels and E. Kring, “Transcutaneous bilirubinometry decreases the need for serum bilirubin measurements and saves money,” *Pediatrics*, vol. 99, no. 4, pp. 599–600, 1997.
- [80] A. A. of Pediatrics Subcommittee on Hyperbilirubinemia *et al.*, “Management of hyperbilirubinemia in the newborn infant 35 or more weeks of gestation.” *Pediatrics*, vol. 114, no. 1, p. 297, 2004.
- [81] “Dräger JM-105,” https://www.draeger.com/en_uk/Hospital/Products/Thermoregulation-and-Jaundice-Management/Jaundice-Management/Jaundice-Screening/Jaundice-Meter-JM-105.
- [82] “Health Level Seven[®] INTERNATIONAL,” <http://www.hl7.org/>.
- [83] “Sinc, System Improvement for Neonatal Care,” <http://sinc.jef.it/>.
- [84] W. H. Organization *et al.*, *WHO child growth standards: length/height for age, weight-for-age, weight-for-length, weight-for-height and body mass index-for-age, methods and development*. World Health Organization, 2006.

- [85] R. Gaillard, M. A. de Ridder, B. O. Verburg, J. C. Witteman, J. P. Mackenbach, H. A. Moll, A. Hofman, E. A. Steegers, and V. W. Jaddoe, “Individually customised fetal weight charts derived from ultrasound measurements: the generation r study,” *European journal of epidemiology*, vol. 26, no. 12, pp. 919–926, 2011.
- [86] Gruppo di Studio Nutrizione e Metabolismo della Società Italiana di Neonatologia, “Guida alla nutrizione parenterale in epoca neonatale,” 2000.
- [87] SIN Società Italiana Neonatologia Gruppo Nutrizione Parenterale Neonatale, “Manuale di Nutrizione Parenterale Neonatale,” 2017.
- [88] N. Bayley, *Bayley scales of infant and toddler development*. Pearson, 2006.
- [89] C. A. Albers and A. J. Grieve, “Test review: Bayley, n.(2006). bayley scales of infant and toddler development—third edition. san antonio, tx: Harcourt assessment,” *Journal of Psychoeducational Assessment*, vol. 25, no. 2, pp. 180–190, 2007.
- [90] T. Moore, S. Johnson, S. Haider, E. Hennessy, and N. Marlow, “Relationship between test scores using the second and third editions of the bayley scales in extremely preterm children,” *The Journal of pediatrics*, vol. 160, no. 4, pp. 553–558, 2012.
- [91] I. Adams-Chapman, C. M. Bann, Y. E. Vaucher, B. J. Stoll, H. D. N. N. R. Network, E. K. S. N. I. of Child Health *et al.*, “Association between feeding difficulties and language delay in preterm infants using bayley scales of infant development,” *The Journal of pediatrics*, vol. 163, no. 3, pp. 680–685, 2013.
- [92] K. Lee, “Use of the bayley scales of infant development-iii by therapists for assessing development and recommending treatment for infants in a nicu follow-up clinic,” 2013.
- [93] A. Knudsen, “The influence of the reserve albumin concentration and ph on the cephalocaudal progression of jaundice in newborns,” *Early human development*, vol. 25, no. 1, pp. 37–41, 1991.
- [94] A. Riskin, A. Tamir, A. Kugelman, M. Hemo, and D. Bader, “Is visual assessment of jaundice reliable as a screening tool to detect significant neonatal hyperbilirubinemia?” *The Journal of pediatrics*, vol. 152, no. 6, pp. 782–787, 2008.

Bibliography

- [95] A. Madan, J. MacMahon, D. Stevenson *et al.*, “Neonatal hyperbilirubinemia,” *Avery’s disease of the newborn. 8th ed. Philadelphia: Saunders*, pp. 1227–56, 2005.
- [96] S. Ip, M. Chung, J. Kulig, R. O’Brien, R. Sege, S. Glick, M. J. Maisels, J. Lau *et al.*, “An evidence-based review of important issues concerning neonatal hyperbilirubinemia,” *Pediatrics*, vol. 114, no. 1, pp. e130–e153, 2004.
- [97] V. K. Bhutani, A. Zipursky, H. Blencowe, R. Khanna, M. Sgro, F. Ebbesen, J. Bell, R. Mori, T. M. Slusher, N. Fahmy *et al.*, “Neonatal hyperbilirubinemia and rhesus disease of the newborn: incidence and impairment estimates for 2010 at regional and global levels,” *Pediatric research*, vol. 74, no. Suppl 1, p. 86, 2013.
- [98] J. Chen and U. Ling, “Prediction of the development of neonatal hyperbilirubinemia in abo incompatibility.” *Zhonghua yi xue za zhi= Chinese medical journal; Free China ed*, vol. 53, no. 1, pp. 13–18, 1994.
- [99] F. Ebbesen, “Recurrence of kernicterus in term and near-term infants in denmark,” *Acta paediatrica*, vol. 89, no. 10, pp. 1213–1217, 2000.
- [100] M. J. Maisels and T. B. Newman, “Kernicterus in otherwise healthy, breast-fed term newborns,” *Pediatrics*, vol. 96, no. 4, pp. 730–733, 1995.
- [101] L. H. Johnson, V. K. Bhutani, and A. K. Brown, “System-based approach to management of neonatal jaundice and prevention of kernicterus,” *The Journal of pediatrics*, vol. 140, no. 4, pp. 396–403, 2002.
- [102] G. K. Suresh and R. E. Clark, “Cost-effectiveness of strategies that are intended to prevent kernicterus in newborn infants,” *Pediatrics*, vol. 114, no. 4, pp. 917–924, 2004.
- [103] F. Nasser, G. A. Mamouri, and H. Babaei, “Intravenous immunoglobulin in abo and rh hemolytic diseases of newborn.” *Saudi medical journal*, vol. 27, no. 12, pp. 1827–1830, 2006.
- [104] M. J. Maisels and A. F. McDonagh, “Phototherapy for neonatal jaundice,” *New England Journal of Medicine*, vol. 358, no. 9, pp. 920–928, 2008.
- [105] C. E. Ahlfors, “Criteria for exchange transfusion in jaundiced newborns,” *Pediatrics*, vol. 93, no. 3, pp. 488–494, 1994.
- [106] S. Murki and P. Kumar, “Blood exchange transfusion for infants with severe neonatal hyperbilirubinemia,” in *Seminars in perinatology*, vol. 35, no. 3. Elsevier, 2011, pp. 175–184.

- [107] J. C. Jackson, “Adverse events associated with exchange transfusion in healthy and ill newborns,” *Pediatrics*, vol. 99, no. 5, pp. e7–e7, 1997.
- [108] D. S. Seidman, D. K. Stevenson, Z. Ergaz, and R. Gale, “Hospital readmission due to neonatal hyperbilirubinemia,” *Pediatrics*, vol. 96, no. 4, pp. 727–729, 1995.
- [109] G. Bertini, C. Dani, M. Tronchin, and F. F. Rubaltelli, “Is breastfeeding really favoring early neonatal jaundice?” *Pediatrics*, vol. 107, no. 3, pp. e41–e41, 2001.
- [110] M. J. Maisels, “Neonatal hyperbilirubinemia and kernicterus—not gone but sometimes forgotten,” *Early human development*, vol. 85, no. 11, pp. 727–732, 2009.
- [111] P. A. Dennery, D. S. Seidman, and D. K. Stevenson, “Neonatal hyperbilirubinemia,” *New England Journal of Medicine*, vol. 344, no. 8, pp. 581–590, 2001.
- [112] S. Ip, S. Glick, J. Kulig, R. O’Brien, and R. Sege, “Management of neonatal hyperbilirubinemia.” *Evidence report/technology assessment (Summary)*, no. 65, p. 1, 2002.
- [113] M. Maisels and J. Watchko, “Treatment of jaundice in low birthweight infants,” *Archives of Disease in Childhood-Fetal and Neonatal Edition*, vol. 88, no. 6, pp. F459–F463, 2003.
- [114] V. K. Bhutani, L. Johnson, and E. M. Sivieri, “Predictive ability of a predischARGE hour-specific serum bilirubin for subsequent significant hyperbilirubinemia in healthy term and near-term newborns,” *Pediatrics*, vol. 103, no. 1, pp. 6–14, 1999.
- [115] T. B. Newman, B. Xiong, V. M. Gonzales, and G. J. Escobar, “Prediction and prevention of extreme neonatal hyperbilirubinemia in a mature health maintenance organization,” *Archives of pediatrics & adolescent medicine*, vol. 154, no. 11, pp. 1140–1147, 2000.
- [116] R. Keren, X. Luan, S. Friedman, S. Saddlemire, A. Cnaan, and V. K. Bhutani, “A comparison of alternative risk-assessment strategies for predicting significant neonatal hyperbilirubinemia in term and near-term infants,” *Pediatrics*, vol. 121, no. 1, pp. e170–e179, 2008.
- [117] M. Sgro, D. Campbell, and V. Shah, “Incidence and causes of severe neonatal hyperbilirubinemia in Canada,” *Canadian Medical Association Journal*, vol. 175, no. 6, pp. 587–590, 2006.

Bibliography

- [118] Y. Maruo, K. Nishizawa, H. Sato, Y. Doida, and M. Shimada, "Association of neonatal hyperbilirubinemia with bilirubin udy-glucuronosyltransferase polymorphism," *Pediatrics*, vol. 103, no. 6, pp. 1224–1227, 1999.
- [119] M.-J. Huang, K.-E. Kua, H.-C. Teng, K.-S. Tang, H.-W. Weng, and C.-S. Huang, "Risk factors for severe hyperbilirubinemia in neonates," *Pediatric research*, vol. 56, no. 5, pp. 682–689, 2004.
- [120] J. F. Watchko, "Identification of neonates at risk for hazardous hyperbilirubinemia: emerging clinical insights," *Pediatric clinics of North America*, vol. 56, no. 3, pp. 671–687, 2009.
- [121] D. De Luca, E. Zecca, P. De Turrís, G. Barbato, M. Marras, and C. Romagnoli, "Using bilicheckTM for preterm neonates in a sub-intensive unit: Diagnostic usefulness and suitability," *Early human development*, vol. 83, no. 5, pp. 313–317, 2007.
- [122] T. Karen, H. U. Bucher, and J.-C. Fauchère, "Comparison of a new transcutaneous bilirubinometer (bilimed®) with serum bilirubin measurements in preterm and full-term infants," *BMC pediatrics*, vol. 9, no. 1, p. 70, 2009.
- [123] S. N. El-Beshbishi, K. E. Shattuck, A. A. Mohammad, and J. R. Petersen, "Hyperbilirubinemia and transcutaneous bilirubinometry," *clinical chemistry*, vol. 55, no. 7, pp. 1280–1287, 2009.
- [124] N. Bosschaart, J. H. Kok, A. M. Newsum, D. M. Ouweneel, R. Mentink, T. G. van Leeuwen, and M. C. Aalders, "Limitations and opportunities of transcutaneous bilirubin measurements," *Pediatrics*, vol. 129, no. 4, pp. 689–694, 2012.
- [125] F. Raimondi, S. Lama, F. Landolfo, M. Sellitto, A. C. Borrelli, R. Maffucci, P. Milite, and L. Capasso, "Measuring transcutaneous bilirubin: a comparative analysis of three devices on a multiracial population," *BMC pediatrics*, vol. 12, no. 1, p. 70, 2012.
- [126] A. R. Gagliardi, M. C. Brouwers, V. A. Palda, L. Lemieux-Charles, and J. M. Grimshaw, "How can we improve guideline use? a conceptual framework of implementability," *Implementation Science*, vol. 6, no. 1, p. 26, 2011.
- [127] R. Grol and J. Grimshaw, "From best evidence to best practice: effective implementation of change in patients' care," *The lancet*, vol. 362, no. 9391, pp. 1225–1230, 2003.

- [128] C. Bielza, M. Gómez, S. Ríos-Insua, J. F. Del Pozo, P. G. Barreno, S. Caballero, and M. S. Luna, “Ictneo system for jaundice management,” *Revista de la Real Academia de Ciencias Exactas Físicas y Naturales*, vol. 92, no. 4, pp. 307–315, 1998.
- [129] C. Longhurst, S. Turner, and A. E. Burgos, “Development of a web-based decision support tool to increase use of neonatal hyperbilirubinemia guidelines,” *The Joint Commission Journal on Quality and Patient Safety*, vol. 35, no. 5, pp. 256–262, 2009.
- [130] “Tool for management of neonatal jaundice.” <http://paediatrics.co.uk/nicu/neonatal-jaundice>.
- [131] J. M. R. Miguélez and J. F. Aloy, “Ictericia neonatal,” *Protocolo de la Asociación Española de Pediatría. Recuperado a partir de <http://www.seneonatal.es/Portals/0/Articulos/38.pdf>*, 2008.
- [132] M. J. Maisels, V. K. Bhutani, D. Bogen, T. B. Newman, A. R. Stark, and J. F. Watchko, “Hyperbilirubinemia in the newborn infant ≥ 35 weeks gestation: an update with clarifications,” *Pediatrics*, vol. 124, no. 4, pp. 1193–1198, 2009.
- [133] M. Atkinson and H. Budge, “Review of the nice guidance on neonatal jaundice,” *Archives of Disease in Childhood-Education and Practice*, vol. 96, no. 4, pp. 136–140, 2011.
- [134] C. Dani, C. Poggi, J. Barp, C. Romagnoli, and G. Buonocore, “Current italian practices regarding the management of hyperbilirubinaemia in preterm infants,” *Acta Paediatrica*, vol. 100, no. 5, pp. 666–669, 2011.
- [135] S. Ip, M. Chung, J. Kulig, R. SEGE, S. GLICKEN, M. MAISELS, J. Lau *et al.*, “American academy of pediatrics subcommittee on hyperbilirubinemia. an evidence-based review of important issues concerning neonatal hyperbilirubinemia,” 2004.
- [136] V. K. Bhutani *et al.*, “Phototherapy to prevent severe neonatal hyperbilirubinemia in the newborn infant 35 or more weeks of gestation,” *Pediatrics*, pp. peds–2011, 2011.
- [137] J. Rennie, S. Burman-Roy, M. S. Murphy, G. D. Group *et al.*, “Neonatal jaundice: summary of nice guidance,” *BMJ*, vol. 340, no. 7757, p. c2409, 2010.
- [138] K. Barrington and K. Sankaran, “Guidelines for detection, management and prevention of hyperbilirubinemia in term and late preterm newborn

Bibliography

- infants (35 or more weeks' gestation)," *Paediatr Child Health*, vol. 12, no. Suppl B, pp. 1B–12B, 2007.
- [139] D. E. van Imhoff, P. H. Dijk, C. V. Hulzebos *et al.*, "Uniform treatment thresholds for hyperbilirubinemia in preterm infants: background and synopsis of a national guideline," *Early human development*, vol. 87, no. 8, pp. 521–525, 2011.
- [140] D. Bratlid, B. Nakstad, and T. Hansen, "National guidelines for treatment of jaundice in the newborn," *Acta Paediatrica*, vol. 100, no. 4, pp. 499–505, 2011.
- [141] M. Kaplan, P. Merlob, and R. Regev, "Israel guidelines for the management of neonatal hyperbilirubinemia and prevention of kernicterus," *Journal of Perinatology*, vol. 28, no. 6, pp. 389–397, 2008.
- [142] "Newborn Service Clinical Guideline. Management of neonatal jaundice." <http://www.adhb.govt.nz/newborn/guidelines/GI/Jaundice.htm>.
- [143] Q. Maternity, "Neonatal clinical guideline: Neonatal jaundice: Prevention, assessment and management. 2009."
- [144] S. Mishra, R. Agarwal, A. Deorari, and V. Paul, "Jaundice in the newborn. aiims-nicu protocols. 2007."
- [145] R. Arlettaz, A. Blumberg, L. Buetti, H. Fahnenstich, D. Mieth, and M. Roth-Kleiner, "Assessment and treatment of jaundice newborn infants 35 0/7 or more weeks of gestation," *Swiss Soc Neonatology*, pp. 1–4, 2007.
- [146] D. De Luca, C. Romagnoli, E. Tiberi, A. A. Zuppa, and E. Zecca, "Skin bilirubin nomogram for the first 96 h of life in a european normal healthy newborn population, obtained with multiwavelength transcutaneous bilirubinometry," *Acta Paediatrica*, vol. 97, no. 2, pp. 146–150, 2008.
- [147] C. Romagnoli, E. Tiberi, G. Barone, M. De Curtis, D. Regoli, P. Paolillo, S. Picone, S. Anania, M. Finocchi, V. Cardiello *et al.*, "Validation of transcutaneous bilirubin nomogram in identifying neonates not at risk of hyperbilirubinaemia: a prospective, observational, multicenter study," *Early human development*, vol. 88, no. 1, pp. 51–55, 2012.
- [148] —, "Development and validation of serum bilirubin nomogram to predict the absence of risk for severe hyperbilirubinaemia before discharge: a prospective, multicenter study," *Italian journal of pediatrics*, vol. 38, no. 1, p. 6, 2012.

- [149] D. Liciotti, M. Contigiani, E. Frontoni, A. Mancini, P. Zingaretti, and V. Placidi, "Shopper analytics: A customer activity recognition system using a distributed rgb-d camera network," in *Video Analytics for Audience Measurement*. Springer International Publishing, 2014, pp. 146–157.
- [150] G. J. Tortora and B. H. Derrickson, *Principles of anatomy and physiology*. John Wiley & Sons, 2008.
- [151] V.-P. Seppa, J. Viik, and J. Hyttinen, "Assessment of pulmonary flow using impedance pneumography," *Biomedical Engineering, IEEE Transactions on*, vol. 57, no. 9, pp. 2277–2285, 2010.
- [152] J. H. Houtveen, P. F. Groot, and E. J. de Geus, "Validation of the thoracic impedance derived respiratory signal using multilevel analysis," *International Journal of Psychophysiology*, vol. 59, no. 2, pp. 97–106, 2006.
- [153] J. P. Cantineau, P. Escourrou, R. Sartene, C. Gaultier, and M. Goldman, "Accuracy of respiratory inductive plethysmography during wakefulness and sleep in patients with obstructive sleep apnea." *CHEST Journal*, vol. 102, no. 4, pp. 1145–1151, 1992.
- [154] J. Allen, "Photoplethysmography and its application in clinical physiological measurement," *Physiological measurement*, vol. 28, no. 3, p. R1, 2007.
- [155] M. A. Carskadon, K. Harvey, W. C. Dement, C. Guilleminault, F. B. Simmons, and T. F. Anders, "Respiration during sleep in children," *Western Journal of Medicine*, vol. 128, no. 6, p. 477, 1978.
- [156] R. Farre, J. Montserrat, M. Rotger, E. Ballester, and D. Navajas, "Accuracy of thermistors and thermocouples as flow-measuring devices for detecting hypopnoeas," *European Respiratory Journal*, vol. 11, no. 1, pp. 179–182, 1998.
- [157] J. Sharp, W. Druz, J. Foster, M. Wicks, and S. Chokroverty, "Use of the respiratory magnetometer in diagnosis and classification of sleep apnea." *CHEST Journal*, vol. 77, no. 3, pp. 350–353, 1980.
- [158] V. P. Harper, H. Pasterkamp, H. Kiyokawa, and G. R. Wodicka, "Modeling and measurement of flow effects on tracheal sounds," *Biomedical Engineering, IEEE Transactions on*, vol. 50, no. 1, pp. 1–10, 2003.
- [159] A. D. Droitcour, T. B. Seto, B.-K. Park, S. Yamada, A. Vergara, C. El Hourani, T. Shing, A. Yuen, V. M. Lubecke, and O. Boric-Lubecke, "Non-contact respiratory rate measurement validation for hospitalized

Bibliography

- patients,” in *Engineering in Medicine and Biology Society, 2009. EMBC 2009. Annual International Conference of the IEEE*. IEEE, 2009, pp. 4812–4815.
- [160] M. Uenoyama, T. Matsui, K. Yamada, S. Suzuki, B. Takase, S. Suzuki, M. Ishihara, and M. Kawakami, “Non-contact respiratory monitoring system using a ceiling-attached microwave antenna,” *Medical and Biological Engineering and Computing*, vol. 44, no. 9, pp. 835–840, 2006.
- [161] D. Dei, G. Grazzini, G. Luzi, M. Pieraccini, C. Atzeni, S. Boncinelli, G. Camiciottoli, W. Castellani, M. Marsili, and J. Lo Dico, “Non-contact detection of breathing using a microwave sensor,” *Sensors*, vol. 9, no. 4, pp. 2574–2585, 2009.
- [162] L. Boccanfuso and J. M. O’Kane, “Remote measurement of breathing rate in real time using a high precision, single-point infrared temperature sensor,” in *Biomedical Robotics and Biomechanics (BioRob), 2012 4th IEEE RAS & EMBS International Conference on*. IEEE, 2012, pp. 1704–1709.
- [163] S. Y. Chekmenev, H. Rara, and A. A. Farag, “Non-contact, wavelet-based measurement of vital signs using thermal imaging,” in *The first international conference on graphics, vision, and image processing (GVIP), Cairo, Egypt, 2005*, pp. 107–112.
- [164] I. Levai, V. Sidoroff, and R. Iles, “An introduction to the non-invasive non-contact assessment of respiratory function,” *Respiratory Therapy*, vol. 7, no. 5, p. 43, 2012.
- [165] A. Aliverti, R. Dellaca, P. Pelosi, D. Chiumello, A. Pedotti, and L. Gattinoni, “Optoelectronic plethysmography in intensive care patients,” *American journal of respiratory and critical care medicine*, vol. 161, no. 5, pp. 1546–1552, 2000.
- [166] R. L. Dellaca, M. L. Ventura, E. Zannin, M. Natile, A. Pedotti, and P. Tagliabue, “Measurement of total and compartmental lung volume changes in newborns by optoelectronic plethysmography,” *Pediatric research*, vol. 67, no. 1, pp. 11–16, 2010.
- [167] M.-C. Yu, J.-L. Liou, S.-W. Kuo, M.-S. Lee, and Y.-P. Hung, “Noncontact respiratory measurement of volume change using depth camera,” in *Engineering in Medicine and Biology Society (EMBC), 2012 Annual International Conference of the IEEE*. IEEE, 2012, pp. 2371–2374.

- [168] F. Benetazzo, A. Freddi, A. Monteriù, and S. Longhi, “Respiratory rate detection algorithm based on rgb-d camera: theoretical background and experimental results,” *Healthcare Technology Letters*, vol. 1, no. 3, pp. 81–86, 2014.
- [169] N. Bernacchia, L. Scalise, L. Casacanditella, I. Ercoli, P. Marchionni, and E. P. Tomasini, “Non contact measurement of heart and respiration rates based on kinectTM,” in *Medical Measurements and Applications (MeMeA), 2014 IEEE International Symposium on*. IEEE, 2014, pp. 1–5.
- [170] H. Aoki, M. Miyazaki, H. Nakamura, R. Furukawa, R. Sagawa, and H. Kawasaki, “Non-contact respiration measurement using structured light 3-d sensor,” in *SICE Annual Conference (SICE), 2012 Proceedings of*. IEEE, 2012, pp. 614–618.
- [171] S. Stick, E. Ellis, P. LeSouëf, and P. Sly, “Validation of respiratory inductance plethysmography (“respitrace”[®]) for the measurement of tidal breathing parameters in newborns,” *Pediatric pulmonology*, vol. 14, no. 3, pp. 187–191, 1992.
- [172] W. J. Daily, M. Klaus, H. Belton, and P. Meyer, “Apnea in premature infants: monitoring, incidence, heart rate changes, and an effect of environmental temperature,” *Pediatrics*, vol. 43, no. 4, pp. 510–518, 1969.
- [173] J. Usher Smith, R. Wareham, J. Lasenby, J. Cameron, P. Bridge, and R. Iles, “Structured light plethysmography in infants and children-a pilot study,” 2009.
- [174] D. E. Odd, R. Lingam, A. Emond, and A. Whitelaw, “Movement outcomes of infants born moderate and late preterm,” *Acta pædiatrica*, vol. 102, no. 9, pp. 876–882, 2013.
- [175] I. Krägeloh-Mann and C. Cans, “Cerebral palsy update,” *Brain and development*, vol. 31, no. 7, pp. 537–544, 2009.
- [176] M. HADDERS-ALGRA, K. R. Heineman, A. F. Bos, and K. J. Middelburg, “The assessment of minor neurological dysfunction in infancy using the touwen infant neurological examination: strengths and limitations,” *Developmental Medicine & Child Neurology*, vol. 52, no. 1, pp. 87–92, 2010.
- [177] S. J. Korzeniewski, G. Birbeck, M. C. DeLano, M. J. Potchen, and N. Paneth, “A systematic review of neuroimaging for cerebral palsy,” *Journal of child neurology*, vol. 23, no. 2, pp. 216–227, 2008.

Bibliography

- [178] M. Burger and Q. A. Louw, “The predictive validity of general movements—a systematic review,” *European journal of paediatric neurology*, vol. 13, no. 5, pp. 408–420, 2009.
- [179] E. C. Cameron, V. Maehle, and J. Reid, “The effects of an early physical therapy intervention for very preterm, very low birth weight infants: a randomized controlled clinical trial,” *Pediatric Physical Therapy*, vol. 17, no. 2, pp. 107–119, 2005.
- [180] C. Einspieler, H. F. Prechtl, F. Ferrari, G. Cioni, and A. F. Bos, “The qualitative assessment of general movements in preterm, term and young infants—review of the methodology,” *Early human development*, vol. 50, no. 1, pp. 47–60, 1997.
- [181] C. Einspieler and H. F. Prechtl, “Prechtl’s assessment of general movements: a diagnostic tool for the functional assessment of the young nervous system,” *Mental retardation and developmental disabilities research reviews*, vol. 11, no. 1, pp. 61–67, 2005.
- [182] L. Adde, M. Rygg, K. Lossius, G. K. Øberg, and R. Støen, “General movement assessment: predicting cerebral palsy in clinical practise,” *Early human development*, vol. 83, no. 1, pp. 13–18, 2007.
- [183] F. Ferrari, G. Cioni, C. Einspieler, M. F. Roversi, A. F. Bos, P. B. Paollicelli, A. Ranzi, and H. F. Prechtl, “Cramped synchronized general movements in preterm infants as an early marker for cerebral palsy,” *Archives of pediatrics & adolescent medicine*, vol. 156, no. 5, pp. 460–467, 2002.
- [184] I. Bernhardt, M. Marbacher, R. Hilfiker, and L. Radlinger, “Inter- and intra-observer agreement of prechtl’s method on the qualitative assessment of general movements in preterm, term and young infants,” *Early human development*, vol. 87, no. 9, pp. 633–639, 2011.
- [185] L. Meinecke, N. Breitbach-Faller, C. Bartz, R. Damen, G. Rau, and C. Disselhorst-Klug, “Movement analysis in the early detection of newborns at risk for developing spasticity due to infantile cerebral palsy,” *Human movement science*, vol. 25, no. 2, pp. 125–144, 2006.
- [186] C. Marcroft, A. Khan, N. D. Embleton, M. Trenell, and T. Plötz, “Movement recognition technology as a method of assessing spontaneous general movements in high risk infants,” *Front. Neurol*, vol. 5, pp. 22–30, 2015.
- [187] N. Kanemaru, H. Watanabe, H. Kihara, H. Nakano, R. Takaya, T. Nakamura, J. Nakano, G. Taga, and Y. Konishi, “Specific characteristics of spontaneous movements in preterm infants at term age are associated

- with developmental delays at age 3 years,” *Developmental Medicine & Child Neurology*, vol. 55, no. 8, pp. 713–721, 2013.
- [188] N. Kanemaru, H. Watanabe, H. Kihara, H. Nakano, T. Nakamura, J. Nakano, G. Taga, and Y. Konishi, “Jerky spontaneous movements at term age in preterm infants who later developed cerebral palsy,” *Early human development*, vol. 90, no. 8, pp. 387–392, 2014.
- [189] L. Adde, J. L. Helbostad, A. R. Jensenius, G. Taraldsen, and R. Støen, “Using computer-based video analysis in the study of fidgety movements,” *Early human development*, vol. 85, no. 9, pp. 541–547, 2009.
- [190] A. R. Jensenius, R. I. Godøy, and M. M. Wanderley, “Developing tools for studying musical gestures within the max/msp/jitter environment,” 2005.
- [191] F. Heinze, K. Hesels, N. Breitbach-Faller, T. Schmitz-Rode, and C. Disselhorst-Klug, “Movement analysis by accelerometry of newborns and infants for the early detection of movement disorders due to infantile cerebral palsy,” *Medical & biological engineering & computing*, vol. 48, no. 8, pp. 765–772, 2010.
- [192] D. Karch, K.-S. Kang, K. Wochner, H. Philippi, M. Hadders-Algra, J. Pietz, and H. Dickhaus, “Kinematic assessment of stereotypy in spontaneous movements in infants,” *Gait & posture*, vol. 36, no. 2, pp. 307–311, 2012.
- [193] M. Fan, D. Gravem, D. M. Cooper, and D. J. Patterson, “Augmenting gesture recognition with erlang-cox models to identify neurological disorders in premature babies,” in *Proceedings of the 2012 ACM Conference on Ubiquitous Computing*. ACM, 2012, pp. 411–420.
- [194] D. Karch, K.-S. Kim, K. Wochner, J. Pietz, H. Dickhaus, and H. Philippi, “Quantification of the segmental kinematics of spontaneous infant movements,” *Journal of biomechanics*, vol. 41, no. 13, pp. 2860–2867, 2008.
- [195] M. Gabel, R. Gilad-Bachrach, E. Renshaw, and A. Schuster, “Full body gait analysis with kinect,” in *Engineering in Medicine and Biology Society (EMBC), 2012 Annual International Conference of the IEEE*. IEEE, 2012, pp. 1964–1967.
- [196] C.-Y. Chang, B. Lange, M. Zhang, S. Koenig, P. Requejo, N. Somboon, A. A. Sawchuk, and A. A. Rizzo, “Towards pervasive physical rehabilitation using microsoft kinect,” in *Pervasive Computing Technologies for Healthcare (PervasiveHealth), 2012 6th International Conference on*. IEEE, 2012, pp. 159–162.

Bibliography

- [197] R. A. Clark, Y.-H. Pua, K. Fortin, C. Ritchie, K. E. Webster, L. Denehy, and A. L. Bryant, “Validity of the microsoft kinect for assessment of postural control,” *Gait & posture*, vol. 36, no. 3, pp. 372–377, 2012.
- [198] R. Wang, G. Medioni, C. Winstein, and C. Blanco, “Home monitoring musculo-skeletal disorders with a single 3d sensor,” in *Proceedings of the IEEE Conference on Computer Vision and Pattern Recognition Workshops*, 2013, pp. 521–528.
- [199] M. Devanne, H. Wannous, S. Berretti, P. Pala, M. Daoudi, and A. Del Bimbo, “3-d human action recognition by shape analysis of motion trajectories on riemannian manifold,” *IEEE transactions on cybernetics*, vol. 45, no. 7, pp. 1340–1352, 2015.
- [200] N. Hesse, G. Stachowiak, T. Breuer, and M. Arens, “Estimating body pose of infants in depth images using random ferns,” in *Proceedings of the IEEE International Conference on Computer Vision Workshops*, 2015, pp. 35–43.
- [201] A. Cenci, D. Liciotti, E. Frontoni, A. Mancini, and P. Zingaretti, “Non-contact monitoring of preterm infants using rgb-d camera,” in *ASME 2015 International Design Engineering Technical Conferences and Computers and Information in Engineering Conference*. American Society of Mechanical Engineers, 2015, pp. V009T07A003–V009T07A003.
- [202] A. Cenci, D. Liciotti, E. Frontoni, P. Zingaretti, and V. P. Carnielli, “Movements analysis of preterm infants by using depth sensor,” in *Proceedings of the International Conference on Internet of Things and Machine Learning (IML 2017)*. Liverpool, UK., 2017.
- [203] J. MacQueen *et al.*, “Some methods for classification and analysis of multivariate observations,” in *Proceedings of the fifth Berkeley symposium on mathematical statistics and probability*, vol. 1, no. 14. Oakland, CA, USA., 1967, pp. 281–297.
- [204] M. D. Olsen, A. Herskind, J. B. Nielsen, and R. R. Paulsen, “Body part tracking of infants,” in *Pattern Recognition (ICPR), 2014 22nd International Conference on*. IEEE, 2014, pp. 2167–2172.
- [205] S. Maldonado-Bascon, S. Lafuente-Arroyo, P. Gil-Jimenez, H. Gomez-Moreno, and F. López-Ferreras, “Road-sign detection and recognition based on support vector machines,” *IEEE transactions on intelligent transportation systems*, vol. 8, no. 2, pp. 264–278, 2007.

- [206] N. Moon, E. Bullitt, K. Van Leemput, and G. Gerig, “Automatic brain and tumor segmentation,” *Medical Image Computing and Computer-Assisted Intervention—MICCAI 2002*, pp. 372–379, 2002.
- [207] G.-Q. Wei, K. Arbter, and G. Hirzinger, “Automatic tracking of laparoscopic instruments by color coding,” in *CVRMed-MRCAS’97*. Springer, 1997, pp. 357–366.
- [208] A. Cohen, E. Rivlin, I. Shimshoni, and E. Sabo, “Memory based active contour algorithm using pixel-level classified images for colon crypt segmentation,” *Computerized Medical Imaging and Graphics*, vol. 43, pp. 150–164, 2015.
- [209] C. Huang, L. Davis, and J. Townshend, “An assessment of support vector machines for land cover classification,” *International Journal of remote sensing*, vol. 23, no. 4, pp. 725–749, 2002.
- [210] D. L. Pham, C. Xu, and J. L. Prince, “A survey of current methods in medical image segmentation, technical report jhu/ece 99–01.” *Baltimore: Department of Electrical and Computer Engineering, The Johns Hopkins University*, 2001.
- [211] R. Girshick, J. Donahue, T. Darrell, and J. Malik, “Rich feature hierarchies for accurate object detection and semantic segmentation,” in *The IEEE Conference on Computer Vision and Pattern Recognition (CVPR)*, June 2014.
- [212] A. Krizhevsky, I. Sutskever, and G. E. Hinton, “Imagenet classification with deep convolutional neural networks,” in *Advances in Neural Information Processing Systems 25*, F. Pereira, C. J. C. Burges, L. Bottou, and K. Q. Weinberger, Eds. Curran Associates, Inc., 2012, pp. 1097–1105. [Online]. Available: <http://papers.nips.cc/paper/4824-imagenet-classification-with-deep-convolutional-neural-networks.pdf>
- [213] D. Ciresan, A. Giusti, L. M. Gambardella, and J. Schmidhuber, “Deep neural networks segment neuronal membranes in electron microscopy images,” in *Advances in neural information processing systems*, 2012, pp. 2843–2851.
- [214] C. Farabet, C. Couprie, L. Najman, and Y. LeCun, “Learning hierarchical features for scene labeling,” *IEEE transactions on pattern analysis and machine intelligence*, vol. 35, no. 8, pp. 1915–1929, 2013.

Bibliography

- [215] S. Gupta, R. Girshick, P. Arbeláez, and J. Malik, “Learning rich features from rgb-d images for object detection and segmentation,” in *European Conference on Computer Vision*. Springer, 2014, pp. 345–360.
- [216] H. Zhu, F. Meng, J. Cai, and S. Lu, “Beyond pixels: A comprehensive survey from bottom-up to semantic image segmentation and cosegmentation,” *Journal of Visual Communication and Image Representation*, vol. 34, pp. 12–27, 2016.
- [217] A. Garcia-Garcia, S. Orts-Escolano, S. Oprea, V. Villena-Martinez, and J. Garcia-Rodriguez, “A review on deep learning techniques applied to semantic segmentation,” *arXiv preprint arXiv:1704.06857*, 2017.
- [218] S. Ioffe and C. Szegedy, “Batch normalization: Accelerating deep network training by reducing internal covariate shift,” in *International Conference on Machine Learning*, 2015, pp. 448–456.
- [219] K. Chatfield, K. Simonyan, A. Vedaldi, and A. Zisserman, “Return of the devil in the details: Delving deep into convolutional nets,” *arXiv preprint arXiv:1405.3531*, 2014.
- [220] K. Simonyan and A. Zisserman, “Very deep convolutional networks for large-scale image recognition,” *arXiv preprint arXiv:1409.1556*, 2014.
- [221] P. Sermanet, D. Eigen, X. Zhang, M. Mathieu, R. Fergus, and Y. LeCun, “Overfeat: Integrated recognition, localization and detection using convolutional networks,” *arXiv preprint arXiv:1312.6229*, 2013.
- [222] L. R. Dice, “Measures of the amount of ecologic association between species,” *Ecology*, vol. 26, no. 3, pp. 297–302, 1945.
- [223] “Boost Library,” <http://www.boost.org/>.
- [224] M. Hadders-Algra, “General movements: a window for early identification of children at high risk for developmental disorders,” *The Journal of pediatrics*, vol. 145, no. 2, pp. S12–S18, 2004.